NANYANG TECHNOLOGICAL UNIVERSITY
SINGAPORE

# DEVELOPMENT OF INNOVATIVE NANO-SATELLITES WITH NEW GENERATION TECHNOLOGIES

**AJIT DENIS MENEZES**

**SCHOOL OF MECHANICAL AND**

**AEROSPACE ENGINEERING**

**2019**

# DEVELOPMENT OF INNOVATIVE NANO-SATELLITES WITH NEW GENERATION TECHNOLOGIES

**AJIT DENIS MENEZES**

School of Mechanical & Aerospace Engineering

A thesis submitted to the Nanyang Technological University
in partial fulfilment of the requirement for the degree of
Master of Engineering

**2019**

## Statement of Originality

I hereby certify that the work embodied in this thesis is the result of original research, is free of plagiarised materials, and has not been submitted for a higher degree to any other University or Institution.

17/08/2020.
Date

Ajit Denis Menezes

## Supervisor Declaration Statement

I have reviewed the content and presentation style of this thesis and declare it is free of plagiarism and of sufficient grammatical clarity to be examined. To the best of my knowledge, the research and writing are those of the candidate except as acknowledged in the Author Attribution Statement. I confirm that the investigations were conducted in accord with the ethics policies and integrity standards of Nanyang Technological University and that the research data are presented honestly and without prejudice.

17/08/2020
.....
Date

.....
Sunil Chandrakant Joshi

## Authorship Attribution Statement

This thesis **does not** contain any materials from papers published in peer-reviewed journals or from papers accepted at conferences in which I am listed as an author.

17/08/2020.
Date

Ajit Denis Menezes

## Acknowledgements

I would like to thank Dr. Sunil Joshi, my supervisor, for his invaluable guidance through the project. Dr. Sunil advised me on the basics of Spacecraft design and the information required to develop an effective design. He also set up meetings with experienced engineers and Space industry professionals to provide details on preparing the CubeSat for testing and launch with a selected launch organisation.

I would also like to thank Mr. Abdullah Azhar Sheikh, for providing the initial tips and advice on the satellite requirements, as well as providing the important files and data necessary to finalise the satellite orbit and start the API documentation for reserving the satellite communication frequency with the International Telecommunication Union (ITU).

I would also like to thank Mr. Rajesh Balaraman, for his continuous support in testing and designing the structure along with the computer simulated models. The models were crucial in deriving the final setup of the CubeSat.

# Contents

# List of Figures

# List of Tables

## Summary

Today's satellite technology although having major focus on CubeSat technology, is far from optimized in terms of power, weight, structure and overall performance. This Master's thesis aims to look at designing, developing and qualifying a 3D printed 1U CubeSat structure that can be successfully launched from the International Space Station (ISS).

Majority of the structure is designed in such a way that it can be 3D printed using the space qualified polymer ULTEM 9085, with minimal use of support material. It is also designed for easy assembly and disassembly. In addition, the structure is optimized and customized to meet the launcher requirements.

The ULTEM structure consists of 6 frames where the side faces have provisions for mounting the solar panels and the top surface has the provision for mounting the antenna. This report also discusses the various mission requirements and non-structural components for the CubeSat.

So far, two successful comprehensive design attempts are included and discussed. The testing is first done using ABAQUS to find some measure of the distortions and stresses that can be experienced by the CubeSat structure. The vibrational models show that the extent of displacements and stress is low.

Next, further testing carried out on real models utilised a rigid base mounted on two different vibration exciters of different sizes. The models are tested based on performance parameters provided by an established launch agency and analysed under a microscope to check for any cracks or major degradation. The ULTEM is also tested for outgassing properties to ensure it is acceptable for Space applications. The results show that the developed structures can survive the high stresses experienced during the launch phase, and display negligible outgassing.

For the Space operation segment, a payload is developed that can measure the temperature of the ULTEM panels and their response to every thermal cycle in Space. The electronic stack is also made up of GomSpace panels that can provide telemetry data and an antenna to transmit data from the payload to the Ground Station. They also manage power with the battery and solar panels.

The combination of the payload, electronic stack and tested hybrid CubeSat structure provide a complete mission in terms of operability and research data gained.

# 1.0 Introduction

The current advancements of 3D Printing have enabled an initiative by Nanyang Technological University (NTU) to explore utilising 3D printing as a method of fabricating a CubeSat structure. The conventional methods of fabricating the CubeSat structure involve using space qualified alloys of Aluminium e.g. Al-6061 and Computer Numeric Control (CNC) Machining. The conventional techniques do produce high strength and high reliability structures but have limited flexibility with regards to design and weight management. With 3D printing, various shapes and configurations are possible, especially if the use of support material is not constrained.

The drawback of using current 3D printing technologies is the time required to print structures, due to the extensive process of melting the base material to a suitable consistency before printing. The equipment needed, and expertise required to make the structures is also expensive. However, with ample amounts of research and development being placed into improving the speed, efficiency and ease of utilising the 3D printing technologies, the cost of using this method of fabrication should be driven downward as it becomes more accessible to all forms of construction.

The current challenge undertaken by this project is to develop a suitable CubeSat structure that can achieve the following,

1. Be fabricated with minimal support material to minimise the time required to print the structural components
2. Sustain the loads during launch, that might reach 5G and 20G shock loads.
3. Deploy cleanly from the launch pod on the ISS or specified launch platform
4. Be able to collect temperature readings from the inner surfaces of the CubeSat to check on the conduction and spread of heat through the CubeSat structure

Point 4 above is especially of interest as two (2) different materials will be utilised in the final assembly of the CubeSat – ULTEM 9085 and Aluminium alloy. The CubeSat will be allowed to tumble in orbit without ADCS and will be fitted with a turnstile type antenna to ensure communication with Earth is still possible regardless of the attitude of the spacecraft. Temperature readings are taken to ensure that the spacecraft is operating within its thermal limits, and extreme thermal stresses are not encountered by any onboard electronic components. All in all, the primary objective of this mission is to test the feasibility of a 3D printed nanosatellite for launch from Earth to orbit.

## 1.1 Unknowns and Objectives

As a guide to develop the CubeSat, to the required standards expected for operation in the harsh environments of space and launch, certain questions must be addressed. NTU is collaborating with an external agency, such as the Japan Aerospace Exploration Agency (JAXA) to launch this CubeSat, so their requirements are investigated. Also, the research should address issues that require analysis to produce a unique and new design and idea. The main research question is,

- What is an effective design for a 3D printed nanosatellite to operate in Low Earth Orbit (LEO)?

Along with this main research question, more sub-questions require addressing to effectively answer the main research question. The sub-questions are as follows,

- What are the design requirements of the CubeSat as stipulated by a launching agency such as JAXA?
- What is the design budget for the CubeSat?
- What are the most likely sources of failure for this CubeSat?
- What is the best power configuration for the CubeSat?
- What are the thermal considerations for the CubeSat, if any?

The final objectives of this project would be to ascertain the following,

1. Design and build a CubeSat structure that can survive the stresses of launch
2. Measure and analyse the temperature differentials of the Aluminium and ULTEM surfaces on the CubeSat structure, while it is in orbit.

## 1.2 Research Approach

To develop an effective 3D printed structure to address the main research question, certain standards or limits must be set and considered. The following considerations apply,

- The design must be lightweight and lighter than a full Aluminium alloy design of similar configuration
- The design should minimise the need for support material. Support material required within the base thickness of the component is allowable.

- The parts in contact with the rails of the pod should be made of Aluminium alloy, so they can be anodised to ensure they are smooth enough slide easily along the pod.
- Under stress, the Aluminium alloy rails should take the bulk of the stresses and not the main ULTEM body.
- The exterior dimensions and rail contact dimensions should follow the standards set by the JAXA design handbook. It may be noted that the requirements by the launchers do not change significantly from each other. If necessary, the satellite can be prepared for any other available launcher with minimal changes to the current design and configuration.
- The structure should be easy to assemble with the interior electronic stack.

To design the structure, the current well-established CubeSat designs that have proven their durability on space missions are studied and adapted to the 3D printing limitations. The model developed is then analysed for stress and displacement patterns using ABAQUS, which in an industry rated engineering tool. After reaching an agreement on the structural integrity of the structure using simulations, a real model is printed and filled with a dummy electronic stack and then placed on a vibration table with sensors to measure relevant data. The real model is taken through several vibration tests at various frequencies and forces (common during launch), to analyse its real response and structural integrity. Finally, the model is place in a pod and tested repeatedly under launch conditions to ensure it will not fail during launch and deploy without issues.

The next challenge would be to build up the electronics stack and test its functionality. GomSpace components are used which consist of a motherboard, a turnstile antenna, solar panels and a battery component. Also utilised are AD8495 chips and K-type thermo-couples to collect temperature readings at crucial parts of the CubeSat. The electronic components need to be connected and tested for proper functionality, and then programmed to operate in orbit under the limitations placed by the power budget and orbit parameters. The electronics is then stacked inside the CubeSat frame such that the centre of gravity of the whole structure is almost exactly in the middle, to prevent off-centre vibrations that can damage the whole structure severely.

## 1.3 Report Outline

This report consists of several chapters to detail the basics of satellite design and operations, as well highlight the process of design and innovations of our 3D printed CubeSat structure. Chapter 1 thus far has been to introduce the objectives and research methodology for this project. Chapter 2 will contain the literature review, to explain all aspects of CubeSat design and its uses, as well as describe the possibility and benefit of designing a 3D printable frame. Chapter 3 will list the requirements of

the CubeSat design and performance. Chapter 4 will delve into the CubeSat operations and the orbit definitions. Chapter 5 will look into the design and development of the CubeSat structure and its analysis. Chapter 6 will describe the setup of the payload and its components. Chapter 7 goes into the conclusion and possible future work that can be done.

# 2.0 Literature Review

## 2.1 Background

CubeSats are miniature satellites that are constructed to perform scientific experiments or explore new technologies while not expending too much overall expense. The major ways in which CubeSats reduce cost is through their minimal mass and their small size. The low mass of the CubeSat would mean that it would not take much rocket thrust to lift them, and the small size means the CubeSats can fit in excess gaps left over by large satellites in certain payloads. Their main purpose is to train amateur satellite builders or to carry out niche experiments on a small scale. The electronics in the CubeSats, being smaller, are more vulnerable to the effects of incoming radiation. Their small size also limits the size of their payloads and limits the size and complexity of the missions that can be carried out. Their low budget also means the CubeSats are not designed for a long mission span, and typically end their missions within a few years or even weeks.

## 2.2 History of CubeSats

The idea of the CubeSat was started in 1999 [1] by the need to educate students on the challenges of building a miniature satellite, and gain engineering skills from the experience. The first CubeSats were launched in 2003 from Russia, and their number has been increasing ever since. The standard specifications for a 1U CubeSat dictate external dimensions of 10 x 10 x 10 cm. Depending on the complexity of the mission and the payload required, more 1U CubeSat units may be stacked together to form 2U, 3U or even 6U CubeSats. There are several providers of CubeSat frames and electronics, which enable builders to assemble CubeSats and prepare for missions with off the shelf components. Various missions have been executed by CubeSats such as temperature measurement and weather analysis. As of mid-2018, more than 2000 CubeSats have been launched into Space, which presents an industry that could benefit from technological improvements.

## 2.3 CubeSat Structure

### 2.3.1 Conventional Developments

The basic make up of a CubeSat consists of the exterior frame, the interior mission-specific electronics and payload, the communication equipment and the solar panels. The exterior frame, for strength and deployment considerations, is usually made of Aluminium alloys. The frame needs to be

light to maximise the allowable weight for the payload, hence low density, high strength materials needs to be utilised to construct the frame. The most common materials being used today are Aluminium alloys. The alloys are specifically either AA-6061 or AA-7075, since these are high strength alloys and can also be surface treated to produce a very smooth surface. The surface is required to be smooth to allow for the effective deployment of the CubeSat from the pod along the pod's rails. Aluminium alloys also have low outgassing, unless they have high proportions of Zinc.

Most CubeSats perform missions pertaining to communications with Earth or between neighbouring satellites, or detecting weather related parameters. They also can collect atmospheric data such as detect lightning discharges. More advanced CubeSat developments allowed for implementation of high end sensors and innovative propulsion techniques to monitor and modify the attitude of the CubeSat.

### 2.3.2 Advanced Developments

Further CubeSat developments in terms of assembly and equipment designs enabled the adoption of more complex missions and more difficult objectives. There has been much advancement over the years starting from the basic missions mentioned in 2.3.1, and some examples are as follows,

**Table 2.1:** Recent CubeSat missions *[2]*

| **Mission Name** | **Launch Date** | **Mission Description** |
|---|---|---|
| MEMS 1A (Pico 21) | 27 January 2000 | Demonstrate low-power low earth orbit "Swarming" or satellite array |
| CP1 | 26 July 2006 | Testing of a sun sensor |
| KKS-1 (KISEKI) | 23 January 2009 | First demonstration of laser ignition thruster based micro propulsion system |
| LightSail-B | 1 December 2018 | Demonstrate deployment of a $32m^2$ solar sail from a 3U CubeSat layout |

Future advancements enable even more complex missions that require more precise equipment and intricacy in assembly and mission planning. Some of these missions consist of demonstrations of low cost and reliable propulsive systems that are simple to implement, miniaturised X-ray imaging telescope technology, demonstrations of mirrors for high contrast imaging and even monitoring of electric fields in Low Earth Orbit.

## 2.4 Non-structural CubeSat Components

Mission specific electronics may consist of a range of electronics, in the form of small devices or implanted on PCB panels and stacked within the frame. Examples of such electronics are cameras, on-board computer panels, signal data processing panels etc. There are several providers of space graded electronics, like Terma and GomSpace, that can provide either basic electronics such as battery units and processing units, or make electronic components customised for a purpose. All the components are able to operate in extreme temperatures, approximately between -40$^{O}$C to 85$^{O}$C. GomSpace provides the on-board computer panel designated the NanoMind A3200, and a signal data processing unit called the NanoCom AX100. Both components pictured below,

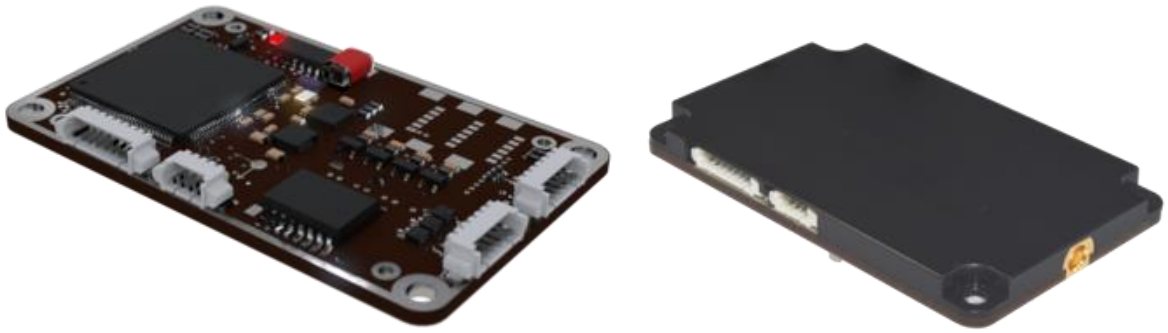

**Figure 2.1:** NanoMind A3200 (left) and NanoCom AX100 (right) *[3]*

The A3200 contains a 3-Axis magnetometer and coil drivers that are able to provide attitude control based on magnetic sensing and actuation [4]. It also has a 3-Axis gyroscope that can be used to implement attitude control. The A3200 interacts with the other subsystems via the CAN and $I^2C$ interface, and is able to store data on a 128 MB NOR serial flash. It also has 8 ADC inputs to interact with SPI devices. The A3200 can be mounted in a NanoDock DMC-3 motherboard along with another daughterboard beside it, to provide its functionality concurrently with the second daughterboard. Finally, the operational temperature of the A3200 is between -30$^{O}$C and 85$^{O}$C.
The NanoCom AX100 is a half-duplex radio transceiver that can handle long range transmissions. It also has multiple interfaces to communicate with the other satellite subcomponents via the $I^2C$, UART, CAN-Bus routes. It is able to handle data rates from 0.1kbps to 115.2kbps. Its operational temperature range is similar to the A3200.

The A3200 and the AX100 would normally form the backbone of the CubeSat operations throughout its lifetime.

GomSpace also provides Solar panels to be fitted on the exterior of a CubeSat. Each Solar panel consists of two solar cells that each have an area of about 30 $cm^2$, with 30% efficiency and able to produce up to 2.3W in Low Earth Orbit. The GomSpace solar panels come in 10 standard configurations. [5] The solar panels are connected to the battery unit to charge the batteries when they are exposed to solar radiation.

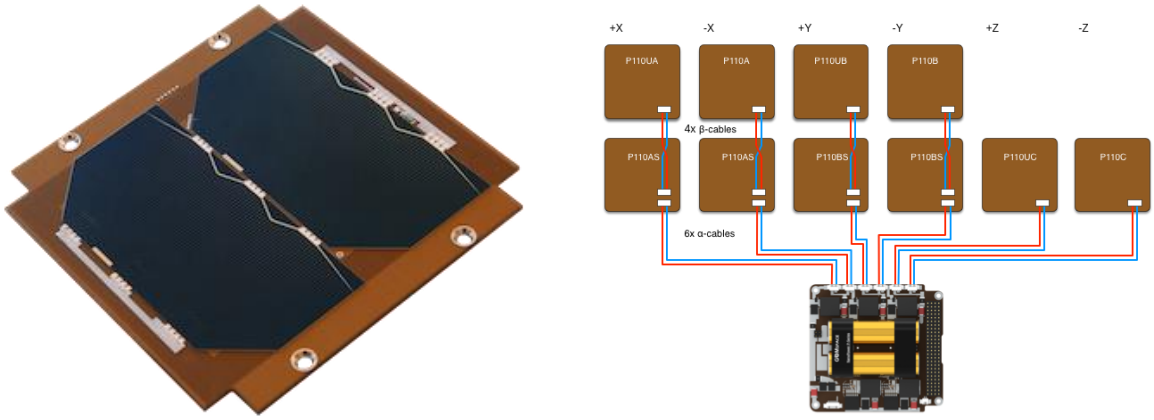


**Figure 2.2:** Solar Panel (left) and Solar Panel setup with P31u battery unit (right) *[6]*

To carry out communications with the ground station, the antenna utilised is essential for its range of transmission and suitable radiation pattern. The radiation pattern is a description of the angular dependence of the strength of the radio waves from the antenna. There are several types of patterns dependent on type of antenna. The simplest antennas are the *monopole* and *dipole* antennas, which have an axially symmetric arrangement. This produces an omnidirectional pattern. An omnidirectional pattern would be suitable for amateur satellites that might not have an effective attitude determination and control system (ADCS), which means it would "tumble" continuously through its orbit. This means it would not have control over its attitude or orientation at any time, including the periods when it is within transmission range of the ground station. An omnidirectional pattern would ensure communication happens regardless of the CubeSat attitude, as long as within a suitably limited range.

In a regular radiation pattern, the radiation from various parts of the antenna interferes at some angles, creating points of out-of-phase interaction which forms "nulls" and points of in-phase interactions which creates "nodes".

Another type of antenna is the *directive* antenna, which directs the radio waves in a primary direction. On the radiation pattern, this shows as a single lobe that is much larger than the other lobes which is called the “main lobe”. If a satellite is fitted with a directional antenna, the operational complexity increases because of the need to implement ADCS. The ADCS will be required to ensure the CubeSat points in a direction suitable to direct the main lobe to connect with the ground station.

GomSpace provides the NanoCom ANT430 omnidirectional canted turnstile antenna, which has a gain range of 1.5 dBi and -1 dBi. The antenna is circular polarised with a frequency range that can be any assigned value between 430 to 440 MHz. The highest gain is along the Z-axis and lower gains are along X- and Y-axes.

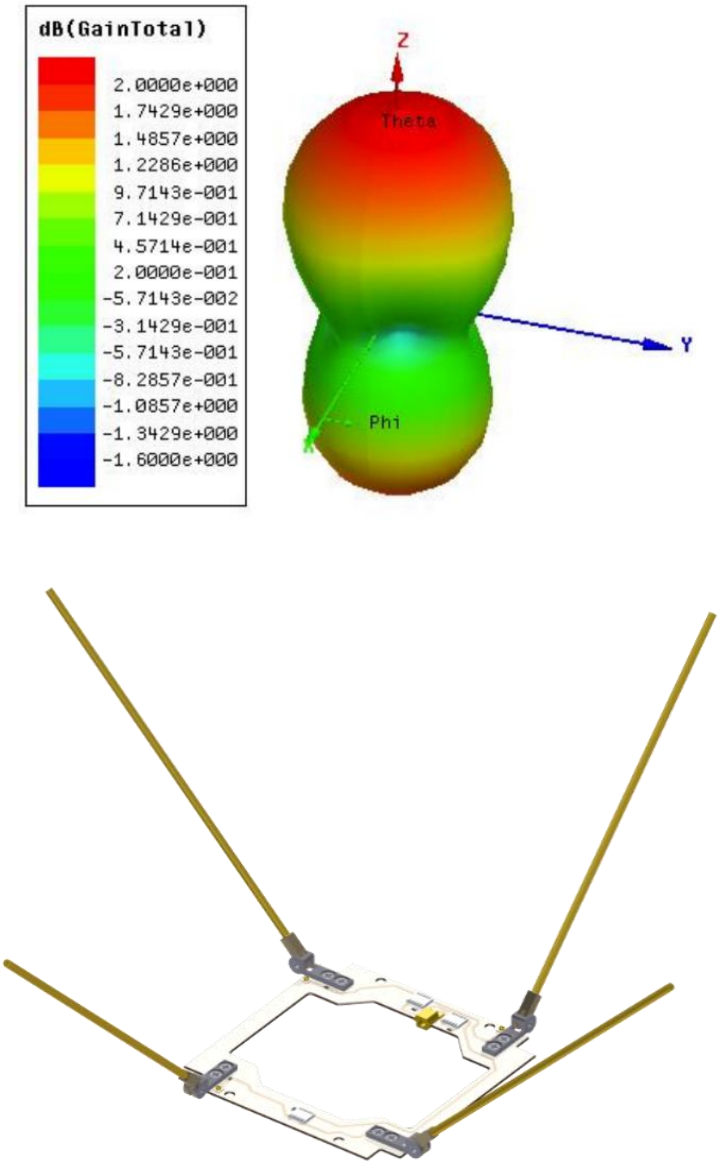


**Figure 2.3:** NanoCom ANT430 radiation pattern (1U setup) *[7]*

The antenna elements are fixed to spring hinges, which allow it to rotate around and align flush with the exterior faces of the CubeSat. The antenna ends can then be tied to the NanoUtil panel with thermal wire. When the CubeSat is released from the pod, the thermal wires will be burned after a pre-set time to release the antenna that were held down. The communication capability of the CubeSat is activated with the antenna release. The requirement to initially hold down the antenna against the satellite faces is to allow the CubeSat to fit inside the launch pod within the limitations set by the launcher.

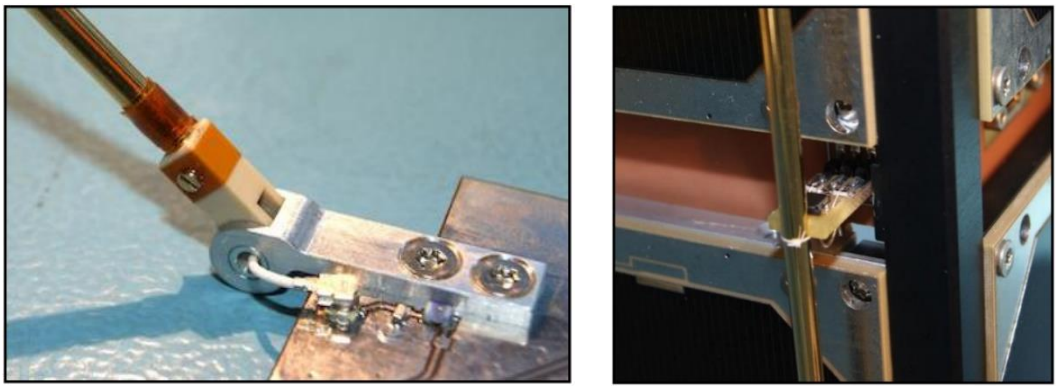

**Figure 2.4:** Antenna spring hinges (left) and thermal wire tie setup (right)


**Figure 2.5:** NanoUtil Top Panel to hold antenna down

The CubeSat for this project and mission will not require the CubeSat to have ADCS, as the satellite surface temperature measurements to take do not require attitude control. Satellites that have ADCS do not normally have it just to accommodate the characteristics of the antenna, but also to align the

satellite in a single direction to fulfil more objectives of the mission. For example, a mission requiring the satellite to collect photos and readings from the sun would require ADCS to ensure the camera and sensing equipment is constantly pointing towards the sun whenever it can.

The lack of an ADCS means the CubeSat will tumble, so the GomSpace ANT430 is a good choice for an antenna due to its omnidirectional property that can accommodate transmissions for a satellite with no attitude control. The CubeSat will also be in Low Earth Orbit and well within the transmission range of the ANT430.

Finally, the CubeSat requires a power source, which comes in the form of batteries that are cyclically charged by the previously mentioned solar panels. Depending on the mission size and power requirements set by the mission objectives, the number of batteries and solar panels is assigned which will also set the size of the CubeSat (1U, 2U, 3U etc.). The CubeSat in this report is a 1U satellite, placing limitations on the mission complexity. Therefore, this project will only be collecting temperature readings from the CubeSat surfaces (to be explained in Chapter 0). To carry out this basic mission, the smallest configuration of the GomSpace power unit can be considered. The NanoPower P31U unit provides up to 30W of power [6], although the CubeSat designed for this mission would require less. The P31U has three photo-voltaic input channels, which can connect to a pair of solar panels each connected in parallel to each other (Input channels are P1 – P6 in Figure ***2.6***).

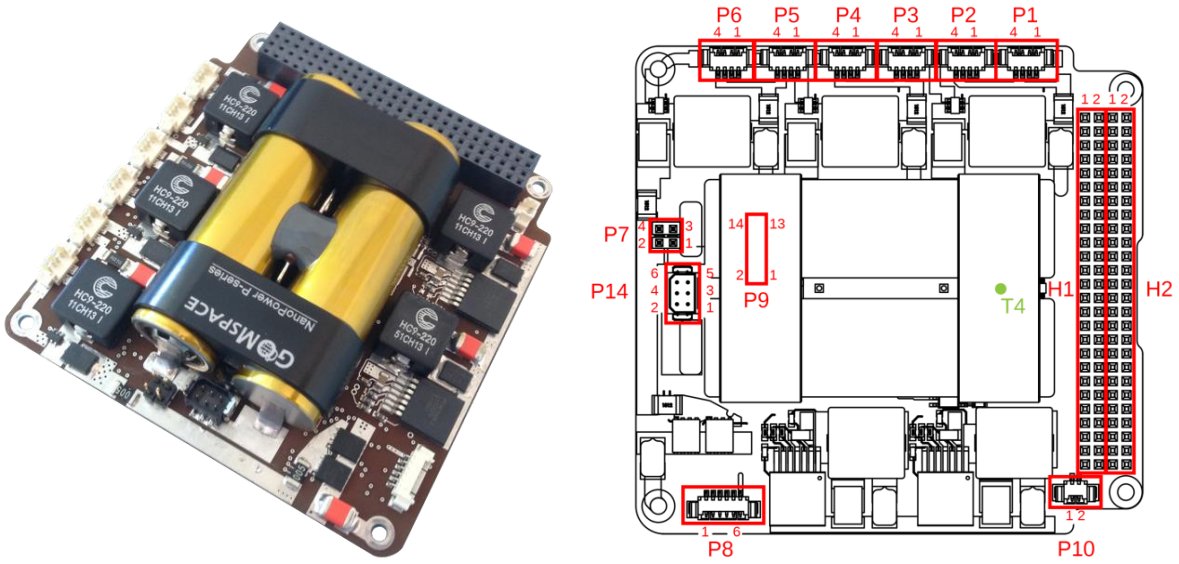


**Figure 2.6:** NanoPower P31U (left) and pin layout (right) *[6]*

The basic satellite non-structural components that make up most regular CubeSats have been detailed above. These components enable the most basic but most important tasks of any satellite mission –

communication and power provision. More components would be required to complete the higher objectives of the mission eg. AD8495 chips and K-type thermocouples used to sense and collect temperature data from the CubeSat surfaces.

## 2.5 Launching of CubeSats

### 2.5.1 Launching from Deployment Pod

The CubeSat is designed as per the launcher requirements, to fit neatly into the launching pod for smooth deployment. Before launching the CubeSat, all electronic and actuation components on the CubeSat are disabled and held inactive until deployment in space. To ensure the components are held inactive, a mechanism is introduced which is a deployment switch or "kill switch" positioned on one or more legs of the CubeSat. During and before launch, the deployment switch is pressed down by the other CubeSat(s) stacked above the current CubeSat and in turn presses down on a microswitch trigger arm. Pressing down on the microswitch trigger ensures the power unit of the CubeSat is held inactive, and the on-board computer is also not operational with the non-functional power unit.

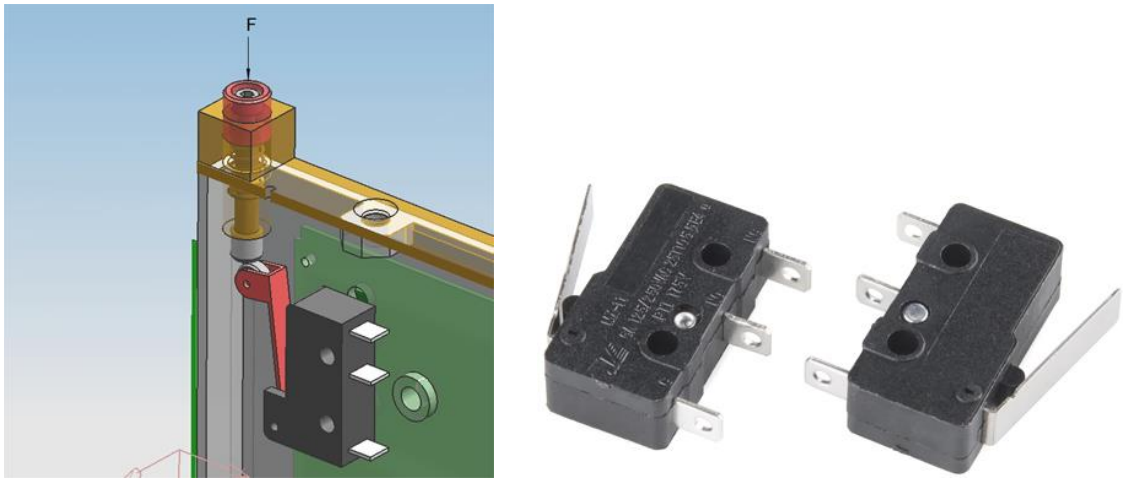


**Figure 2.7:** Deployment Switch mechanism example (left) *[8]* and CubeSat micro-switches *[9]*

The CubeSat will be sent to the ISS and placed in a deployer pod and might be fitted on a multiple deployment platform that can hold and activate several deployer pods together. For example, JAXA provides its own deployer called the JEM Small Satellite Orbital Deployer (J-SSOD). The following steps for launch and deployment of any CubeSat with JAXA are usually carried out,

1. Satellite Install Cases with CubeSats installed are launched and carried to the ISS

2. In the Kibo module on the ISS, the Satellite Install Cases are fitted on the Multi-Purpose Experiment Platform (MPEP). The MPEP is then installed on the airlock slide table to be transferred outboard.
3. The J-SSOD/MPEP setup is then picked by Kibo's Japanese Experiment Module Remote Manipulator System (JEMRMS) and transferred outboard to the CubeSat releasing point.
4. The spring on the Satellite Install Case is activated and launches the CubeSats out of the pod in the direction nadir-aft $45^{O}$ (MPEP points in this direction), opposite to the ISS travel direction.

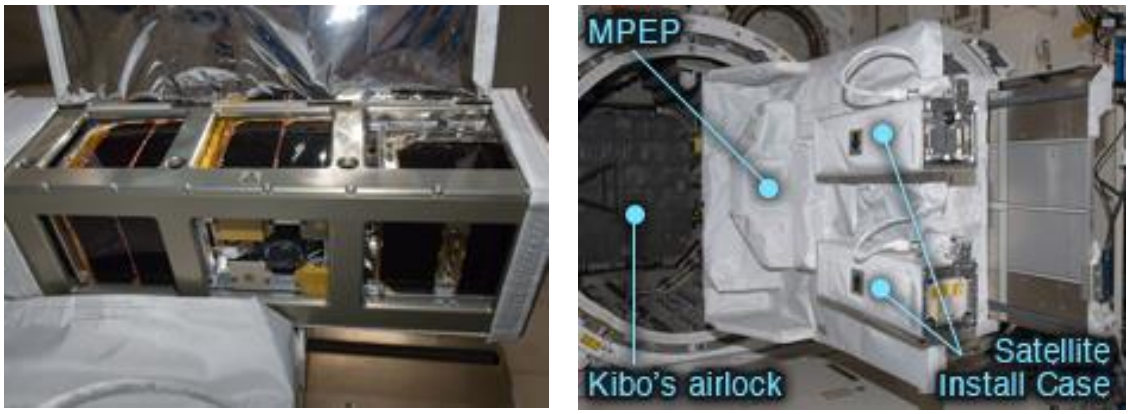


**Figure 2.8:** Satellite Install Case (left) and MPEP system with J-SSODs (right) *[10]*

**Figure 2.9:** CubeSats deployed from J-SSOD/MPEP *[10]*

The following specifications apply for usage and performance of the J-SSOD,

**Table 2.2:** J-SSOD Specifications *[11]*

| **Item** | **Specification** |
|---|---|
| Installable satellite size | CubeSat size 1U, 2U, 3U or 6U* |
| Installable satellite mass | 1.33 kg or less per 1U, 6U size satellite is 14 kg or less |

| Item | Specification |
|---|---|
| Insertion orbit | Elliptical orbit with altitude of 380 km - 420 km (depends on ISS altitude)<br>Inclination: 51.6° |
| Ballistic coefficient | 120kg/$m^2$ or less (to make satellites decayed faster than ISS orbit) |
| Insertion direction | Nadir-aft 45° from the ISS nadir side, in terms of ISS body coordinate system<br>(to avoid collision with the ISS) |
| Insertion velocity | 1.1 - 1.7 m/sec |
| Life expectancy on orbit | about a year (depends on ballistic coefficient, released altitude, solar activity, etc.) |

The success of this deployment system has been exemplified by JAXA and its Kibo module. The first CubeSats using the J-SSOD were deployed into orbit in October 2012, which consisted of three Japanese satellites and two U.S. satellites. The next deployment consisting of four satellites (three U.S. and one Vietnamese satellites) was carried out in November 2013. Between February and March 2014, 33 CubeSats were deployed using the NanoRacks made deployer from Kibo.

### 2.5.2 Launching from Polar Satellite Launch Vehicle (PSLV)

The Indian Space Research Organisation (ISRO) launched their satellites via the PSLV, which is a third generation launch vehicle for India. From 1994 to 2017, the PSLV has completed 39 consecutively successful launches, and has deployed almost 260 satellites from India and customers from abroad. The ISRO PSLV also launched the Chandrayaan-1 in 2008 and the Mars Orbiter Spacecraft in 2013 that travelled to the Moon and Mars respectively. [12]

The PSLV specifications are as follows –
Height: 44 m
Diameter: 2.8 m
Number of Stages: 4
Lift Off Mass: 320 tonnes (XL)
Variants: 3 (PSLV-G, PSLV - CA, PSLV - XL)
First Flight: September 20, 1993


**Payload Fairing -** Can place multiple payloads into orbit, thus multi-payload adaptors are used in the payload fairing.

**PS4 -** Fourth and final stage of PSLV and it uses two liquid engines for propulsion. PS4 is responsible for the correct injection of PSLV's payloads into their respective desired orbits.

**PS3 -** Third and penultimate stage of PSLV, and it uses a solid rocket for propulsion.

**PS2 -** Second stage of PSLV and is powered by the Vikas liquid engine, developed in the early 90s.

**PS1 -** First stage of PSLV and provides the launcher the high thrust that is required for lift off. It uses the S139 solid rocket booster that contains 138 tonnes of HTPB

**Strap on Boosters -** While the PSLV-G uses 6 HTPB based solid strap-on motors of 9 tonnes each and PSLV-XL uses 6 extended strap-ons of 12 tonnes each, the PSLV-CA (core alone version) does not use any strap-on motors.

**Figure 2.10:** PSLV Stages Specifications

The PSLV utilised its several stages to reach the desired altitude, before the fairing sequentially injects the satellites into orbit at the desired inclinations.

## 2.6 3D Printing Technology

The realm of mission specific electronics having been delved into, a case can be made to adapt the structure of the CubeSat to keep up with current fabrication trends. The up and coming industry rated fabrication technique is 3D printing. 3D printing enables us to create any shape possible, with the addition of support material where required.

There are currently ten types of 3D printing techniques available [13] –

- Fused Deposition Modelling (FDM)
- Stereolithography (SLA)
- Digital Light Processing (DLP)
- Selective Laser Sintering (SLS)
- Material Jetting (MJ)
- Drop on Demand (DOD)
- Binder Jetting (BJ)
- Direct Metal Laser Sintering (DMLS)
- Selective Laser Melting (SLM)
- Electron Beam Melting (EBM)

### 2.6.1 Printing of Satellite Structure

The most common method of printing that is utilised as well is FDM. Figure 2.11 shows one setup of a 3D printing device that utilises the FDM technique. In this setup, there is a platform in a heated chamber that acts as a base for the printed structure that is built with micro-thin layers of the required material. The base material is passed through a hot nozzle, melted and selectively deposited on the platform to build up the model.

The support material can be seen in the figure as well, where the slanted sections of the structure cannot be printed without printing supports first to prevent a collapse of the part due to gravity. Printing the supports adds time to the completion of the structure, which can be an issue when trying to adapt the fabrication of the part to mass production.

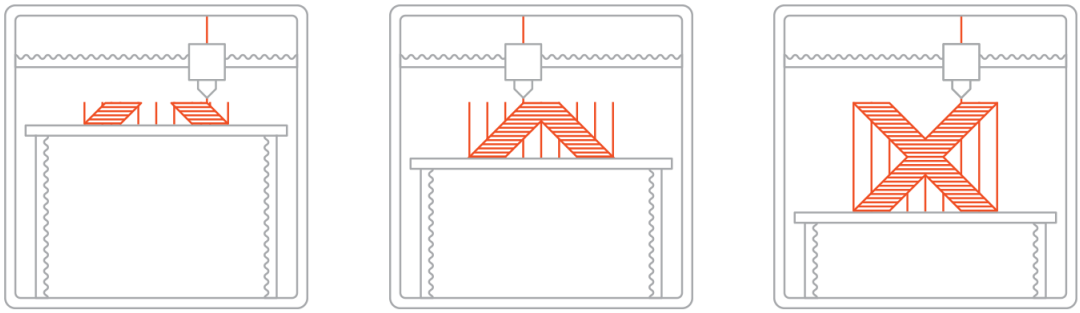

**Figure 2.11:** General representation of a 3D printing device [13]

The downside of 3D printing is that it takes a long time to finish up a model, since the base material needs to be melted first and then set into the structure at high resolution. However, heavy investments are being placed into further research and development of this technique, and there is a high possibility the productivity and speed of 3D printing will increase tremendously over the next decade.

Past attempts have been made to utilise 3D printing as a tool to fabricate CubeSat structures and launch them into space. A high-level composite known as Windform XT 2.0 was utilised to develop the CubeSat frame of Printsat and launched in 2015 but lost in the failure of the launch platform [14]. Another organisation known as "Made In Space" is exploring 3D printing structures in space using ULTEM 9085 as the base material, which opens up new possibilities of constructing complex structures in Space and avoiding the extreme forces experienced of launching the structure from Earth to Space [15]. In both these cases, either cost or complexity is high.

### 2.6.2 Suitable Materials

ULTEM 9085

ULTEM 9085 is a flame-retardant high-performance thermoplastic that is ideal for 3D printing requirements and fast prototyping. The material also has a high strength-to-weight ratio and has a solid FST (flame, smoke and toxicity) rating. Engineers and designers can utilise ULTEM 9085 to produce complex, functional parts for advanced prototypes without the need to turn to conventional tooling that have their own limitations.

The basic properties of ULTEM 9085 are as follows [16],
Tensile Modulus: 2.15 GPa
Outgassing, Total Mass Loss (TML): ASTM E595 / 0.41% (1.00% maximum)
Specific Gravity: 1.34
Poisson Ratio: 0.41

Aluminium Alloy 6061 or 7075

Aluminium alloy 6061 is a precipitation hardened Aluminium alloy. Silicon and Magnesium are the major alloying components in Al-6061. Al-6061 is a high strength alloy that is for general purpose use but has been accepted as a space grade quality material.

The basic properties of Aluminium alloy 6061 are as follows,
Tensile Modulus: 68 GPa
Specific Gravity: 2.70
Poisson Ratio: 0.33

### 2.6.3 CubeSat Orbit

There are two types of satellite orbits for any operational satellite – circular and elliptical. The satellite can orbit either in the same direction as the rotation of the earth (posigrade) or in the opposite direction (retrograde). The following parameters also define the orbit of a satellite and its positional properties –

- Orbital nodes: Points where the ground track moves between hemispheres
    - Ascending node: Ground track moves from southern to northern hemisphere
    - Descending node: Ground track moves from northern to southern hemisphere
- Longitude of ascending node (Ω): Angle of ascending node from a reference direction. For a geocentric orbit, the reference plan is Earth's equatorial plane, and the First Point of Aries as the origin of longitude. The longitude of ascending node is called the right ascension of the ascending node (RAAN).
- Radius of orbit, or altitude of satellite from the surface of the earth
- Angle of elevation: Angle at which the satellite appears above the horizon. The angle places limitations on the correspondence with the ground station as the signals from the satellite might be blocked by nearby objects that are much taller than said ground station. This problem would exist in Singapore where there are many high-rise buildings.
- Angle of inclination: Angle of orbit relative to the equatorial plane.
- Apogee: The point where the satellite is farthest from the earth. Relevant for elliptical orbits. For satellites in an elliptical orbit, it is usually planned for the satellite to be at apogee when over the ground station, so it can remain in correspondence with the ground station for the

longest period possible. This is because at apogee and near it the velocities of the satellite are at a minimum for the most period of time.

- Perigee: The point where the satellite is nearest to the earth. Relevant for elliptical orbits.
- Mean anomaly: Angle that defines the position of the satellite in the orbit.

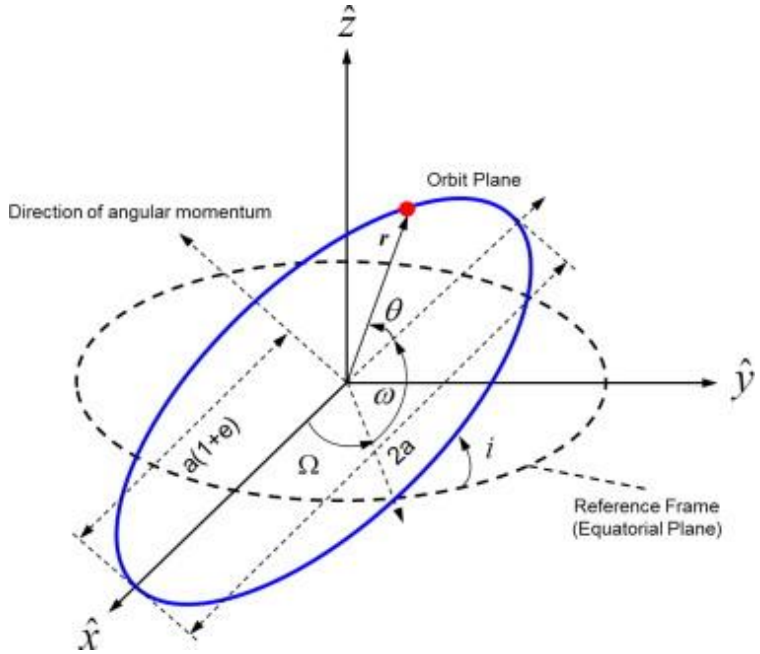


**Figure 2.12:** Orbital elements *[17]*

For circular orbits, they are defined mainly by their radius of orbit,

**Table 2.3:** Circular orbit definitions

| **Orbit Name** | **Orbit Altitude (km above earth surface)** | **Comments** |
|---|---|---|
| Low Earth Orbit (LEO) | 200 – 1,200 | -- |
| Medium Earth Orbit (MEO) | 1,200 – 35,790 | -- |
| Geosynchronous Orbit | 35,790 | One orbit per day, either posigrade or retrograde. Might not be stationary |
| Geostationary Orbit (GEO) | 35,790 | One orbit per day, posigrade. Always stationary. |
| High Earth Orbit (HEO) | > 35,790 | -- |

## 2.7 Concluding Remarks

A CubeSat frame was designed with a hybrid composition of two materials: Aluminium and ULTEM. ULTEM is one of the more affordable materials to 3D print, but with higher strength characteristics than ABS. ULTEM 9085 specifically is a high performance FDM thermoplastic, and therefore the 3D printed parts required were completed with FDM. In FDM, the material is guided through a hot nozzle which melts the material. The melted material is then deposited on a platform along a predetermined path, to gradually build up the structure

The possibility of creating a design that is affordable to develop, uses minimal support material to expedite the fabrication process, and stays well within the requirements placed by the launcher without excessive modifications required was explored. Furthermore, the use of ULTEM that has not been used together on a CubeSat that is to be launched from Earth, and temperature readings of the ULTEM components can be measured while the CubeSat is in orbit. This will first confirm the feasibility of ULTEM as a suitable material for to fabricate a “To Launch” CubeSat and give us an indication of the thermal interaction between Aluminium and ULTEM over a long period in the extreme environment of Space. The successful launch of the first design can pave the way for future improvements in terms of performance, weight saving and fine-tuning of the interior components are specialised for the design. Also, with advancements in 3D printing technologies, more “support material free” design improvements can be made.

# 3.0 Current CubeSat Requirements

The design on the satellite is based upon the underlying mission which decide the material composition, its functions, the testing and verification process and the configurations. The requirements derived were based on the mission requirements and the data that needed to be collected effectively. To ensure all aspects of the mission and its requirements are met, the requirements have to mapped based on the systems engineering approach. [18]

## 3.1 Requirements Discovery Tree

A Requirements Discovery Tree (RDT) will be created to consider all the engineering aspects of the mission, without considering the requirements tabulated in Appendix D. The tree building process begins with the mission statement –

*"The mission shall demonstrate the feasibility and suitability of a 3D printed CubeSat structure in the extreme environment of space and launch"*

Considering that the positive result of the mission is the ability of the CubeSat to stay intact throughout the launch and orbit lifetime, a simple indicator is required to understand the condition of the CubeSat. That indicator can be the interior temperature of the CubeSat on its interior surfaces. The mission statement consists of three mission objectives:

- Design and construct a 3D printed structure with minimal support material and cost
- Measure the temperature of each one of the six interior surfaces of the CubeSat
- Demonstrate the satellite can handle the vibrational loads of launch

## 3.2 Requirements Description

This section shall provide an overview of the reasoning behind the requirements in the requirements tree.

### 3.2.1 Payload Support Requirements

Tree A-1 consists of three requirements to explain the payload of the CubeSat. The data that is obtained from the payload had to collected or accumulated first. The CubeSat shall store temperature

data from the temperature sensing which would allow analysis of the temperature variations along the orbit after the data is transmitted to the ground station.

The data needs to be transmitted to the ground station for analysis. It will communicate with the ground station at a rate of 9.6kbps, to allow for efficient sending of the temperature data collected throughout the last orbit.

The payload needs to be operated with power as well. The very low power required by the components involved (<1W) can afford to include the continuous operation of the payload along all phases of orbit. The design of the electronics and CubeSat structure will maintain it at operation temperatures not below -40 $^{O}$C and not higher than 70$^{O}$C. The derived temperature ranges are based on payload specifications.

## 3.3 Satellite Bus Operations

The satellite bus requirements are defined in Table A-2. The GomSpace battery has a maximum capacity of 38.5 Wh, and the mission design will ensure operation of the CubeSat will continue as long as the battery voltage exceeds 12.8V. Considering the minimum scale of the mission operation this scenario is unlikely. There are also power input of 3.3V and 5V on the electronic stack to power the various sub-components. The components are also equipped with protection from overcurrent.

Next, the considerations have to be made for sending of the payload data to the ground station, and also receiving of commands and downlinking of telemetry. The antenna and transmitter will work together to transmit data at 437.5 MHz, and be able to send data from the payload as well as basic information such as telemetry and systems' health. There should be provision to store data where required prior to transmission. There should be a 2x64 MB flash memory for storage of science and housekeeping data.

When the CubeSat is in eclipse, or when communication is not possible, the CubeSat should be able to function autonomously. It should be able to continue collecting data from the payload and transmit if required, if the battery capacity is sufficient to prevent a systems breakdown and allow for another orbit to charge the batteries.

The various components in the electronic stack are connected firmly and the wires are not interlinked or coiled strongly at any point to prevent shorting. Standard PC104 connectors are used to stack the PCB panels to allow the unit to perform as one.

## 3.4 Technical Constraints

The Tree B-1 is a collection of technical constraints. For a start, the CubeSat needs to comply with the launcher regulations. This means it has to pass the standards placed on strength, durability and frequency resonance. The CubeSat may experience vibrations as strong as 30G during launch and should survive such conditions without significant damage. The main body of the CubeSat will remain within a (10 x 10 x 10) cm and allow for further extensions if required based on the launch mechanism and setup.

The CubeSat will also be equipped with a suitable power switch mechanism, preferably a trigger switch, to power up the electronics on board the CubeSat only after it has deployed safely from the launcher. Most launchers require at least two trigger mechanisms in case one of them should fail. Based on the mission objective and the extent of data required, the CubeSat is designed for a lifespan of 1 year. The materials placed on board the CubeSat also must not have outgassing limits exceeding 1%, or excessive release of volatile mass, to ensure material does not settle on the sensitive electronic components during Space operation.

The launch phase is a very small fraction of the entire satellite lifespan. The remainder of its lifetime will be used to test the reliability of the structure with vast temperature variations, and also to collect temperature data from the relevant satellite surfaces.

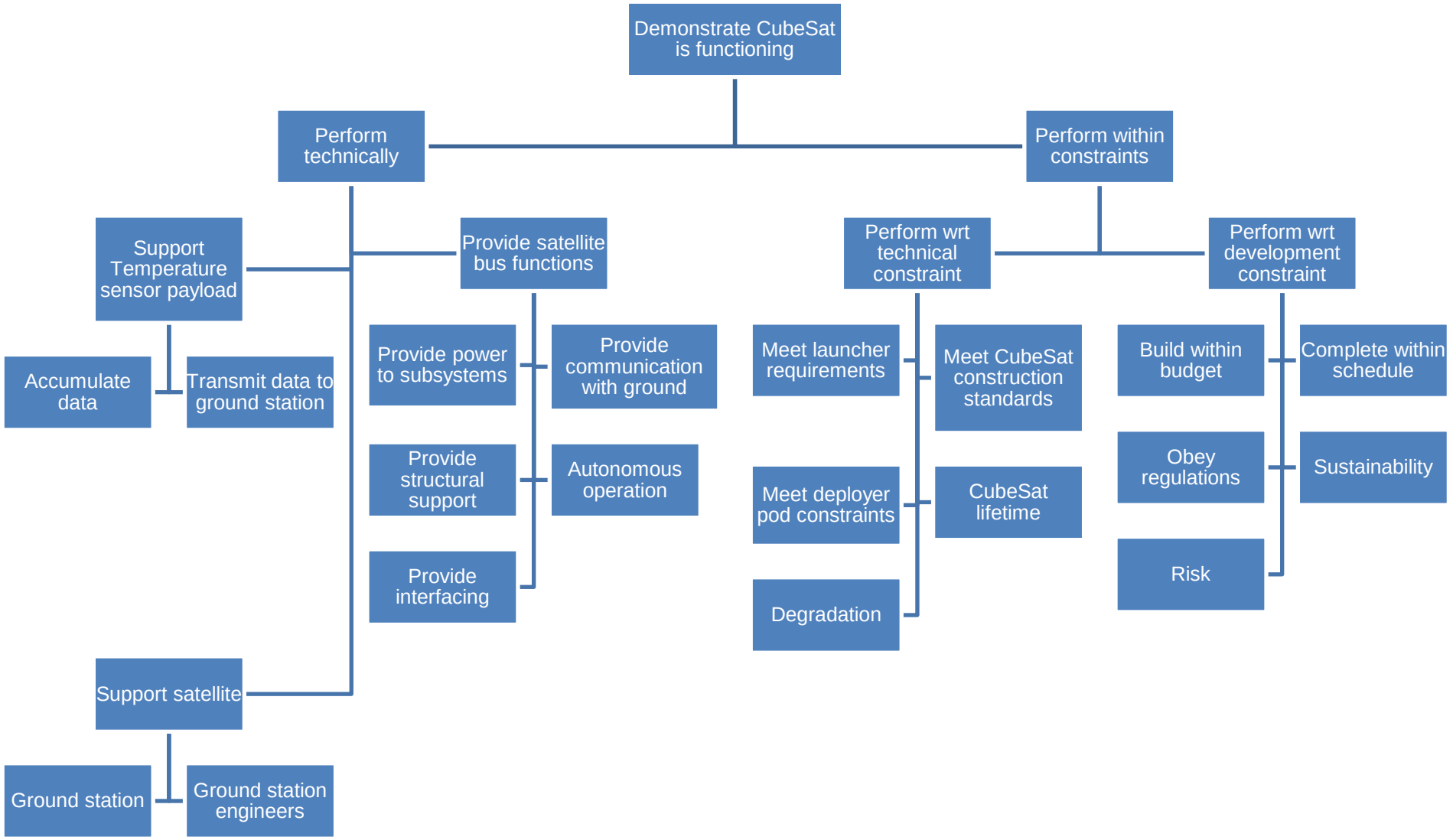


**Figure 3.1:** CubeSat Requirements Discovery Tree, A-1

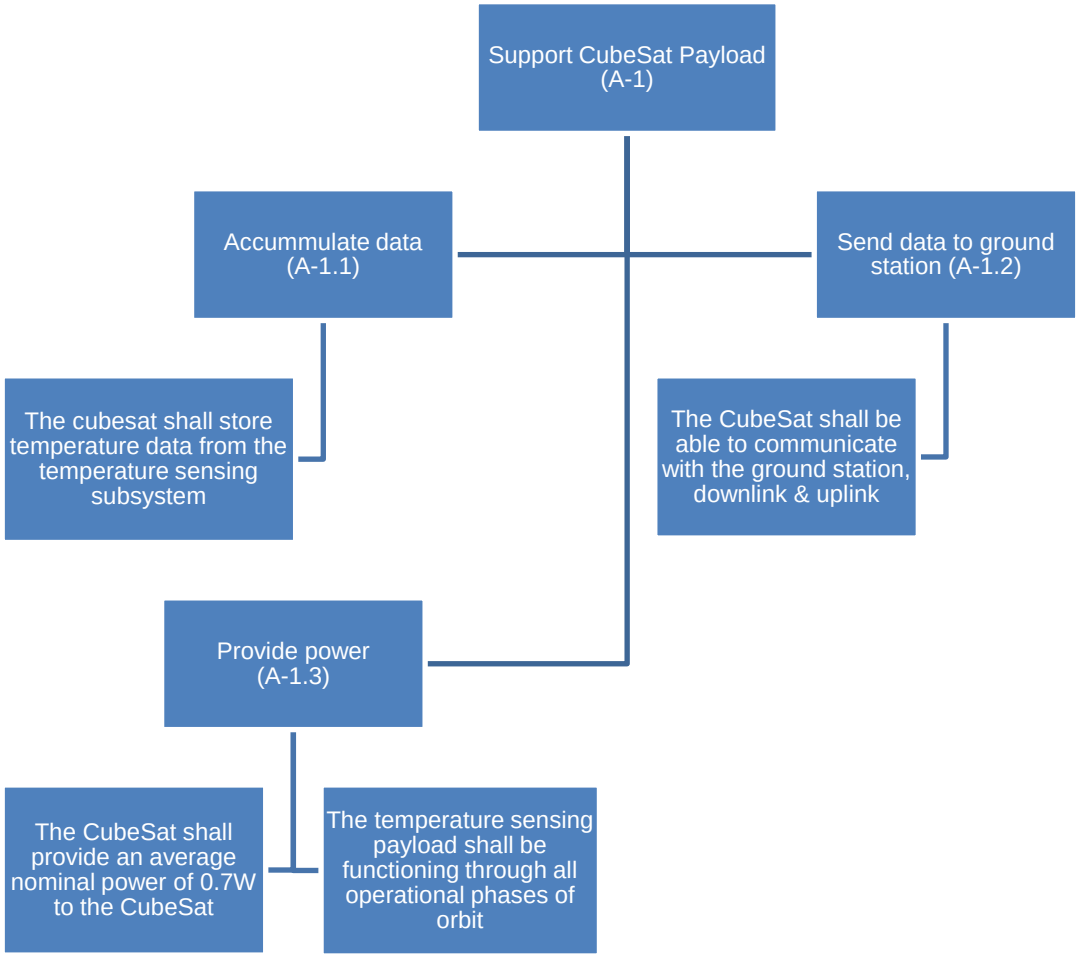


**Figure 3.2:** CubeSat Requirements Discovery Tree, A-2

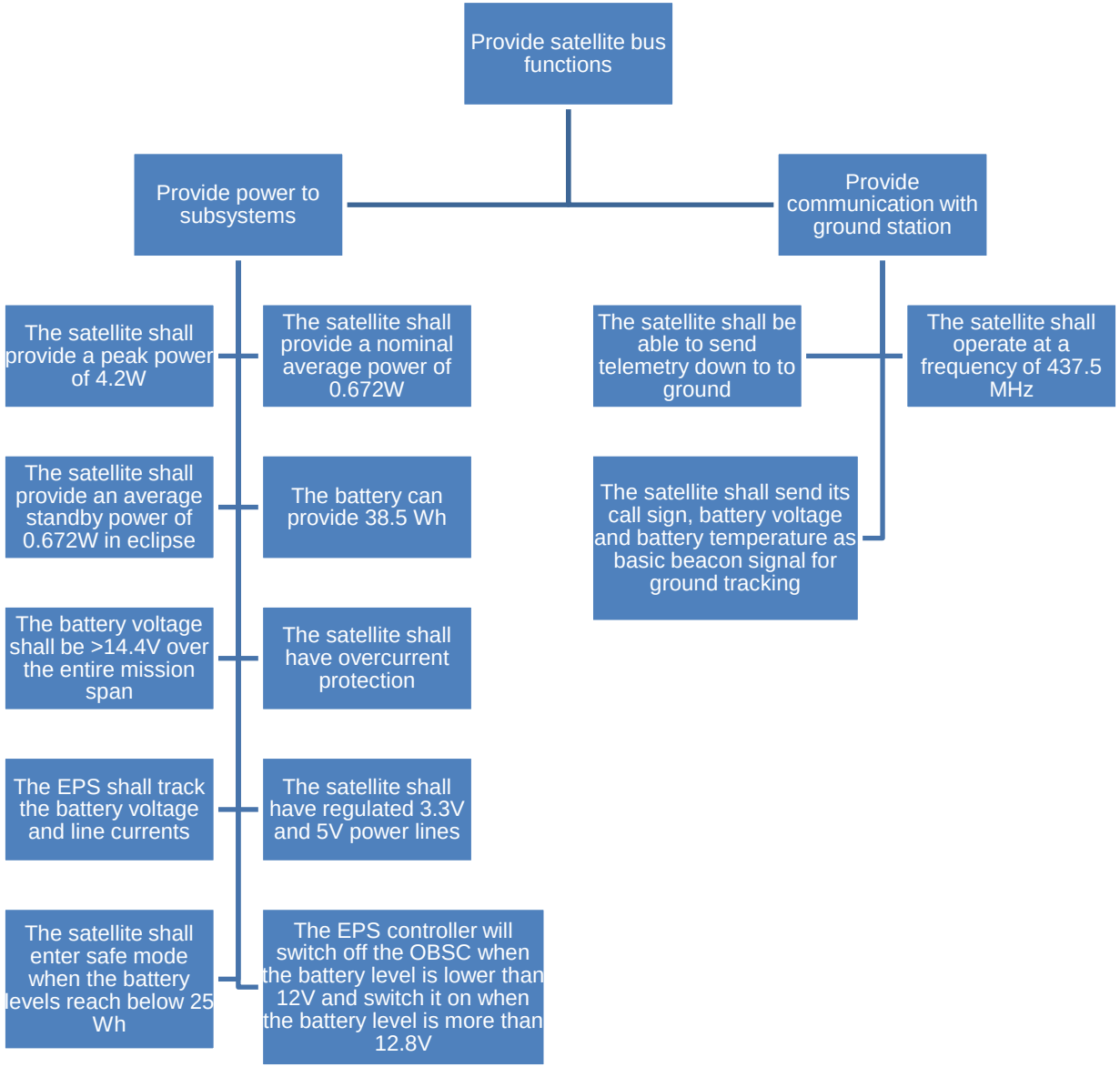


**Figure 3.3:** CubeSat Requirements Discovery Tree, A-3

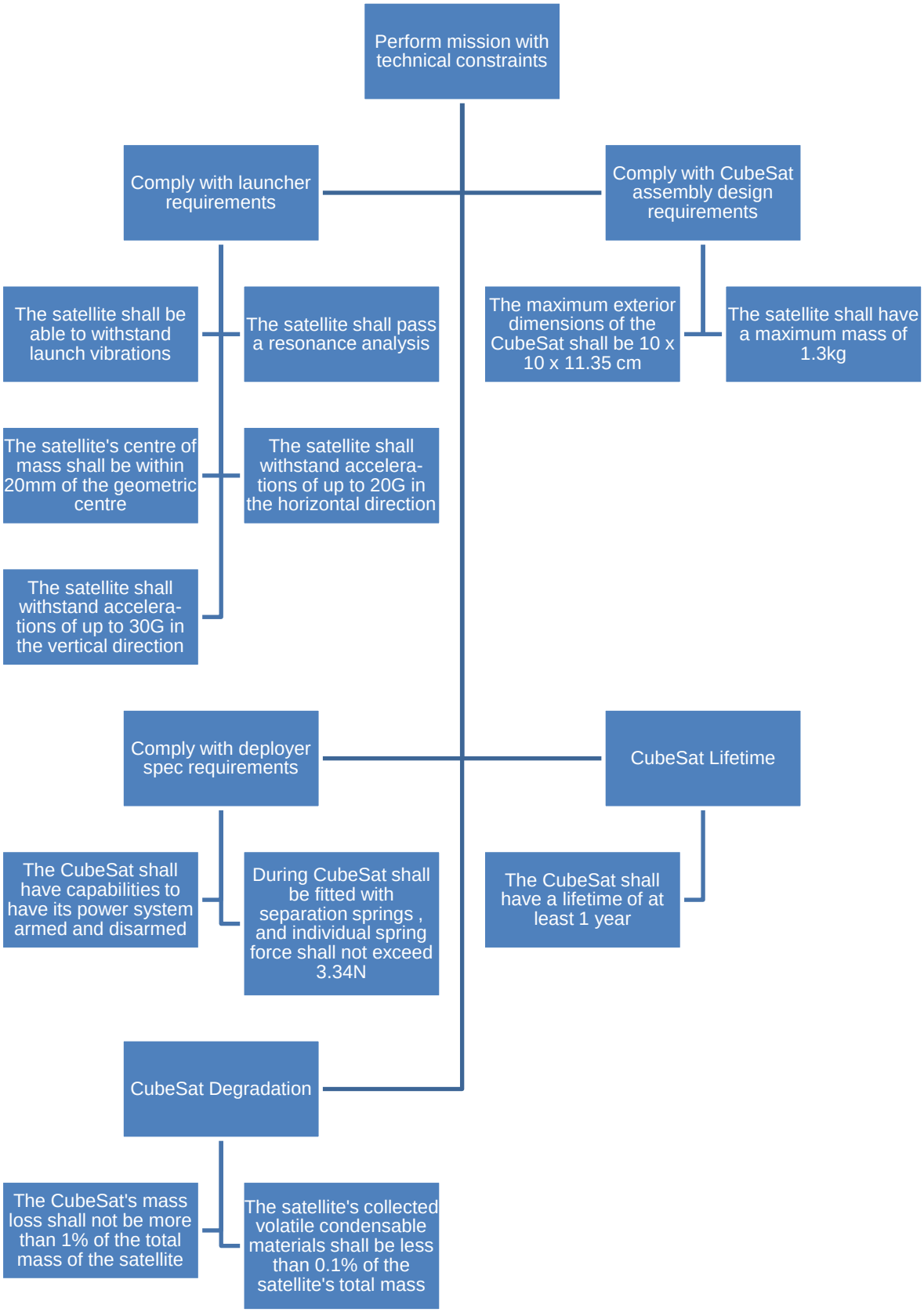


**Figure 3.4:** CubeSat Requirements Discovery Tree, A-4

# 4.0 CubeSat Development

The CubeSat being developed will be the first 3D printed nanosatellite developed by a Singaporean institute and launched into Space. This section shall describe the process of developing the final structural design, the challenges involved and the tentative layout of the onboard electronics and communications. This section will also mention the current parameters selected and their implications on the satellite operations.

## 4.1 Mission Specifications

### 4.1.1 CubeSat Orbit

In a JAXA orbit (as a reference) where the CubeSat will be launched from the ISS, the CubeSat will orbit at an altitude of 400km (Earth's radius is 6,378km), with an inclination of 51.6 degrees. The table below summarises the orbit parameters for this CubeSat,

**Table 4.1:** CubeSat Orbit Parameters (JAXA launch)

| | | |
|---|---|---|
| Height of Apogee (ha): | 400.0 | km |
| Height of Perigee (hp): | 400.0 | km |
| Semi-Major Axis (a): | 6,778.1 | km |
| Eccentricity (e): | 0.000000 | |
| Inclination (I): | 51.60 | ° |
| Argument of Perigee ($\omega$): | 180.0 | ° |
| R.A.A.N. ($\Omega$): | 7.13 | ° |
| Mean Anomaly (M): | 0.00 | ° |
| Period: | 92.561 | minutes |
| dw/dt: | 3.7397 | deg./day |
| dW/dt: | -5.0002 | deg./day |
| Mean Orbit Altitude: | 400.00 | km |
| Mean Orbit Radius: | 6,778.14 | km |
| Sun Synchronous Inclination: | 97.03 | ° |
| Elevation Angle (d): | 0.0 | ° |
| Slant Range (S): | 2,294.0 | km. |

The ideal scenario for the CubeSat is to have a perfectly circular orbit to have equal amounts of sunlight where the satellite is in daylight at any point in time. The orbit inclination and altitude should give us eclipse periods that are between 30 – 40% of the orbit duration [18]. Based on the orbit period, the eclipse period might be between 27 and 37 minutes. This would play a role on the charging rate of the battery and the requirement for enough power through all modes of operation. Based on the mission profile of the CubeSat, the operation modes are split into the following,

- Launch mode: Battery is full charged, and all equipment is not active
- Safe mode: Only the equipment needed for basic operations and survival are active. This should include the receiver, electrical power system (EPS) and the on-board computer (OBC).
- Nominal mode: Satellite bus is functioning as required. The transmitter can be activated by uplink.
- Communication mode: Satellite bus is functioning as required. The transmitter is on.
- Eclipse mode: Same as nominal mode.

Considering the longest eclipse period possible is 40%, the duty cycles have to be allocated to ensure power is utilised conservatively. The duty cycle to consider most important is that of the communication mode, which is 10 minutes based on AGI STK analysis. This will account for less than 1% of the total orbit time, which will be dominated by the nominal mode and the eclipse mode. Table 4.2 below shows the duty cycles derived for each mode,

**Table 4.2:** Duty cycle for each operational mode

| Mode | Duty cycle per orbit [%] |
|---|---|
| Launch mode | 0 |
| Safe mode | 0 |
| Nominal mode | 59.10 |
| Communication mode | 0.90 |
| Eclipse mode | 40.00 |

Based on simulation data on operating a satellite at 400km altitude and approximately 51.6 degrees inclination and elevation of at least 10 degrees, the satellite has 2 passes over Singapore that fulfil the parameters (Appendix D). That gives us allowance to use one communication orbit, transit back to nominal mode followed by eclipse mode, and then run a few orbits to allow the batteries to charge fully before the next pass over Singapore. The transmitter can be requested to transmit the data via a signal sent from the ground station. In the case of the ground station not having the capacity to

transmit to the satellite, an alternative transmission pattern must be used to ensure the ground station will receive at least one full transmission each day from the satellite without prompting.

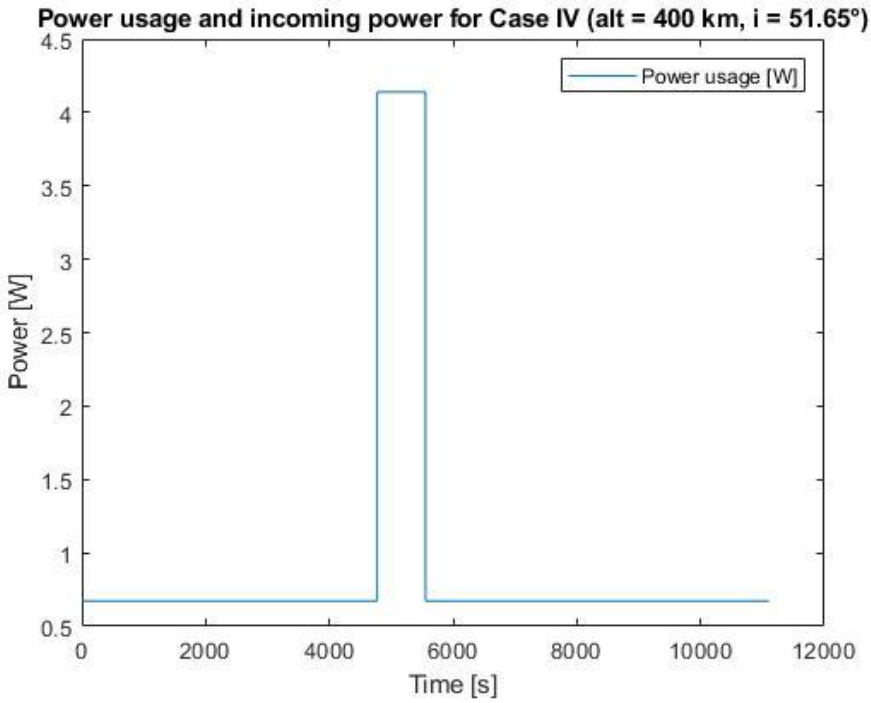


**Figure 4.1:** Power usage of CubeSat over 2 orbits

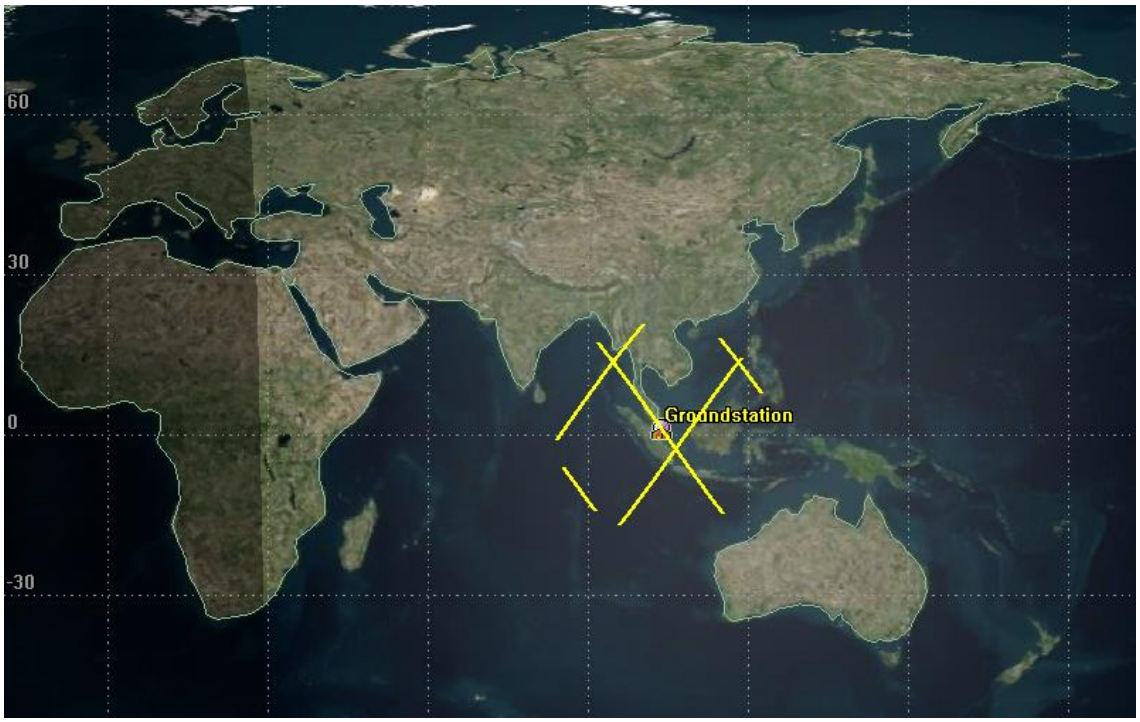


**Figure 4.2:** Ground tracks showing paths when satellite is in contact with ground station

For the given modes, the desired power budget can be calculated as follows,

**Table 4.3:** Power budget for CubeSat. All values are given in Watts

| Power mode | Nominal | COMMS | Eclipse | Safe | Launch |
|---|---|---|---|---|---|
| **Payload** | 0.01 | 0.01 | 0.01 | 0 | 0 |
| **OBC** | 0.13 | 0.13 | 0.13 | 0.13 | 0 |
| **Nanodock** | 0.02 | 0.02 | 0.02 | 0.02 | 0 |
| **Transmitter** | 0 | 2.89 | 0 | 0 | 0 |
| **Receiver** | 0.19 | 0.19 | 0.19 | 0.19 | 0 |
| **EPS Board** | 0.21 | 0.21 | 0.21 | 0.21 | 0 |
| ***Subtotal*** | 0.56 | 3.43 | 1.36 | 0.55 | 0 |
| Margin | 0.20 | 0.20 | 0.20 | 0.20 | 0.20 |
| ***TOTAL*** | 0.672 | 4.12 | 0.672 | 0.66 | 0 |

Using the duty cycle percentages shown in Table 4.2 and multiplying them with the corresponding power values shown in Table 4.3, and then adding the final power values provides the average required incoming power per orbit which is calculated to be 0.7 Watts (W). It can now be verified if the power components provided are sufficient to power the CubeSat according to the required operational scenario. GomSpace NanoPower P31us EPS and five (5) GomSpace Solar panels are provided power for the CubeSat through its operational lifetime.

The P31us unit has three photovoltaic power converters, which can connect two solar cell lines on opposite sides. On this CubeSat, there is one (1) solar panel on each one of five sides of the satellite. The last side of the CubeSat holds the GomSpace ANT430 antenna panel. Using a reverse diode in the connection between each solar panel and the corresponding power converter will prevent current from flowing to the panel that is not exposed to incoming solar radiation. The circuit block diagram detailing the solar panel setup is shown in Figure 4.5. Other factors are also accounted for that can affect the estimate on the incoming solar power, such as array efficiency, UV degradation and the effect of changing temperatures. The array efficiency has been estimated to be 90 % [19]. The solar panels are tested at $25^{O}$C while they operate at $75^{O}$C in Space, which combined with UV degradation results in 3% less efficiency at the end-of-life. To minimise power required and with the benefit of the turnstile antenna ANT430, no ADCS control is implemented which means the CubeSat will tumble throughout its orbit. This will allow equal durations of solar radiation on the CubeSat faces with the solar panels and is expected to enable a distributed temperature range around the structure.

Next to calculate is the necessary battery capacity during eclipse, which can be derived from the Equation (1) below,

$$C_r = \frac{P_e \,.\, T_e}{DoD \,.\, N \,.\, n} \tag{1}$$

in which $P_e$ is the power of the satellite, $T_e$ is the eclipse time of the satellite, DoD is the depth of discharge of the battery, N is the number of batteries and n is the charging and discharging efficiency. N is set to 1 in this analysis, DoD is set at 30% and n is set at 90%. Using this equation comes to a battery capacity of 1.54 Wh. The battery pack P31us that is being utilised is rated at 38.5 Wh.

The optimal communication cycle (battery capacity chart shown in Figure 4.3) considers that data can be transmitted down to the ground station at the exact region of orbit where the ground station is able to have sufficient data downlink connectivity with the CubeSat (without any uplink to the CubeSat from the ground station). This is a very ideal and almost unrealistic scenario since it would be difficult to time the downlink such that it would always be in the communication zone (as the launch scenario might vary).

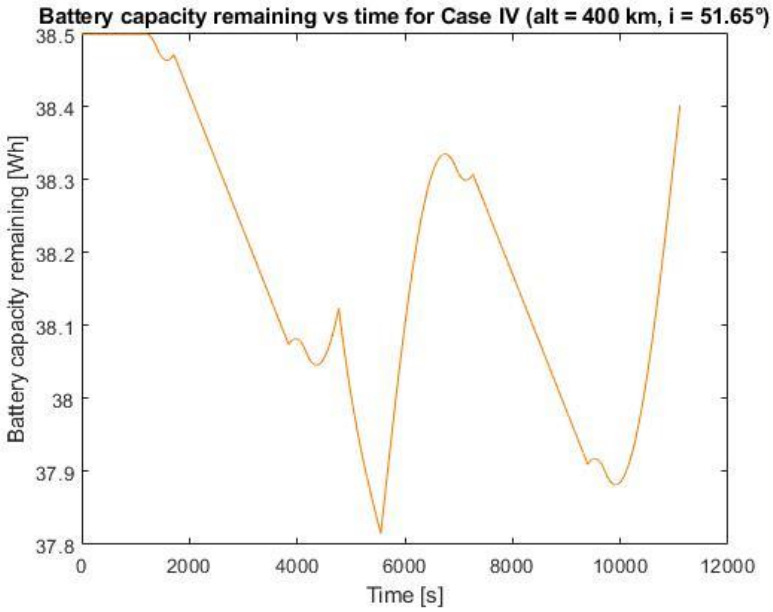


**Figure 4.3:** Battery power levels over 2 orbits with communication orbit (ideal scenario)

Two scenarios can therefore be considered – (1) transmit the data every 10 minutes to have a higher probability of being within the desired uplink/downlink region during data transmission or (2) transmit throughout the orbit. For both scenarios, the transmission can only happen during one orbit. For the subsequent "X" (value to be determined based on power budget chart) orbits transmission does not occur, but the CubeSat operates just the basic components while charging the P31U unit with the solar panels. The battery capacity charts for the 2 scenarios are shown below,

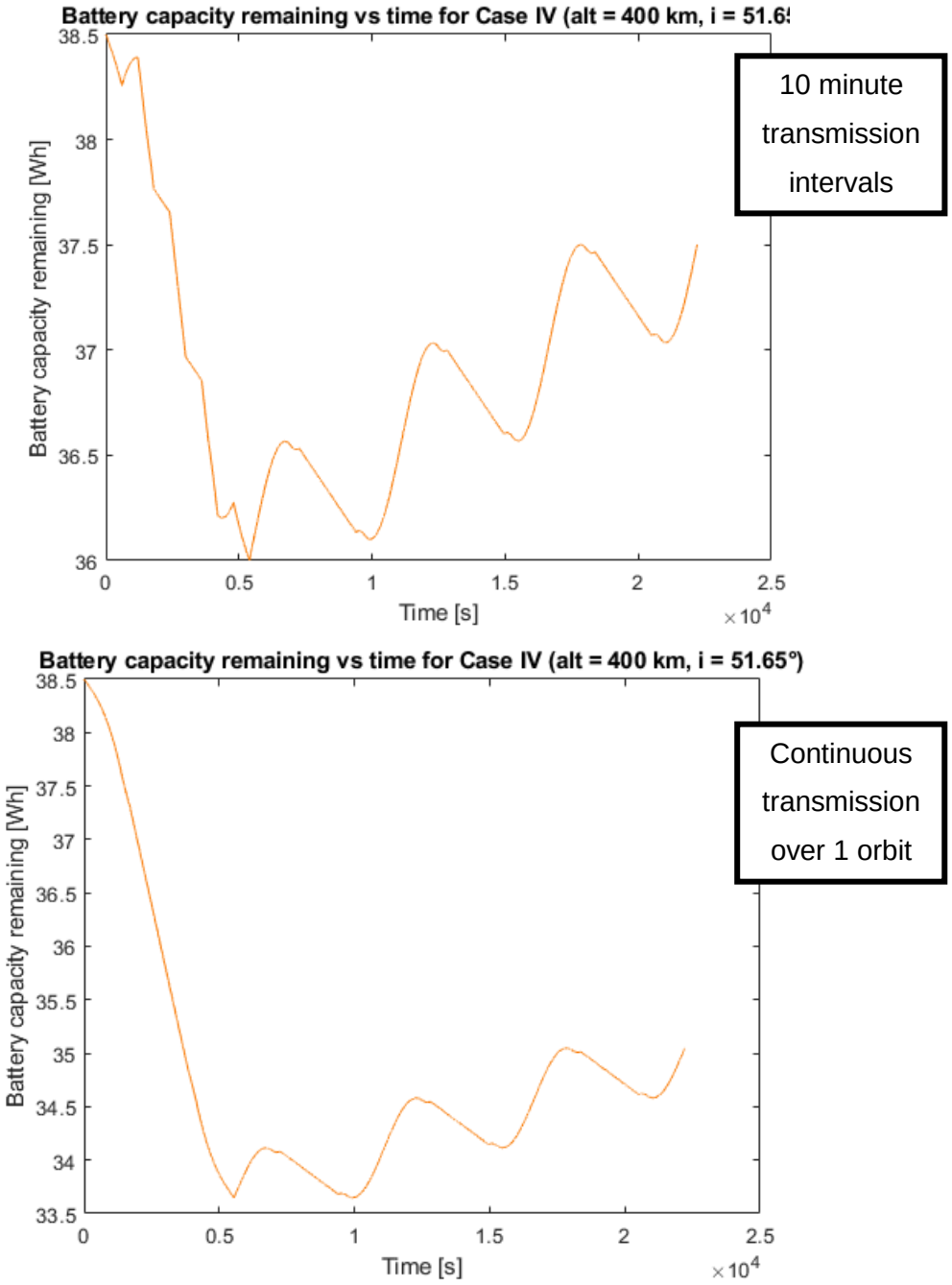


**Figure 4.4:** Battery power levels over 2 orbits with communication orbit (10 minute transmission intervals and continuous transmission over one orbit)

As per Figure 4.4, it can be seen that with ten minute transmission intervals, you would require another five charging orbits to allow the battery to charge to full capacity. For the continuous transmission over one orbit, another 13 charging orbits are required for every transmission orbits. This is for conservative transmission methods.

Using the design parameters and altitude of the CubeSat, the orbital lifespan of the satellite is calculated. The coefficient of drag $C_D$ of the satellite is assumed to be 2.2. The radiation pressure

coefficient $C_R$ is assumed to be 1.0. The sun-facing area of the satellite is set to be $0.03m^2$ and the m/A of the satellite is set at 100 kg $m^{-2}$. Using these values and the "Jacchia 1970 lifetime" density model, it is estimated the CubeSat can remain in orbit for 2.5 years. This orbit is sufficient to collect a sufficient volume of data and also test the durability of an ULTEM-Aluminium matrix structure in the extreme environment of space with its large temperature variances along the orbit.

**Table 4.4:** Link Budget

| | |
|---|---|
| Launch agency | JAXA / ISRO (to be decided) |
| Launch location | Japan (JAXA) or India (ISRO) |
| Expected launch date | Late-2019 |
| Apogee | 400km (JAXA) or 460km (ISRO) |
| Perigee | 400km (JAXA) or 460km (ISRO) |
| Orbit inclination | 51.6 degrees (JAXA) or 45 degrees (ISRO) |
| Orbit period | 1.5 hours |
| UHF | 437.5 MHz |
| Symbols / second | 9600 |
| Canted Turnstile ANT430 | Omnidirectional |

**Table 4.5:** Downlink

| **Parameter:** | **Value:** | **Units:** |
|---|---|---|
| **Spacecraft:** | | |
| Spacecraft Transmitter Power Output: | 1,0 | watts |
| In dBW: | 0 | dBW |
| In dBm: | 30,0 | dBm |
| Spacecraft Total Transmission Line Losses: | 0,5 | dB |
| Spacecraft Antenna Gain: | 0 | dBi |
| Spacecraft EIRP: | **-0,5** | dBW |
| **Downlink Path:** | | |
| Spacecraft Antenna Pointing Loss: | 0 | dB |
| S/C-to-Ground Antenna Polarization Loss: | 3 | dB |
| Path Loss: | 153 | dB |
| Atmospheric Loss: | 2,1 | dB |
| Ionospheric Loss: | 0,4 | dB |
| Rain Loss: | 0,0 | dB |
| Isotropic Signal Level at Ground Station: | **-159,0** | dBW |
| **Ground Station (EbNo Method):** | | |
| Ground Station Antenna Pointing Loss: | 0,5 | dB |
| Ground Station Antenna Gain: | 17 | dBi |
| Ground Station Total Transmission Line Losses: | 0,5 | dB |
| Ground Station Effective Noise Temperature: | 1003[5] | K |
| Ground Station Figure of Merrit (G/T): | -13,5 | dB/K |
| G.S. Signal-to-Noise Power Density (S/No): | 59,7 | dBHz |
| System Desired Data Rate: | 9600 | bps |
| In dBHz: | 39,8 | dBHz |
| Telemetry System Eb/No for the Downlink: | 15,8 | dB |
| Demodulation Method Selected: | GMSK | |
| Forward Error Correction Coding Used: | Conv. R=1/2,K=7 & R.S. (255,223) | |
| System Allowed or Specified Bit-Error-Rate: | 1,0E-05 | |
| Eb/No Threshold: | 7,8 | dB |
| System Link Margin: | 8,0 | dB |

**Table 4.6:** Uplink

| **Parameter:** | **Value:** | **Units:** |
|---|---|---|
| **Ground Station:** | | |
| Ground Station Transmitter Power Output: | 25,0 | watts |
| In dBW: | 14,0 | dBW |
| In dBm: | 44,0 | dBm |
| Ground Stn. Total Transmission Line Losses: | 1,6 | dB |
| Antenna Gain: | 17 | dBi |
| Ground Station EIRP: | 29,4 | dBW |
| **Uplink Path:** | | |
| Ground Station Antenna Pointing Loss: | 0,5 | dB |
| Gnd-to-S/C Antenna Polarization Losses: | 3,0 | dB |
| Path Loss: | 153 | dB |
| Atmospheric Losses: | 2,1 | dB |
| Ionospheric Losses: | 0,4 | dB |
| Rain Losses: | 0,0 | dB |
| Isotropic Signal Level at Spacecraft: | -129,6 | dBW |
| **Spacecraft (Eb/No Method):** | | |
| Spacecraft Antenna Pointing Loss: | 0 | dB |
| Spacecraft Antenna Gain: | 0 | dBi |
| Spacecraft Total Transmission Line Losses: | 0,2 | dB |
| Spacecraft Effective Noise Temperature: | 234 | K |
| Spacecraft Figure of Merrit (G/T): | -23,9 | dB/K |
| S/C Signal-to-Noise Power Density (S/No): | 75,1 | dBHz |
| System Desired Data Rate: | 9600 | bps |
| In dBHz: | 39,8 | dBHz |
| Command System Eb/No: | 35,3 | dB |
| Demodulation Method Selected: | GMSK | |
| Forward Error Correction Coding Used: | Conv. R=1/2,K=7 & R.S. (255,223) | |
| | | |
| System Allowed or Specified Bit-Error-Rate: | 1,0E-05 | |
| Eb/No Threshold: | 7,8 | dB |
| System Link Margin: | **27,5** | dB |

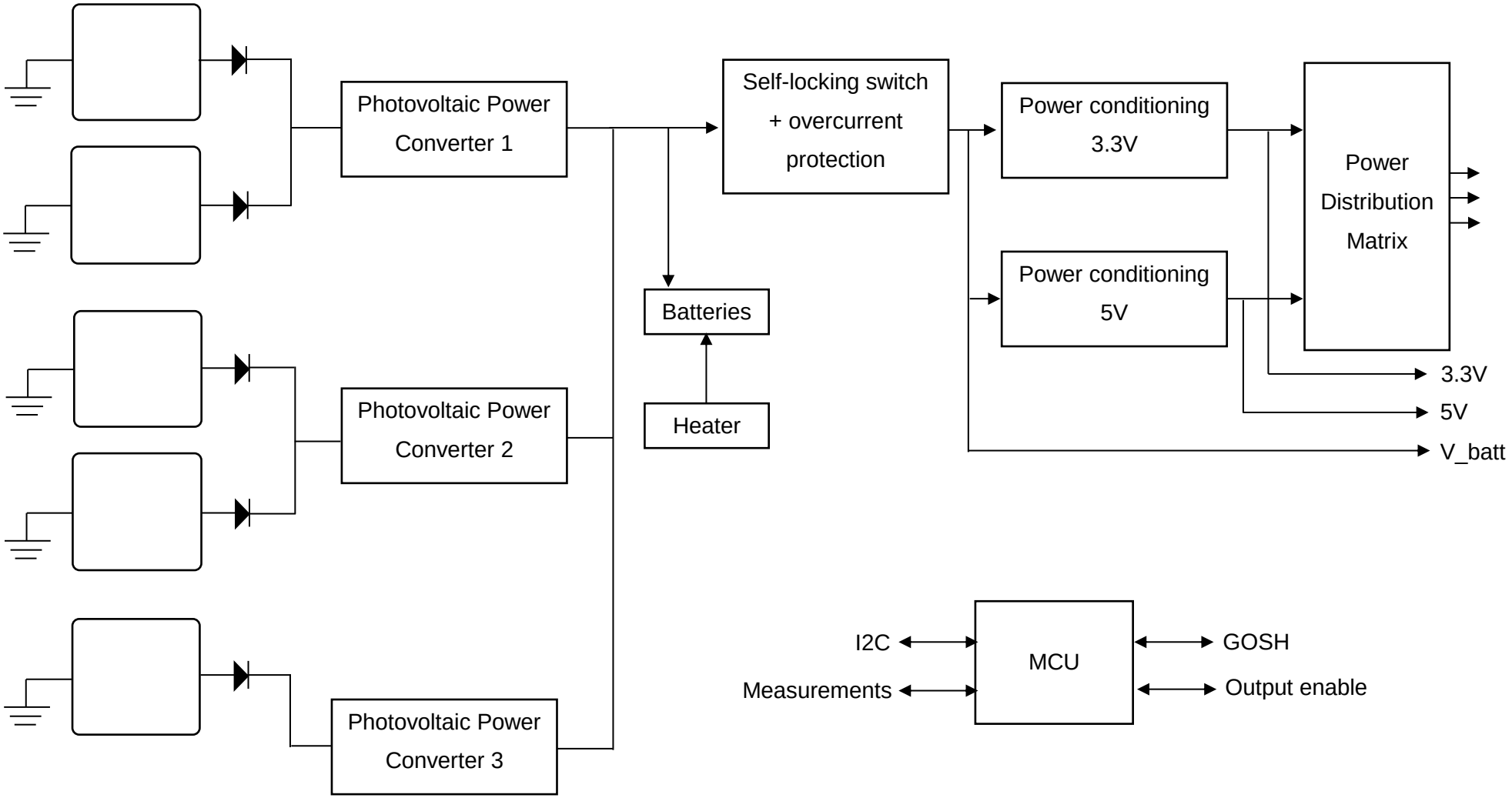


**Figure 4.5:** Solar Panel Setup

# 5.0 Structure Development

The 3D printed structure has been developed while keeping in line with certain set rules to limit expense and time for fabrication of the structure as explained in Chapter section 1.2.

## 5.1 Structure Design

Design of the CubeSat structure required the use of industry rated engineering tools SolidWorks and Abaqus. SolidWorks was used to create the digital models of the designs and create the models for 3D Printing, while Abaqus was used to test the static response of the model to high G forces and test its response to steady state modal vibrations. Design of the structure followed two routes – 1) Open side design and 2) Partially covered side design. The reasons for choosing either design are as follows,

*Open side design (Design A)*

- Lightest possible structure
- Least number of assembly parts
- Less parts that hence limits additional vibrational modes at low frequencies

*Partial covered side design (Design B)*

- Overall durability is higher
- Easier to assemble in preferred "stacking" technique

A visual representation of the two designs is as follows,

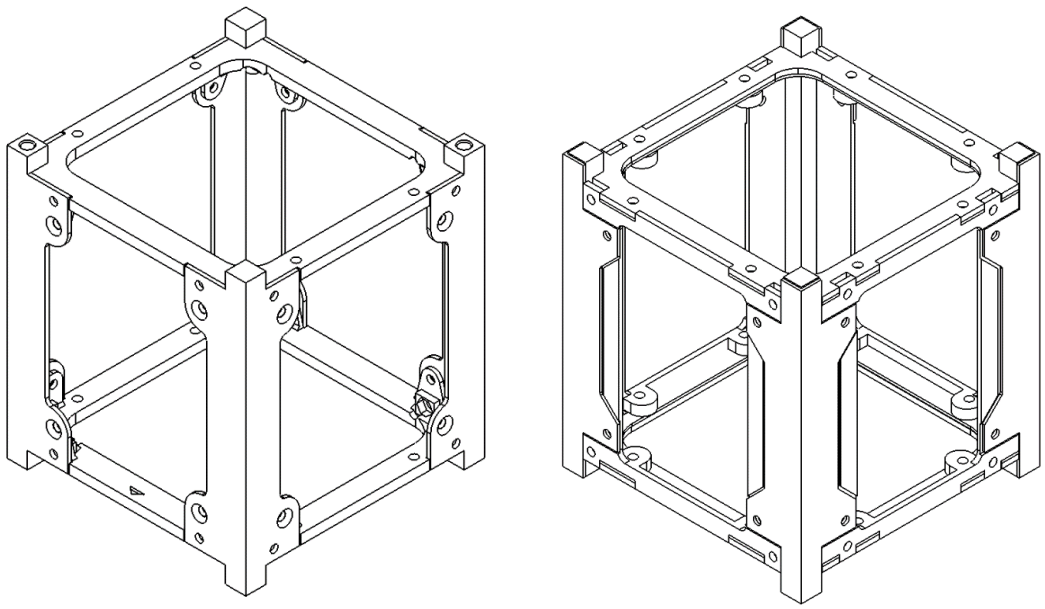

**Figure 5.1:** Drawings of Structures, Design A (left) and Design B (right)

The stacking method mentioned under Design B refers to the ability to build the CubeSat from the base and adding the components by stacking or fixing them in layers on the structure. This means there is no need to fit in parts with difficulty as other parts will not stand in the way of fitting the parts in with the structure.

In Design A, there are 6 structure components – 4 Aluminium rails and 2 ULTEM 9085 panels. The challenge is developing the Aluminium rods and panels with consideration of that the support material should be minimised. This adds to the complexity in the shape of the Aluminium rails to add the cubic support legs (top leg 6.5mm and bottom leg 7mm) on the rails, and the rod supports and rail connectors on the ULTEM panels which are facing the opposite direction from the cubic supports.

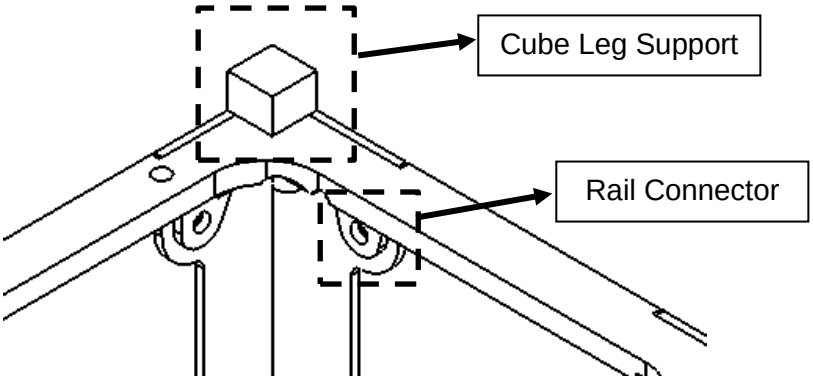


**Figure 5.2:** Cube Leg Support and Rail Connector (Design A)

Along with the design preference to have a pre-set cavity to contain the nuts that enable the tightening of the bolts that would hold the structure together, this presents a challenge to contain so many features within the limited area near the cube supports without the presence of additional side panels. The dimensions of the GomSpace panels restrict the positions of the rod support extrusions, so a solution must be found to position the rail connector screw holes, so the screws do not contact the PCB panel support rods and also hold the structure together effectively. Finally, assembly of Design A is tricky as the rails with the cubic leg supports will hinder the stacking or placement of the top ULTEM panel, since it will have to go beneath the leg supports to be assembled properly. This would present a situation where one of the rails cannot be added until the last assembly step, which is not an optimal scenario to consider.

As a foremost objective to ensure the general acceptability of the structure for engineering friendliness, Design B should be pursued. Although Design B is heavier and has more structural components, it is still much lighter than the conventional full Aluminium structures available on the market. The weight savings can be attributed to the much lower density of ULTEM as compared to Aluminium. In this regard, focus is placed on testing the stress handling ability of the ULTEM panels in its interaction with the Aluminium rails. To do so, it would be best to maximise the area and

volume of the ULTEM pieces against the Aluminium rails, to maximise their exposure to external forces that are applicable during launch mode.

In the case of Design A, it is clear that the ULTEM panels are quite excluded from majority of the forces that a CubeSat would experience, as an equal majority of the area and volume is taken up by the Aluminium rails. In Design B, however, a large majority of the exposed surface is taken by ULTEM. In fact, 80% of the CubeSat surface is made up of ULTEM. This would mean that in Design B the ULTEM pieces play a greater role in keeping the structure together against launch forces. This would help us support the case in qualifying ULTEM as a suitable material to use for 3D printing nanosatellite structures and consider using it as a major material over metal which is heavy and difficult to 3D print if that option is being considered. To 3D print using metallic base materials, a very large and bulky amount of metallic feed material is required to print a relatively much smaller amount of object material which is expensive and wasteful. This problem is avoided with plastics because of their lower density, melting temperature and better propensity to form 3D printed structures with ease.

## 5.2 Structure Performance Analysis

### 5.2.1 First Design Analysis

The first design, based on Design B, allows smooth motion of the CubeSat in the deployment pod and reduces weight to a minimum, which includes having a hybrid standoff surface made up of ULTEM and Aluminium alloy and variations from the JAXA standards. As mentioned in the previous section, the preferred design is tested using appropriate engineering software. In this case, the digital model of the design is run through simulated force-stress scenarios and vibrational studies using Abaqus.

First, the vibrational modes of the CubeSat are figures using suitable constraints based on the orientation of the CubeSat when it is placed in the launch pod. In a typical launch pod, the CubeSats or nanosatellites are stacked inside the pod with their contact points being the cubic leg supports described in section 5.1. The strict adherence to dimensional limits and specific materials for certain contact points is required to ensure that not a single CubeSat is stuck inside the pod and causes a blockage in the pod that prevents the free deployment of the nanosatellites behind it in the pod queue.

Therefore, in the frequency study to determine the modal frequencies of the CubeSat, the top and bottom cubic support legs are fixed in place. The study is then initiated under the desired constraints, and the modal frequencies are found to be well in excess of 100Hz (which is the minimum standard set by the JAXA Design Handbook [20]). The first ten (10) modal frequencies established are in 3 range sets: 605 – 635Hz, 830 – 875Hz and 1,250 – 1,265Hz.

The model was then tested under heavy static stress conditions and modal steady state vibration studies. The studies were done separately considering a maximum vertical force of 30g and maximum horizontal force of 20g. These forces can be experienced at certain high acceleration periods during launch, either as a few periodic vibrations or as a single shock application.

For the static vertical force (run over one second of a ramp increase in force), just the bottom cubic leg supports were fixed, and the remaining areas of the CubeSat were left free to move. The 30g force was applied as a pressure force on the four top cubic leg supports, which each presented a pressure application area equal to 8.5 mm squared, which is 72.25 $mm^2$. Assuming a CubeSat mass of 1kg, that would mean a force of 75 N was applied on each leg, which would translate to a pressure of 1.04 MPa per leg. Based on these conditions and the study results, the maximum stress experience by the structure was 16.7 MPa and displacement of 1.06 mm. The maximum displacement was only at the 4 cubic leg supports though, but the Aluminium rails had minimal distortion.

For the static horizontal force, the top and bottom cubic leg supports were fixed. The 20g forced was applied on the side surfaces of 2 Aluminium rails, since these areas would be in contact with the rail receivers in the pod and will likely be the first to experience the force. This would simulate 100 N of force per rail surface, which is equivalent to 0.1 MPa of pressure. The maximum stress measured is 37.8 MPa and maximum deviation is 0.53 mm. The highest displacement is near the ULTEM panel cavity, and not on the Aluminium rails.

Data was collected from four (4) data points on the model, and their response to the forces plotted on a chart. The data points of interest on the model are shown in Figure 5.3.

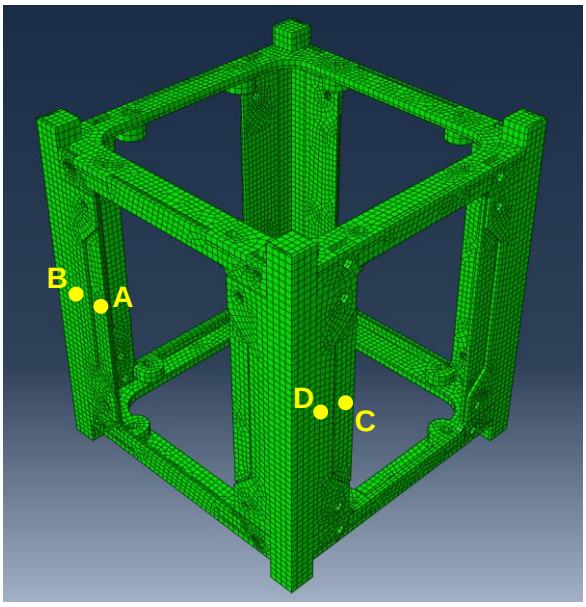


**Figure 5.3:** Abaqus test model data points placements

The data gathered at the selected points was then plotted and analysed. The side surfaces of the CubeSat are of high interest because excessive bending or buckling at these regions can cause a permanent distortion in the shape of the CubeSat and affect its deployment. The horizontal force application under steady vibrations naturally resulted in the highest registered displacements but are much less than 1mm in magnitude. The data gathered can be seen in Figures A-1 and A-2 in Appendix A.

When looking at the stress distributions in response to the horizontal vibrations, the stresses experienced by the Aluminium rails are higher than those seen on the ULTEM parts. This is a good occurrence because the Aluminium rails should absorb the higher levels of stress but the ULTEM panels also experience some of the loads. In this case, the ULTEM panels experience stresses 2-5 times less than that by the Aluminium rails.

For the vertical vibrations at 30G magnitude, the side displacements and stresses are much less as most of the force responses are experienced by the components perpendicular to the force application. However, getting data of the side surface is useful to check on the effective distortion of the structure, which could affect its deployment if the displacement is too severe. The data gathered, shown in Figures A-3 and A-4 in Appendix A, show that the displacements points on the components are very minor as they are on the scale of $10^{-6}$ m. The stress magnitudes are also very low, on the scale of just a few thousand pascals.

The stress and displacement areas of the structure under stress was also analysed, to find the areas of highest stress and displacement. Figure 5.4 and Figure 5.5 below show the contour maps for the pressure application under static conditions,

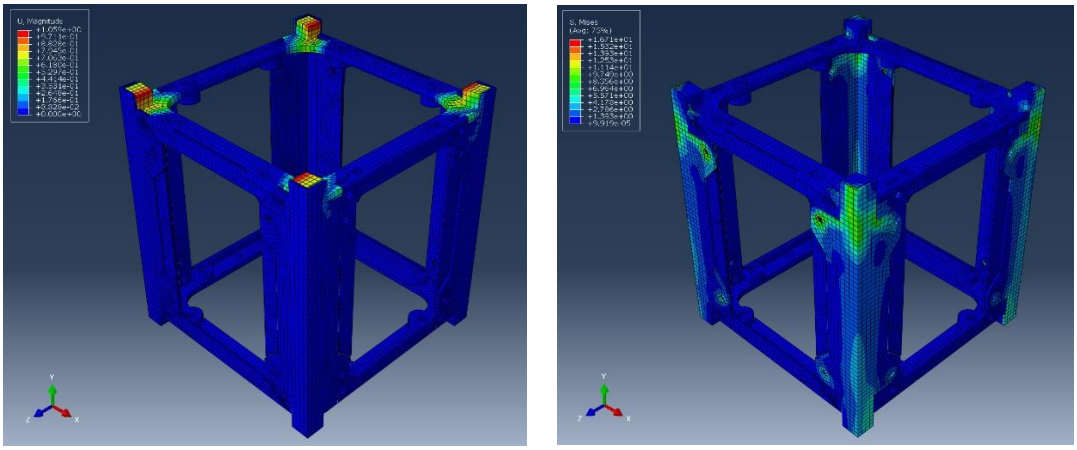

**Figure 5.4:** Contour maps for 30G vertical pressure force application, static case. Displacement contour (left) and stress contour (right)

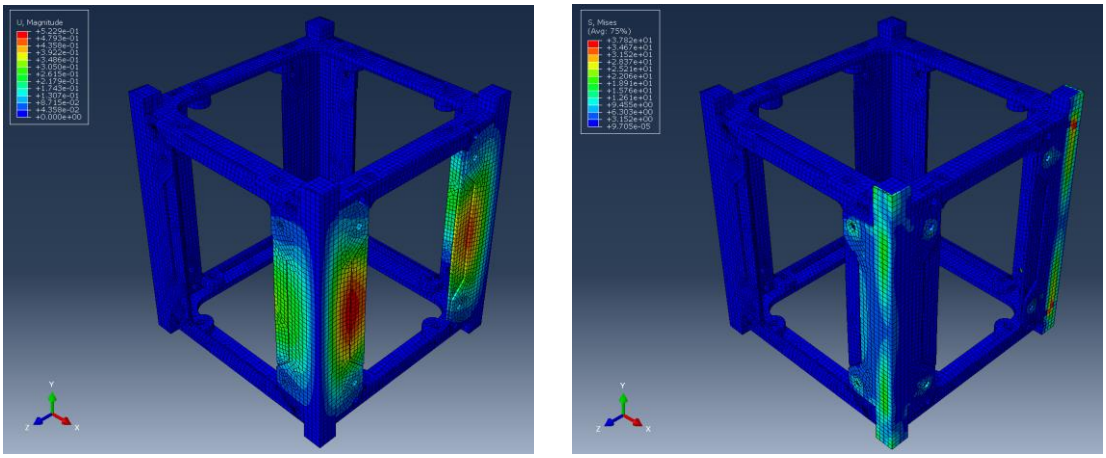

**Figure 5.5:** Contour maps for 20G side pressure force, static case.
Displacement contour (left) and stress contour (right)

**Table 5.1:** Maximum Stress and Displacement Values

| Pressure Force (g) | Direction | Max. Stress | Max Displacement |
|---|---|---|---|
| 30 | Vertical | 17 MPa | 1.06e-3 m |
| 20 | Horizontal | 37 MPa | 5.3e-4 m |

### 5.2.2 Second Design for General Acceptance

The variations from JAXA discussed are not accepted due to strict standards placed by the launch agencies, which are expected for any launch agency. To minimise conflict on design variations, the rail designs are changed to make the standoff area with just one material – Aluminium alloy.

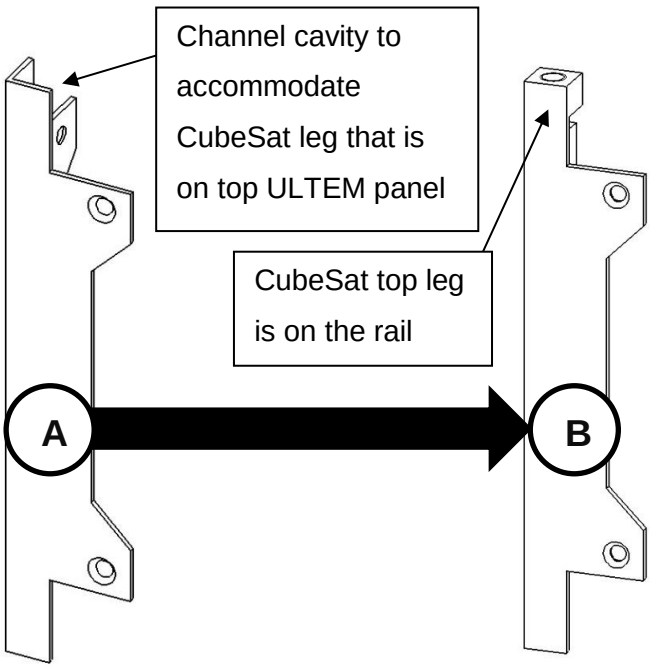


**Figure 5.6:** Rail Design Variation

The drawback of the new rail design with the CubeSat leg added is that it cannot be made easily with conventional fabrication techniques eg. CNC machining. It can be made effectively with metallic-based 3D printing, although such a process would be material and cost intensive. 3D printing the rail would however enable research on the performance of a 3D printed metallic part in Space.

### 5.2.3 Second Design Analysis

The second design follows Design A more closely but adds elements of Design B and is analysed with different conditions from a launcher with more allowance on design and material variations. In the new conditions, the satellite is tested under two scenarios with specific parameters – one test was done with regular sinusoidal vibrations, and the second test was done under random vibration conditions. The tests were carried out on computer simulations as well as real setups with suitable vibration exciters. The satellite was also fixed at a different point – the bottom plate of the CubeSat structure instead of the standoff areas on the rails. The test conditions are described in Tables Table ***5.2*** and Table ***5.3***.

**Table 5.2:** Sinusoidal Vibration Test Levels for Micro Satellites

| | Frequency Range (Hz) | Qualification Level | Acceptance Level |
|---|---|---|---|
| Longitudinal Axis | 5.0 – 8.0 | 34.5 mm (DA) | 23 mm (DA) |
| | 8.0 - 100 | 4.5g | 3g |
| Lateral Axis | 5.0 – 8.0 | 24 mm (DA) | 16 mm (DA) |
| | 8.0 - 100 | 3g | 2g |
| Sweep rate | | 2 Oct/min | 4 Oct/min |

**Table 5.3:** Random Vibration Test Levels for Micro Satellites

| Frequency (Hz) | Qualification | Acceptance |
|---|---|---|
| | PSD ($g^2$ / Hz) | PSD ($g^2$ / Hz) |
| 20 | 0.002 | 0.001 |
| 110 | 0.002 | 0.001 |
| 250 | 0.034 | 0.015 |
| 1000 | 0.034 | 0.015 |
| 2000 | 0.009 | 0.004 |
| g RMS | 6.7 | 4.47 |
| Duration | 2 min/axis | 1 min/axis |

Before gathering the results on the two test scenarios, the modal frequencies of the second design

were gathered to ensure they comply with general launch standards, which state it must exceed at least 100Hz. A frequency study was carried out, and the results showed that the first frequency mode is at 415 Hz, which is much higher than the requirements and means the CubeSat will not reach resonance within the expected performance envelope for launch.

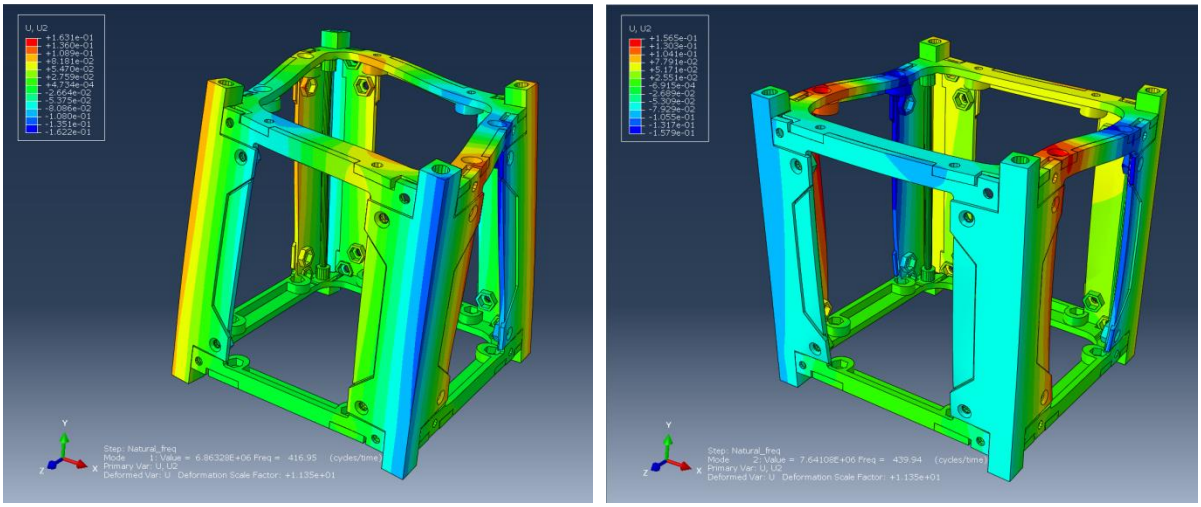

**Figure 5.7:** Frequency Study Results for Second Design

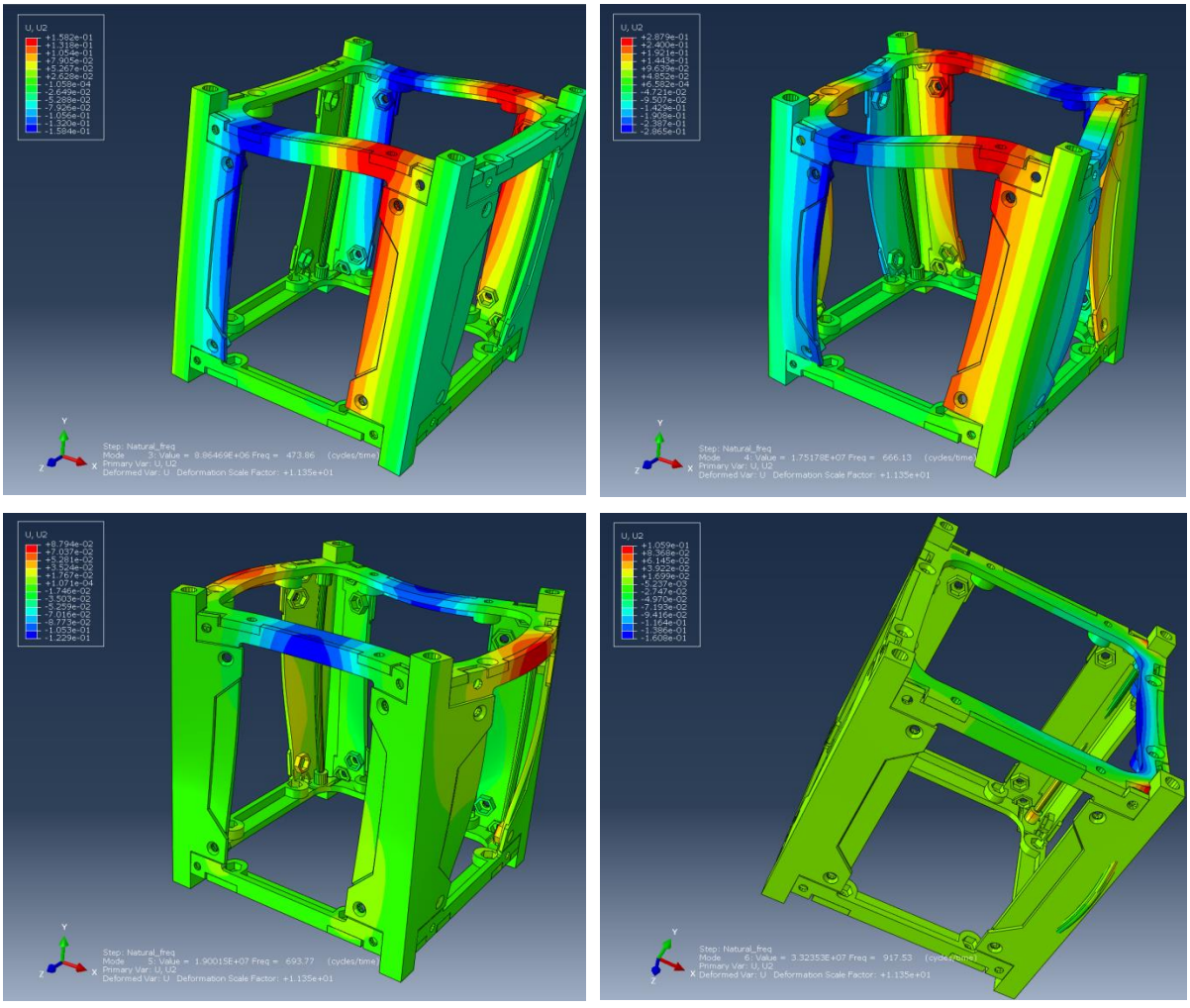

**Figure 5.8:** More Frequency Study Results for Second Design

The base plate was fixed (via an encastre boundary condition), and an acceleration mapped onto a frequency progression chart was applied to the model. The model was subjected to sinusoidal vibrations with associated g values shown in Tables Table ***5.2***. The results showed that the displacements were in the order of $10^{-9}$m with pressure not exceeding 200,000 pascals, which are well within the strength and endurance limits of the materials used.

The vibrations followed the chart values shown in Appendix E. Results gathered (Appendix F) also showed that the displacements on the ULTEM panels are minimal, on the order of $10^{-17}$m to $10^{-20}$m. The random vibrations cover the conditions through majority of the launch. The results show that the CubeSat will remain well within the displacement limits that would prevent any physical interactions with the satellites in proximity of the CubeSat in the Polar Satellite Launch Vehicle (PSLV).

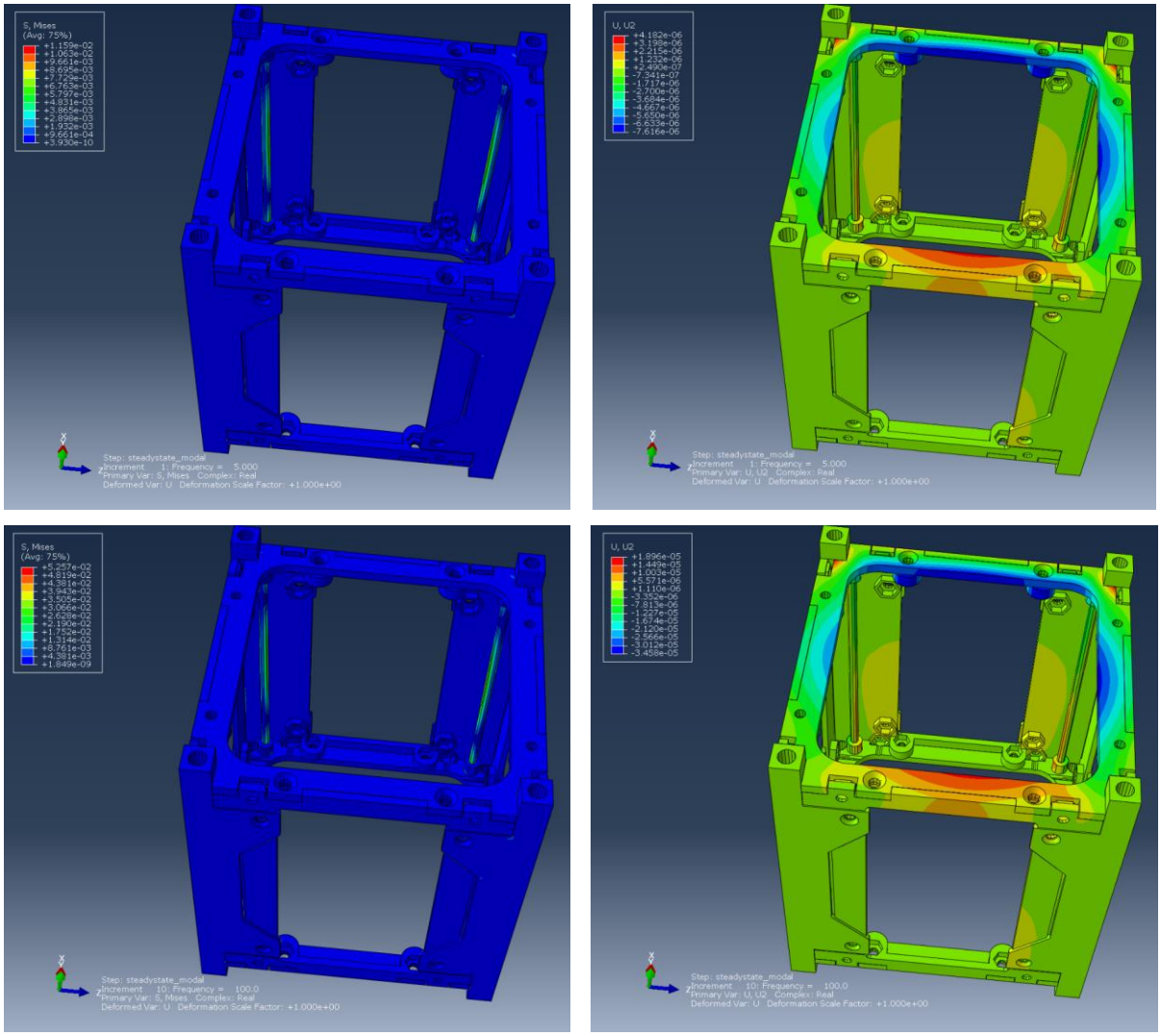

**Figure 5.9:** Deformation & Stress Contour Maps for 5Hz (top) and 100Hz (bottom)

## 5.3 Live Testing of First Design

The live testing of the first design structure was done using a large vibration platform to simulate maximum 4.5g sinusoidal vibrations and 6.7g random vibrations. The CubeSat structure should be able to withstand high gravitational loads which would be common during the launch phase of the mission. The typical loads generated and tested are almost standard across all launch agencies, with the major differences being the type of fixtures provided on the launchers.

In the testing performed for this CubeSat structure, the dummy "PCB" panels were developed and stacked inside the test CubeSat structure, to provide the mass distribution like the expected final, launch-ready CubeSat setup. Based on the GomSpace datasheets, the masses of the acquired components are given and used to calculate the mass of the CubeSat, along with the mass of the payload. The payload is a PCB panel with sensors to measure temperature of the ULTEM structure surface.

**Table 5.4:** CubeSat Weight Breakdown

| **Component** | **Quantity** | **Unit Mass (g)** | **Tot. Mass (g)** |
|---|---|---|---|
| CubeSat Frame | 1 | 116 | 116 |
| NanoMind A3200 | 1 | 14 | 14 |
| NanoCom AX100 | 1 | 24.5 | 24.5 |
| Motherboard DMC-3 | 1 | 51 | 51 |
| NanoPower P31u | 1 | 270 | 270 |
| Antenna ANT430 | 1 | 30 | 30 |
| NanoUtil Top | 1 | 20 | 20 |
| P110A Solar Panel | 1 | 26 | 26 |
| P110B Solar Panel | 1 | 26 | 26 |
| P110UA Solar Panel | 1 | 57 | 57 |
| P110UB Solar Panel | 1 | 57 | 57 |
| P110UC Solar Panel | 1 | 65 | 65 |
| Payload | -- | 100 | 100 |
| | | ***Margin*** | 0.20 |
| | | ***TOTAL (g)*** | 1,035 |

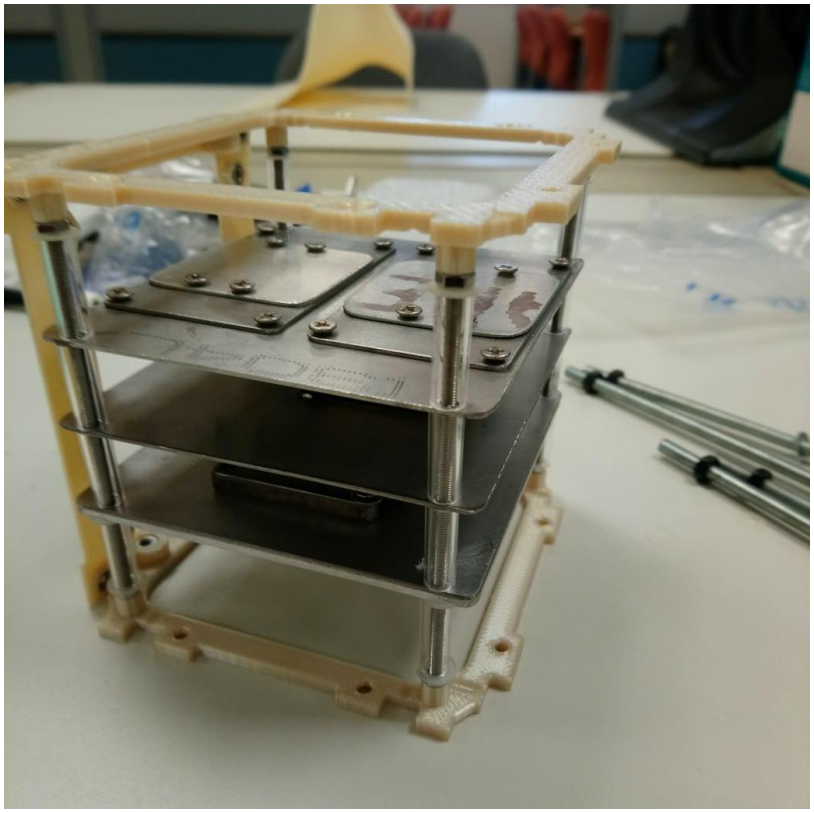

**Figure 5.10:** Stacking of dummy components inside CubeSat

### 5.3.1 Testing of CubeSat Structure

The assembled test CubeSat was then secured to an acrylic base, and then on a mounting platform that is fixed to a vibrator (with rail standoffs secured), in this case a Brüel & Kjær Type 4808 Vibration Exciter, with its associated acceleration vs. Frequency performance chart shown in Figure 5.11.

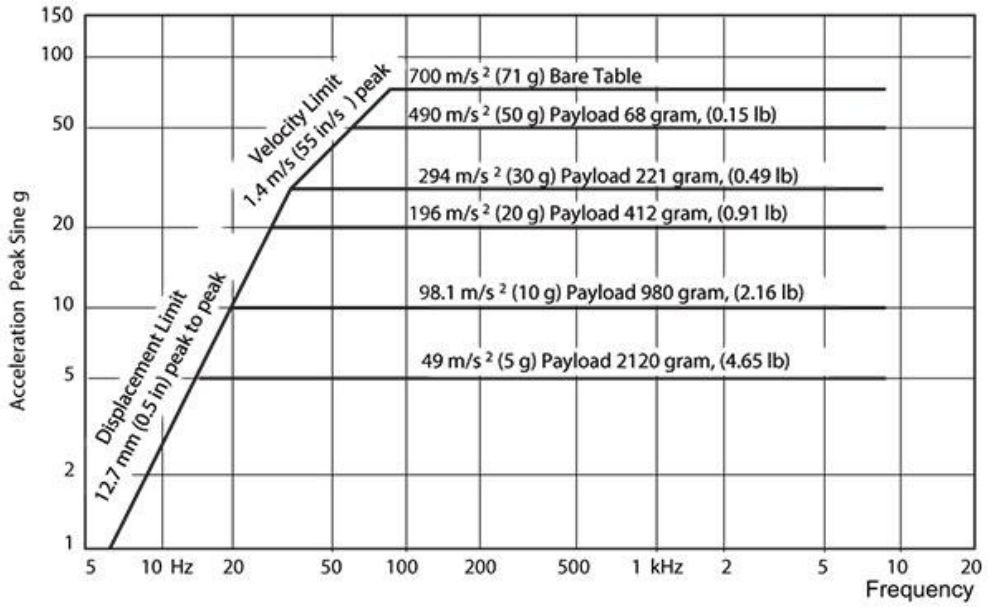


**Figure 5.11:** Acceleration vs. Frequency chart for selected Vibration Exciter

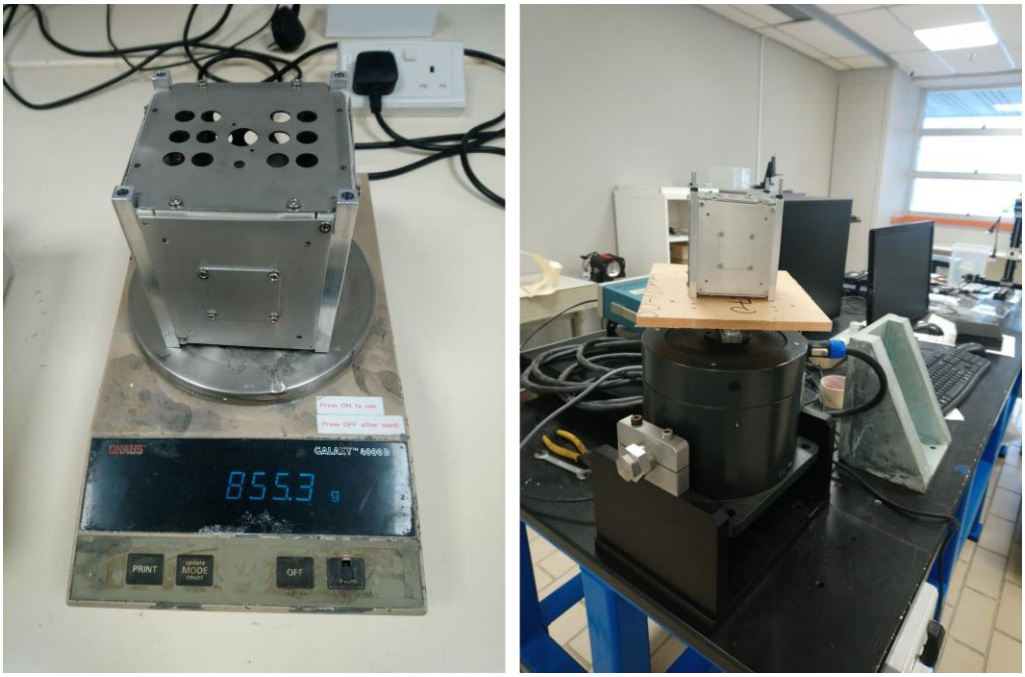


**Figure 5.12:** Mass measurement and setup of CubeSat on Brüel & Kjær Type 4808 Vibration Exciter

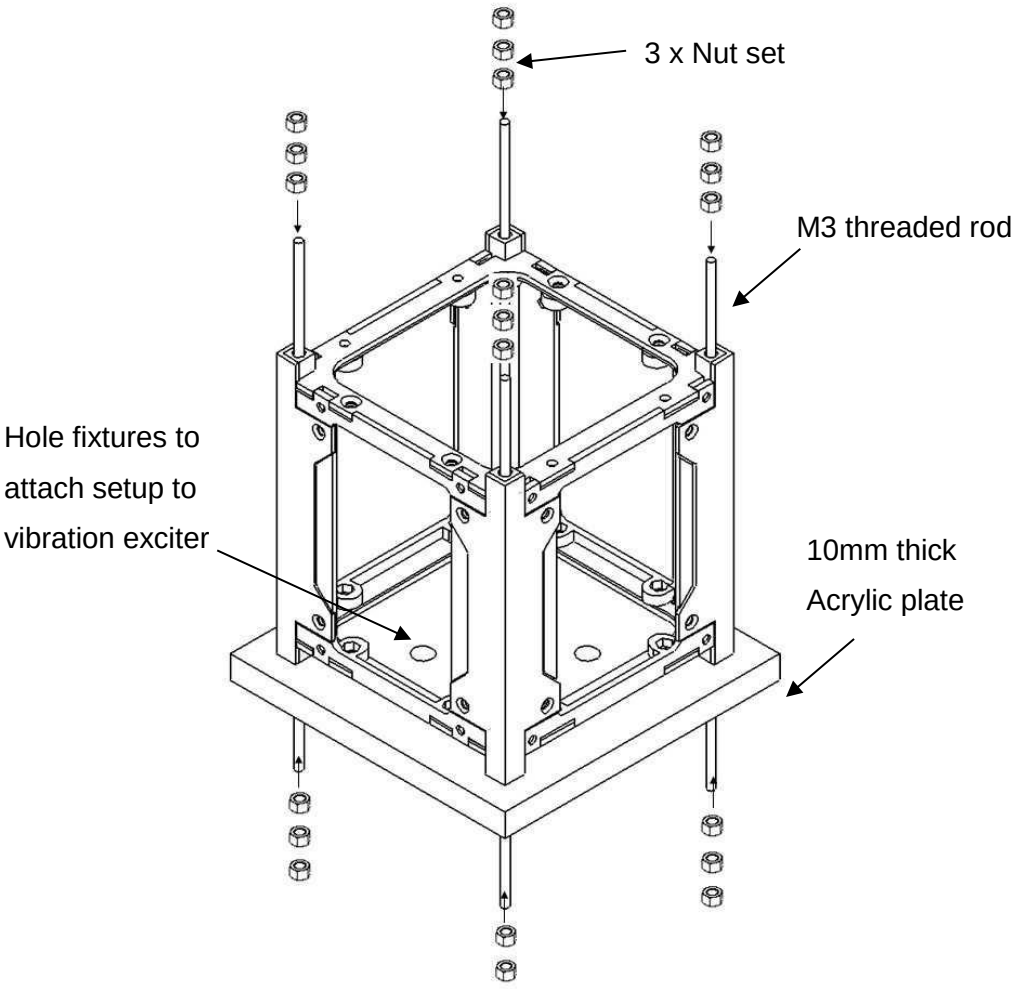


**Figure 5.13:** Basic setup of structure on vibration exciter

The final weight of the structure measured was 855.3g, which is almost exactly the weight expected for the final CubeSat structure without the 20% weight margin. The acrylic base with the bottom attachment and support rods all added an additional 1 kg to the mass of the test structure. As per Figure 5.11 this would limit the acceleration to a maximum of 5g. Due to the safety limitations of the machine, only 4g magnitude forces were achieved at a frequency of 100Hz.

To properly ascertain the integrity of the structure for launch vibrations, the base structure with the dummy components needs to be tested on a stronger vibration exciter. After testing, the structure must be analysed minutely, preferably through a microscope to find any defects that have occurred due to the vibrations. The defects must be identified and analysed to determine if they would cause a failure in the CubeSat structure.

The structure with the acrylic base plate and bottom attachment was then transferred to a larger vibration exciter – TIRA TV55240/LS. The TV55240 can generate much higher vibration frequencies and accelerations and has the software compatible with procedures required to qualify the structural integrity of a CubeSat structure for launch. For the mass of about 1kg, the maximum gravitational load that can be applied is near 50g, which is much higher than our test requirement.

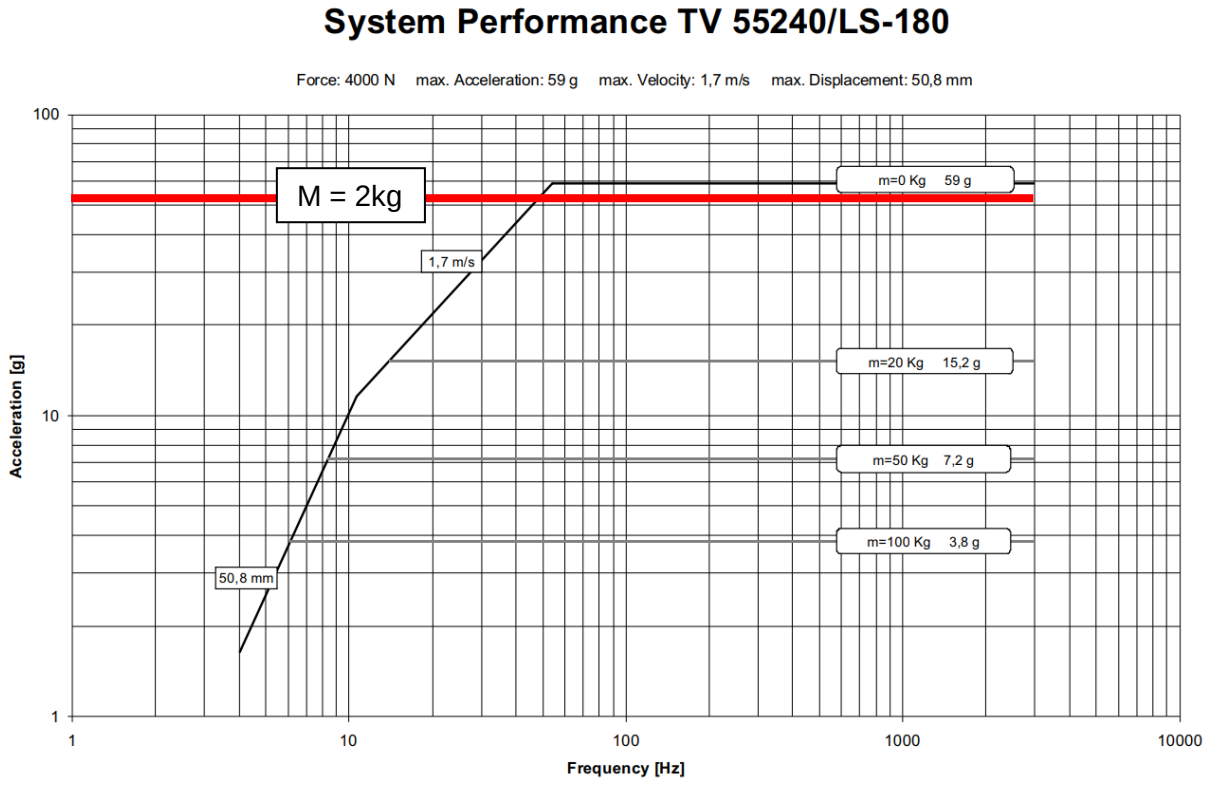


**Figure 5.14:** Performance chart for TIRA TV55240/LS vibration exciter

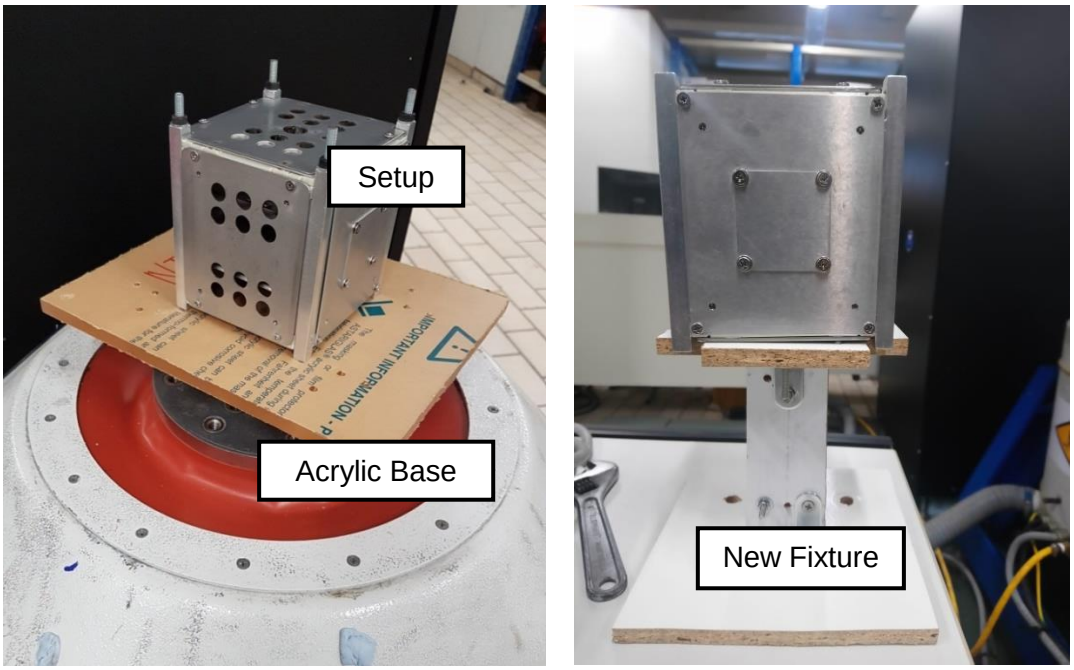


**Figure 5.15:** Setup of CubeSat on large Vibration Exciter – JAXA standard (left) and ISRO standard (right)

The CubeSat was also refit at new fixture points. Instead of fixing the CubeSat with the rail standoffs, it is fixed with the bottom plate that is a condition utilised in the PSLV environment. The new setup with the revised fixture base is shown in Figure 5.15. The new fixture provides the boundary conditions similar to what is expected on the ISRO launch setup. In this setup, the rails are completely exposed to the vibrations during testing and place a greater emphasis on the structural integrity of the ULTEM and Aluminium setup. The setup was exposed to the same conditions mentioned in Tables 5.2 and 5.3. After testing, the CubeSat was disassembled. Considering that the rails are not fixed to a base and are free to move with the vibrations, the ULTEM panels would be exposed to more stress variations of higher magnitude.

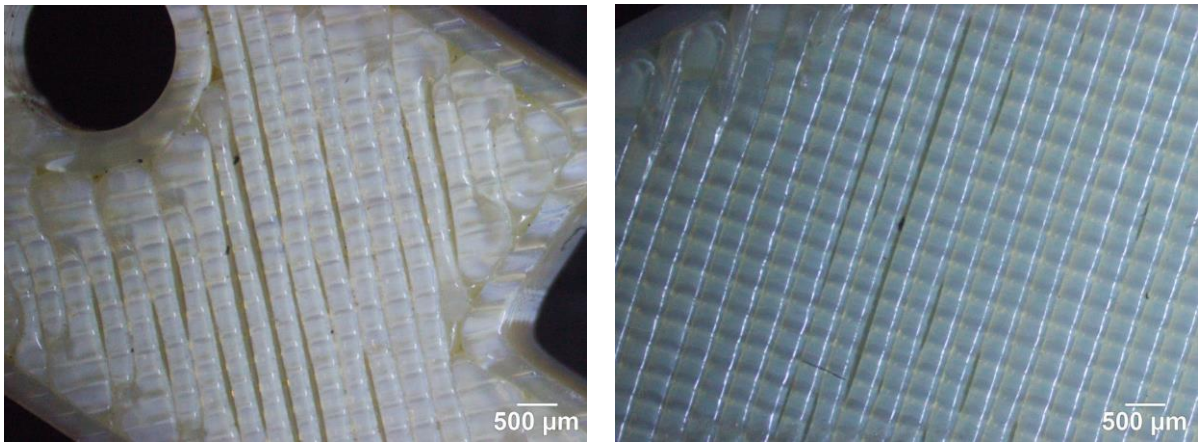


**Figure 5.16:** In-surface defects on ULTEM

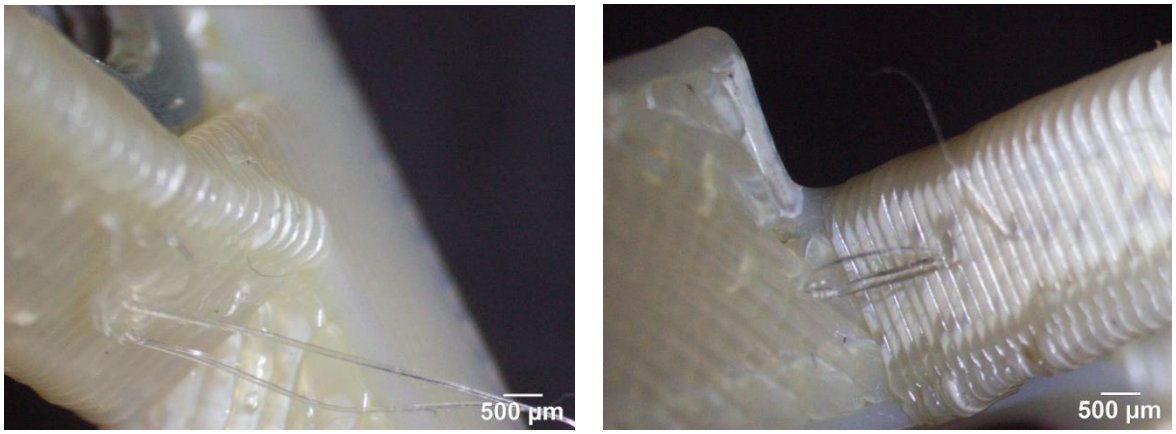


**Figure 5.17:** Filaments dislodged from ULTEM surface

The ULTEM panels were observed under a microscope, to find any major cracks in the material. Although there were no cracks found, there were interesting observations made on the ULTEM surface of two types: in-surface and out-surface. In-surface observations refer to gaps found on the surface layer of the ULTEM panels at some locations (see Figure 5.16**:** In-surface defects on ULTEM). These separations are actually defects from the 3D printing process when fabricating the ULTEM panels, based on the settings of the machine. The dislodged filaments are out-surface damages (see Figure 5.17) that are defects from the 3D printing process as well. The filaments are material strings that have not adhered well due to either 1) the complexity of the shape based on curvature and edges or 2) an excessive length of travel for the material being printed.

## 5.4 Outgassing Test

A major issue to consider when sending equipment into space or their containment structures is the materials being used to construct the setup. There are a select few materials that can be utilised for space based on their density, durability and outgassing properties. The material that needs some further testing in our design is ULTEM, which although has been approved and tested by other engineering institutes, would provide further assurance of its quality if tested again for this project.

The testing for outgassing has a fixed procedure. The samples, initially conditioned in 298K at 50% humidity, were exposed to a temperature of 398K at 10 millibars of pressure (near 7 torrs) for 24 hours. An absolute vacuum was difficult to achieve based on the limitation of the equipment, so the final outgassing measurements would have some minor errors attached to them. The samples were weighed before and after the test procedure, to find the percentage change in mass which will relate to the loss (or outgassing) of volatile mass. The outgassing percentage calculated was between 0.8 – 0.9%.

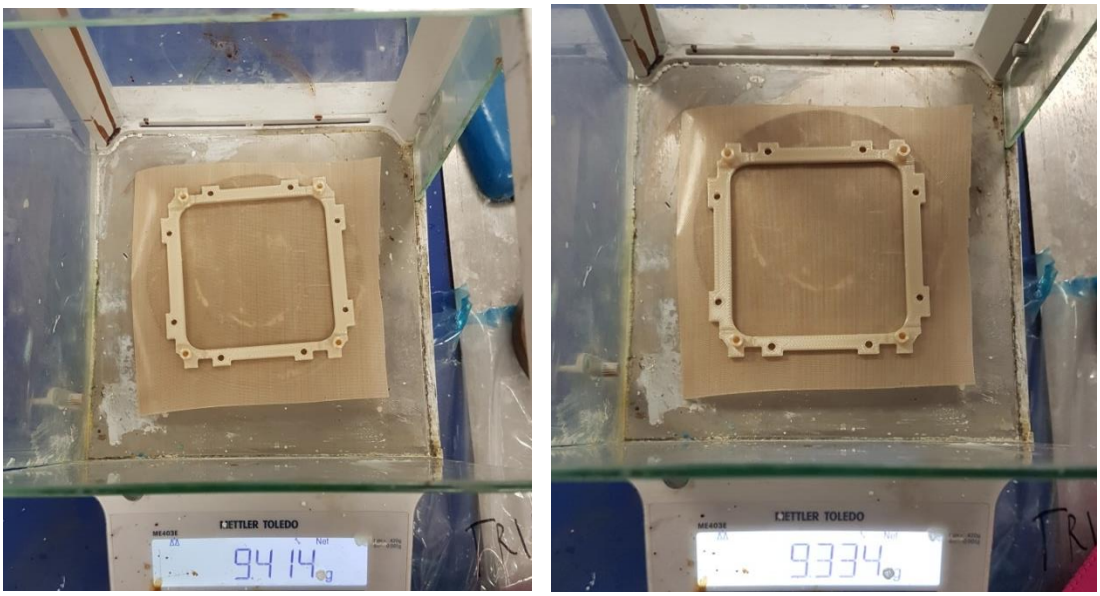


**Figure 5.18:** One measurement set of Top ULTEM panel

As seen in Figure 5.18**:** One measurement set of Top ULTEM panel, the initial mass of the ULTEM is higher than that measured after the outgassing test procedure. The outgassing percentage is calculated as such,

$$Outgassing\ level = \frac{(Mass\ before\ testing) - (Mass\ after\ testing)}{Mass\ before\ testing} * 100$$

$$= \frac{9.414 - 9.334}{9.414} * 100\%$$

$$= \mathbf{0.86}\% \ (< 1\%)$$

The requirement for a space grade material is that the outgassing percentage be below 1% [21]. The requirement for outgassing is to ensure that excessive material mass does not vaporise and from the base parts and settle on the interior components, which can affect their sensitivity and operational life.

## 5.5 Concluding Remarks

The tests have shown that the combination of ULTEM and Aluminium works sufficiently well to ensure a durable structure that can survive the launch environment. The materials have passed the tests that assessed the strength and their outgassing limits. The materials have achieved the required performance standards while keeping within the weight limits required for a 1U CubeSat.

# 6.0 Payload Development

A major mission to consider is to measure the temperature variations around the satellite as it orbits the Earth. A study can be made of the progression of temperature around the ULTEM frame through its interaction with the Aluminium rails. For this purpose, a simple setup consisting of several AD8495 chips, with K-type thermocouples and connecting with the ADC inputs on the On-board computer (OBC) is used. The component is setup is shown below,

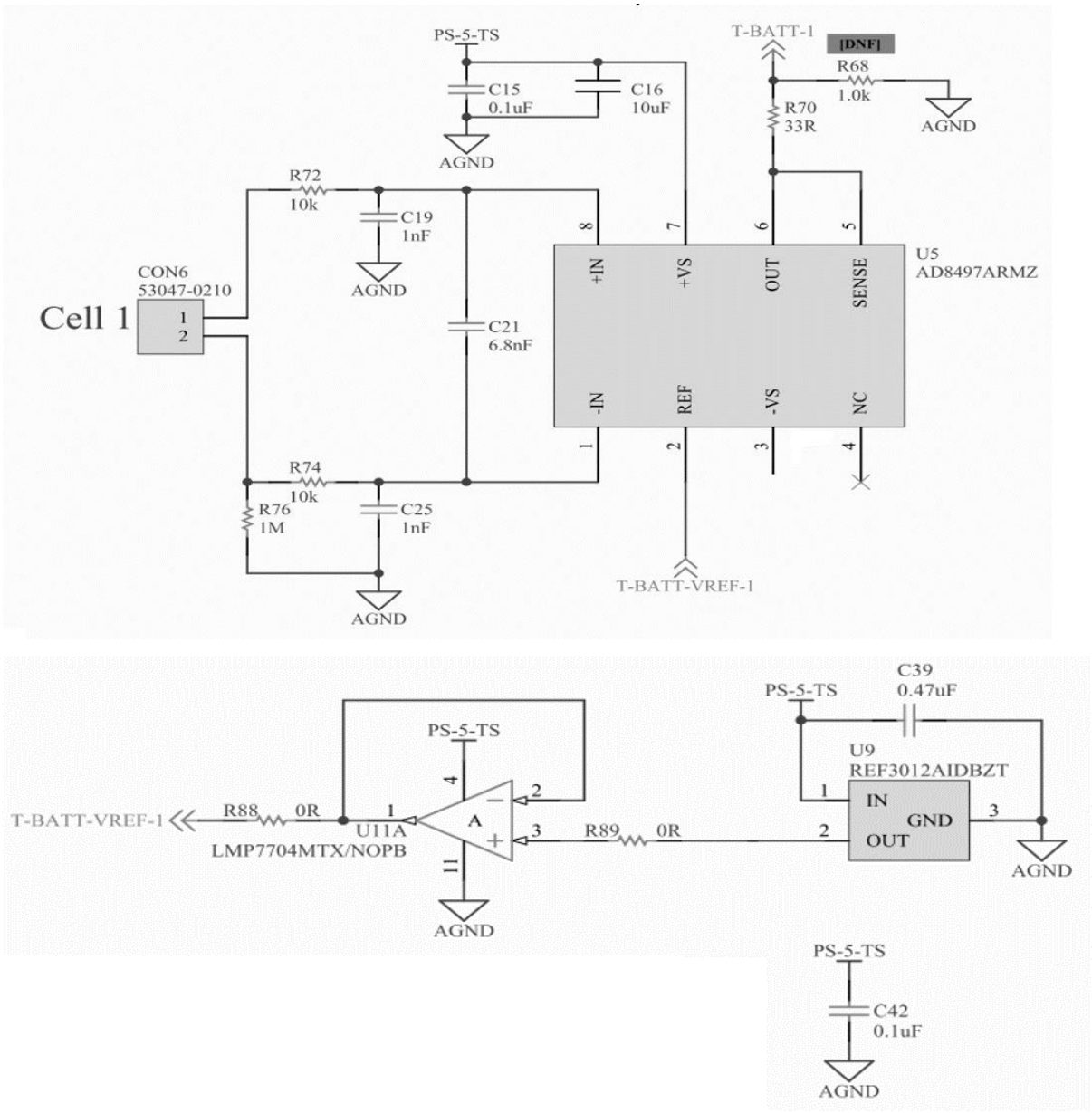


**Figure 6.1:** Temperature sensor circuit (1 AD8495 chip)

There will be six or eight AD8495 chips used to measure the temperatures in pairs on each Aluminium and ULTEM surface. Each AD8495 chip will measure the voltage of their respective connected thermocouples and produce an output based on the differential between the thermocouple voltage and the reference input (comparison between the “hot” and “cold/reference” junctions). The

differential voltage will be sufficiently amplified and then passed to the output pin to direct to the ADC pins on the OBC. The data can then be collected, processed and stored for future transmission to the ground station. The thermocouples utilised will be K-type with exposed welded tip, and temperature sensing range of -75$^{O}$C to 250$^{O}$C.


**Figure 6.2:** K-type thermocouple (left) and AD8495 ARMZ Thermocouple Amplifier (right)

The selection of the AD8495 is based on its ability to produce a high output for every degree change in temperature, and its low power consumption. Also, it has an operational temperature range of -40$^{O}$C to 125$^{O}$C that is sufficient based on the predicted temperature range experience by the CubeSat components [22].

The connection of the reference junction to the LMP7704 and REF3012 components would allow us to level shift the output to account for negative temperatures, while using a single power supply. If reference is connected straight to ground, an additional power supply would be required to produce negative voltage to account for negative temperature measurements, which would add complexity to the system hence the decision to utilise level shifting. The combination of the two 10kΩ resistors, 1.0nF and 6.8nF capacitors form a differential filter with a cutoff frequency of 1,100Hz (final cutoff frequency is to be decided).

The output from the temperature circuit can be fed to the on-board computer via ADC channels, and then stored and transmitted on the next pass over the ground station. GomSpace has provided the GomSpace Shell (GOSH) to present a console like environment for the user. GOSH enables us to send commands and set parameters of the A3200 [4]. The specific A3200 pins responsible for ADC inputs are specified in the GomSpace datasheet, and a diagram layout displayed below,

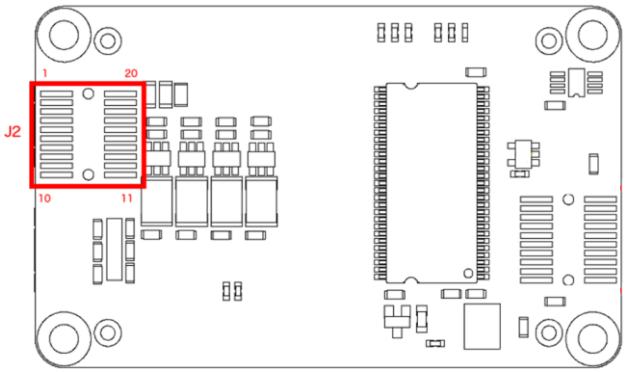


| A3200 Description | Connector ID | Connector PIN |
|---|---|---|
| I²C 2 SDA | J2 | 1 |
| I²C 2 SCL | J2 | 2 |
| AD0 | J2 | 7 |
| AD1 | J2 | 8 |
| AD2 | J2 | 9 |
| AD3 | J2 | 10 |
| AD4 | J2 | 11 |
| AD5 | J2 | 12 |
| AD6 | J2 | 13 |
| AD7 | J2 | 14 |

**Figure 6.3:** GomSpace A3200 pins for ADC input *[4]*

The NanoMind A3200 is fitted on the NanoDock DMC-3 panel, and the mentioned Pins (PA05 – PA11) will contact the metallic contacts from the A3200 with the ones on the DMC-3. The DMC-3 has header pins that connect to the I/O pins PA05 – PA11 and can therefore collect data from external components and transfer them to the A3200 on-board computer. The header pins and the table of connections are shown in the next figure,

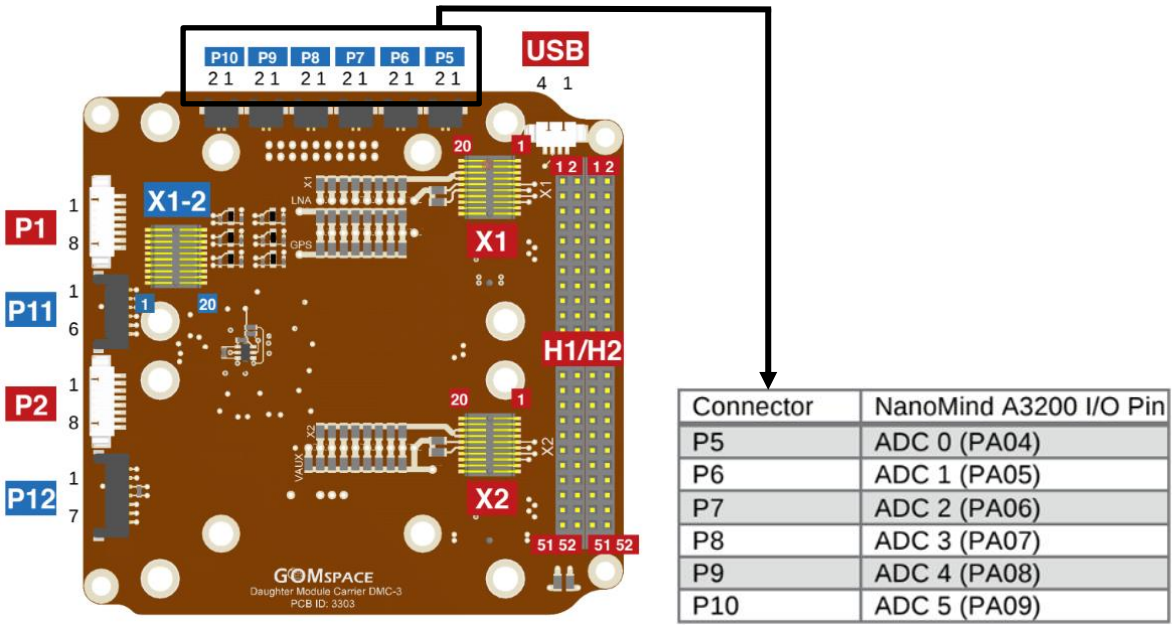


| Connector | NanoMind A3200 I/O Pin |
|---|---|
| P5 | ADC 0 (PA04) |
| P6 | ADC 1 (PA05) |
| P7 | ADC 2 (PA06) |
| P8 | ADC 3 (PA07) |
| P9 | ADC 4 (PA08) |
| P10 | ADC 5 (PA09) |

**Figure 6.4:** NanoDock DMC-3 ADC pin connectors *[3]*

Communication to and from the NanoCom AX100 can then occur through the USART pins on the main connector. The AX100 uses the CubeSat Space Protocol (CSP) to transfer data between the various subsystems on-board the CubeSat and between the CubeSat and the ground station. The USART pins are Pins 9 and 10 in the FSI main connector highlighted in the figure below,

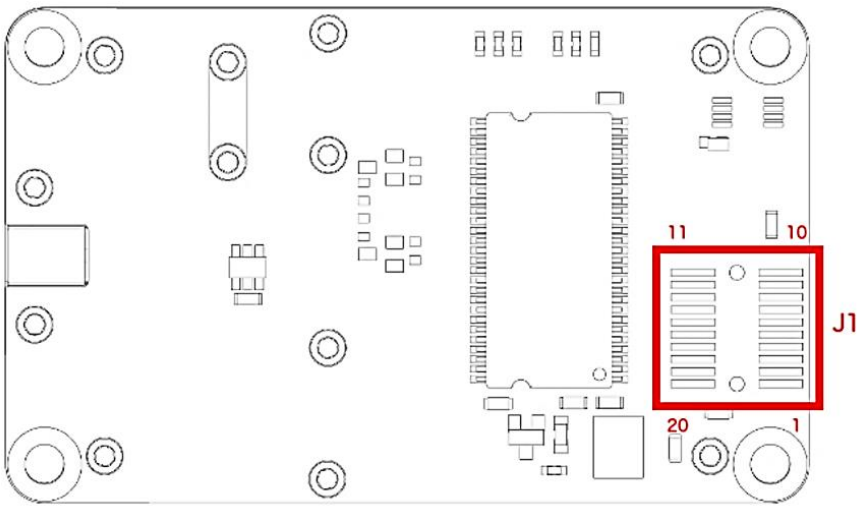


**Figure 6.5:** NanoCom AX100 bottom surface with FSI pins *[23]*

Now going back to the NanoDock DMC-3, it has 4 x 20 position FSI pin connectors and another 20-position pin connector for the A3200. In Figure 6.4 the connectors X1-2, X1 and X2 can be seen. There are X3 and X4 connectors on the bottom side of the DMC-3 panel as well. The communication layout of the connectors is as follows,

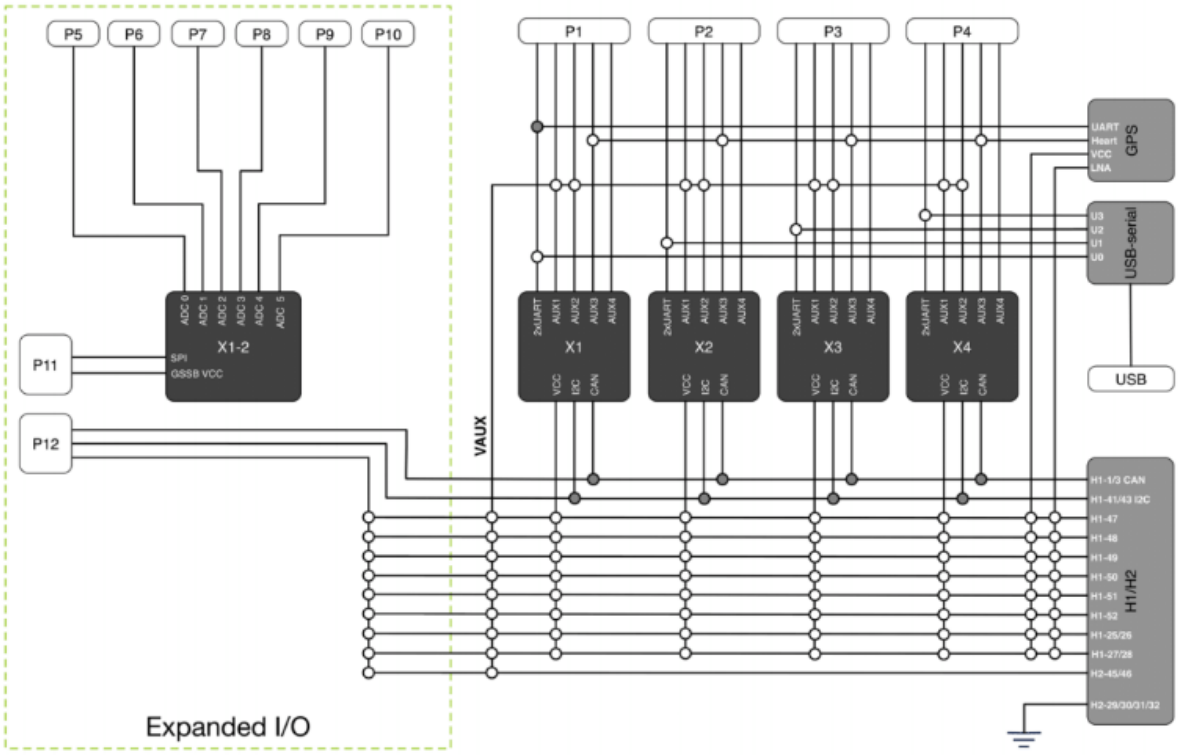


**Figure 6.6:** NanoDock DMC-3 connection block diagram *[3]*

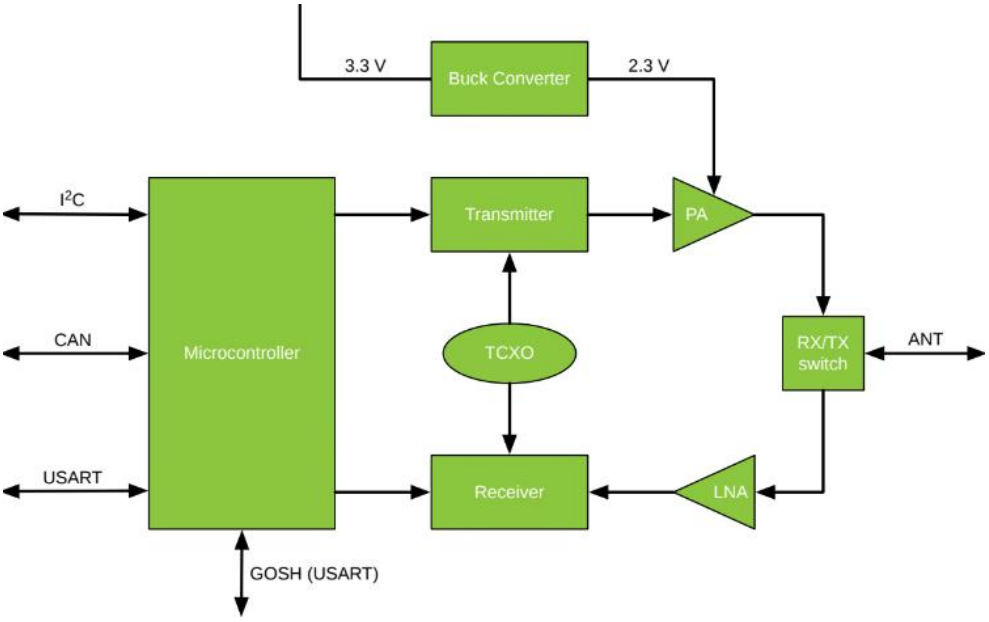


**Figure 6.7:** NanoCom AX100 operation block diagram [3]

# 7.0 Conclusion & Future Work

## 7.1 Conclusion

With the consistent use of conventional machining and Aluminium alloys, CubeSats of today have limited range in terms of structure and their functional layout. Also, with the need to limit weight due to the high density of the metallic alloys used in the CubeSat frame, the range of devices that can be mounted on various parts of the structure is limited as well. 3D Printing therefore provides the possibility of using a range of other materials that cannot be effectively machined with conventional techniques. It was noted that 3d printing is versatile enough to print complex satellite frames using space-qualified materials. Accordingly, printing using FDM and ULTEM was planned. ULTEM has sufficient strength and durability and lower densities than the conventional space qualifies Aluminium alloys. As highlighted before, 3D printing also efficiently develops shapes and features that would be difficult to achieve with conventional machining techniques. To ascertain the feasibility of 3D printing materials for use in Space, the experiments in this report test the strength of the materials based on launch conditions.

With regards to the design of the CubeSat, it depends on three factors – 1) design standards placed by the launcher, 2) optimising weight savings and fabrication efficiency within the current technology and 3) the CubeSat should be assembled and disassembled easily. Design limitations from launchers are placed to adapt to the launch methods.

The basic standards are that the dimensions of the main body of the CubeSat should be (10 x 10 x 10) cm. For a launcher that uses a POD based launch system, rails are designed around the CubeSat main body. It is also required that the rail surfaces of the CubeSat must be very smooth (< Ra 1.6 µm) to allow proper travel inside the POD which can be achieved only with specific Aluminium alloys. A POD based CubeSat design also requires the CubeSat have extensions of defined heights to provide space to install a trigger switch mechanism (which activates the CubeSat once it deploys) to fit properly in the POD. In fact, all launchers require a defined trigger switch mechanism which would require some design on the CubeSat. All considerations were taken in developing a model that can test both the reliability of ULTEM as a structure material and also permit the CubeSat to be used with any distinguished launcher.

The current model tested has considered minimising support material. The amount of support material required to develop each of the 6 ULTEM panels is less than 5% of the total volume of each panel. The model's bolt holes, indentations and corner radii were designed such that assembly and disassembly of the CubeSat frame should be simple and there are no sharp corners that can injure. However, the designs can still go through further improvements to reduce weight and reduce the

dependence on bolts to connect the pieces together. However, this would need advancements in 3D printing to allow better control in depositing material to build the model with minimal support material. The current design is sufficient to test the high stress endurance of ULTEM 9085 when it is used as the primary material to contain and interact with the payload.

The model was subjected to 30g vertical and 20g horizontal pressure forces to find the baseline response of the ULTEM panels. After more design reviews based on limitations placed by launchers, a second design version was developed and tested on ABAQUS with test parameters set by a reliable launcher. The results show that the hybrid ULTEM – Aluminium structure performs very well with minimal distortions and stresses.

After the computer simulations were completed, the actual test model was developed to be tested using small and large vibration exciters. The test model was developed in 3 parts as follows –

1. For 3D printing the ULTEM panels, a list of 3D printing agencies was listed and ranked based on location, reliability and versatility of services. The selected 3D printing company printed the ULTEM panels with some coordination with the project team, to ensure the model submitted for fabrication can meet both the design standards of the launcher and also the production limits of the 3D printer.
2. The Aluminium rails were also developed using conventional techniques, as Aluminium based 3D printing is not economical and viable to make an Aluminium part that is thin and durable enough to withstand the forces during launch.
3. Finally, the electronic panels (made up of the GomSpace equipment and the payload panel) were developed. Development of the electronic panels started with an intensive study of the parameters of the original panel eg. Mass, centre of gravity. Each dummy panel was made up of different sized plates and a mixture of metals, to ensure the final panel met the exact mass and centre of gravity characteristics of the original panel.

The final parts were then assembled together to complete the test CubeSat structure. A sturdy base was made with Acrylic to mount the CubeSat on the vibration exciter. Test were then carried out as per the parameters in Tables Table ***5.2*** and Table ***5.3***.

After the testing on the vibration exciter, the ULTEM panels were then inspected under a microscope to check for any major cracks or other material degradation due to the testing. If cracks are found, the panels have failed the test as any major cracks would affect the structural integrity of the CubeSat and jeopardise the mission. However, no cracks were found and only defects in the structure that occur during fabrication were observed. It is concluded that the structure survived the test launch vibrations with negligible damage, if any.

The payload of the CubeSat will be the temperature monitoring components and circuit, that will measure the temperatures of the Aluminium rails and ULTEM panels, for analysis to review the heat conductivity of these materials in space and while interacting with each other throughout the orbits. The payload panel was also designed to account for the constrained space inside the CubeSat frame. The wiring configuration between panels in the electronic stack was also modelled with Solidworks to look at it from a three dimensional view.

3D printing a material might create different properties of the material as compared to the material in standard form, and the thermal conductivity might be one of the basic properties that would be affected. The difference in properties is caused mainly due to voids and pores present in the microstructure of the ULTEM panels, as described in 5.3.1. Thermal conductivity is a very essential property to consider materials for Space due to the extreme temperature variations spacecraft experience regularly. The payload can assist to some degree in finding the thermal performance of ULTEM in Space. Checking the temperature variations around the CubeSat to ensure the heat is distributed considerably throughout the structure would ensure heat is not localised to an extreme degree on any one side of the CubeSat at any time during its orbit.

The total work accomplished opens the following possibilities –

1. It is possible to design a customised CubeSat structure with different shapes unique to the capabilities of 3D printing
2. The materials used with 3D printing can withstand the launch vibrations, if coupled with a metallic alloy. More research needs to be done on a model that is completely 3D printed with minimal support material.
3. There are defects and limitations to achieving 3D printed materials that have properties similar to the same material in bulk form. As 3D printing techniques evolve, the defects can be minimised further to fabricate more reliable parts.
4. 3D printed structures can also serve as support structures to mount inside sturdier frames, and these support structures can hold devices that would be difficult to mount on conventionally made frames or developing the frame to contain the devices might be difficult to achieve through conventional fabrication methods.

## 7.2 Future Work

Future work on the CubeSat revolves around the build-up of the electronics, completion of the payload electronics, thermal testing of the structure and final testing of the CubeSat before launch. Some GomSpace components require software upgrades and reconfiguration before being implemented in the electronic stack.

The build up of the GomSpace components consists of connecting the electronic panels through designated pins to coordinate power and data to and from the payload. The programming of the components is done with FreeRTOS and Linux Terminal coding. Based on the manuals provided by GomSpace, the communication parameters of the AX100 transmitter can be set, and the task list of the CubeSat to be executed during its orbit is programmed on the A3200 on-board computer. The final configuration is tested to ensure all the electronics work as required after deployment from the launcher.

Thermal testing of the CubeSat is required to confirm the systems are able to survive the thermal cycles present in Space. This is a pre-test scenario of the temperature endurance of the CubeSat, along with the payload systems which find the temperature variations across the structure during orbit.

Before launch, all the structural components are fabricated again and the whole structure is re-assembled, tested and loaded into the launcher.

The general timetable for future work is as follows –

| **Activity** | **Jul – Sep ‘19** | **Oct – Nov ‘19** | **Dec – Jan ‘20** | **Feb – Mar ‘20** | **May – Jul ‘20** |
|---|---|---|---|---|---|
| Upgrade of GomSpace component software | | | | | |
| Programming of GomSpace crucial components | | | | | |
| Final fabrication, assembly and qualification | | | | | |
| Final discussions and administrations pre-launch | | | | | |
| Possible satellite launch | | | | | |

Further research is required to optimise the structural layout of the CubeSat to limit the number of bolts required. In the model developed for this project, the support material for 3D printing the parts was minimised to shorten the time required to make the model and limit the wastage of materials. However, with further advancements in 3D printing technology and possibly other techniques, shapes can be developed that limit both the number of bolts as well as the support material. This serves to reduce both the fabrication time and the assembly or disassembly time.

With regards to the analysis on the response of the structure in the extremes of space, more research may be carried out on developing a payload that can detect the distortions in the structure as it proceeds through its orbit and thermal cycles. This can be especially important if there are less bolts involved in keeping the structure together, as the differences between the Aluminium and ULTEM can be more exposed due to the limited fixed contact points.

# 8.0 Bibliography


[1] "About CubeSats," Innovative Solutions in Space (ISIS), [Online]. Available: https://www.isispace.nl/cubesats/. [Accessed 2 Jun 2018].

[2] E. Kulu, "Nanosatellite & CubeSat Database," [Online]. Available: http://www.nanosats.eu. [Accessed 10 October 2018].

[3] G. A/S, "NanoDock Motherboard DMC-3 Datasheet: Daughter module carrier for 4 daughterboards," [Online]. Available: https://gomspace.com/UserFiles/Subsystems/datasheet/gs-ds-nanodock-dmc-3-19.pdf. [Accessed 19 September 2018].

[4] G. A/S, "NanoMind A3200 Datasheet: On-board Computer System for mission critical space applications," [Online]. Available: https://gomspace.com/UserFiles/Subsystems/datasheet/gs-ds-nanomind-a3200-114.pdf. [Accessed 15 September 2018].

[5] G. A/S, "P110 Datasheet," [Online]. Available: https://gomspace.com/UserFiles/Subsystems/datasheet/gs-ds-nanopower-p110-29.pdf. [Accessed 2 October 2018].

[6] G. A/S, "NanoPower Power Packs: Descriptions of GomSpaces Power Packs for 1U, 2U and 3U," [Online]. Available: https://gomspace.com/UserFiles/Subsystems/datasheet/gs-ds-nanopower-powerpack-12.pdf. [Accessed 21 September 2018].

[7] G. A/S, "NanoCom ANT430 Datasheet: 70 cm band Omnidirectional UHF CubeSat antenna," [Online]. Available: https://gomspace.com/UserFiles/Subsystems/datasheet/gs-ds-nanocom-ant430-34.pdf. [Accessed 2 October 2018].

[8] S. S. Laboratory, "TIsat-1: Structures, Mechanics and Materials," [Online]. Available: http://www.spacelab.dti.supsi.ch/tiSat1.html. [Accessed 5 October 2018].

[9] S. Electronics, "Mini Microswitch - SPDT (Lever, 2-pack)," [Online]. Available: https://www.sparkfun.com/products/13013. [Accessed 5 October 2018].

[10] M. Wada, "A Bridge Connecting Humans and Space," Japan Aerospace Exploration Agency (JAXA), [Online]. Available: http://global.jaxa.jp/article/2014/interview/vol86/. [Accessed 25 September 2018].

[11] J. A. E. A. (JAXA), "JEM Small Satellite Orbital Deployer (J-SSOD)," [Online]. Available: http://iss.jaxa.jp/en/kiboexp/jssod/. [Accessed 25 September 2018].

[12] ISRO, "Polar Satellite Launch Vehicle," [Online]. Available: https://www.isro.gov.in/launchers/pslv. [Accessed 8 July 2019].

[13] B. Yusuf, "All 10 Types of 3D Printing Technology in 2018," [Online]. Available:

https://all3dp.com/1/types-of-3d-printers-3d-printing-technology/. [Accessed 1 October 2018].

[14] M. S. University, "PrintSat," 2015. [Online]. Available: https://ssel.montana.edu/printsat.html.

[15] R. Clinton, "NASA's In Space Manufacturing Initiatives," 2017. [Online].

[16] J. T. Inc., "Ultem 9085," [Online]. Available: https://www.javelin-tech.com/3d/stratasys-materials/ultem-9085/. [Accessed 15 May 2018].

[17] Y. Shin, Y. Seyoung, S. Yongmyung and J. Ho, "Radiation effect for a CubeSat in slow transition from the Earth to the Moon," Advances in Space Research, 2015.

[18] C. Pollier, "System design and orbit analysis for SpooQySat-1," 2016.

[19] W. Larson, Space Mission Analysis and Design, El Segundo, California: Microcosm Press, 2010.

[20] JAXA, "JEM Payload Accommodation Handbook - Vol. 8," Japan Aerospace Exploration Agency, 2013.

[21] E. S. Agency, "General Requirement for Outgassing," [Online]. Available: http://esmat.esa.int/Services/outgassing_data/outgassing_data.html. [Accessed 14 May 2019].

[22] J. Friedel, Thermal Analysis of the CubeSat CP3 Satellite, California Polytechnic State University, 2011.

[23] G. A/S, "NanoCom AX100 Datasheet: Long-range software configurable VHF/UHF transceiver," [Online]. Available: https://gomspace.com/UserFiles/Subsystems/datasheet/gs-ds-nanocom-ax100-33.pdf. [Accessed 19 September 2018].

[24] B. Yost, "Structures, Materials and Mechanisms," NASA State of the Art Report of Small Spacecraft Technology, 2018. [Online]. Available: https://sst-soa.arc.nasa.gov/06-structures-materials-and-mechanisms. [Accessed 4 October 2018].

[25] Stratasys, "Stratasys Direct Manufacturing Builds the First 3D Printed Parts to Function on the Exterior of a Satellite," [Online]. Available: https://www.stratasysdirect.com/resources/case-studies/3d-printed-satellite-exterior-nasa-jet-propulsion-laboratory. [Accessed 24 September 2018].

[26] NASA, "CubeSat 101," *NASA CubeSat Launch Initiative*, 2017.

[27] M. Matney, "How to Calculate the Average Cross Sectional Area," *The Orbital Debris, Volume 8, Issue 2*, 2004.

# Appendix A: ABAQUS Vibration Model Results

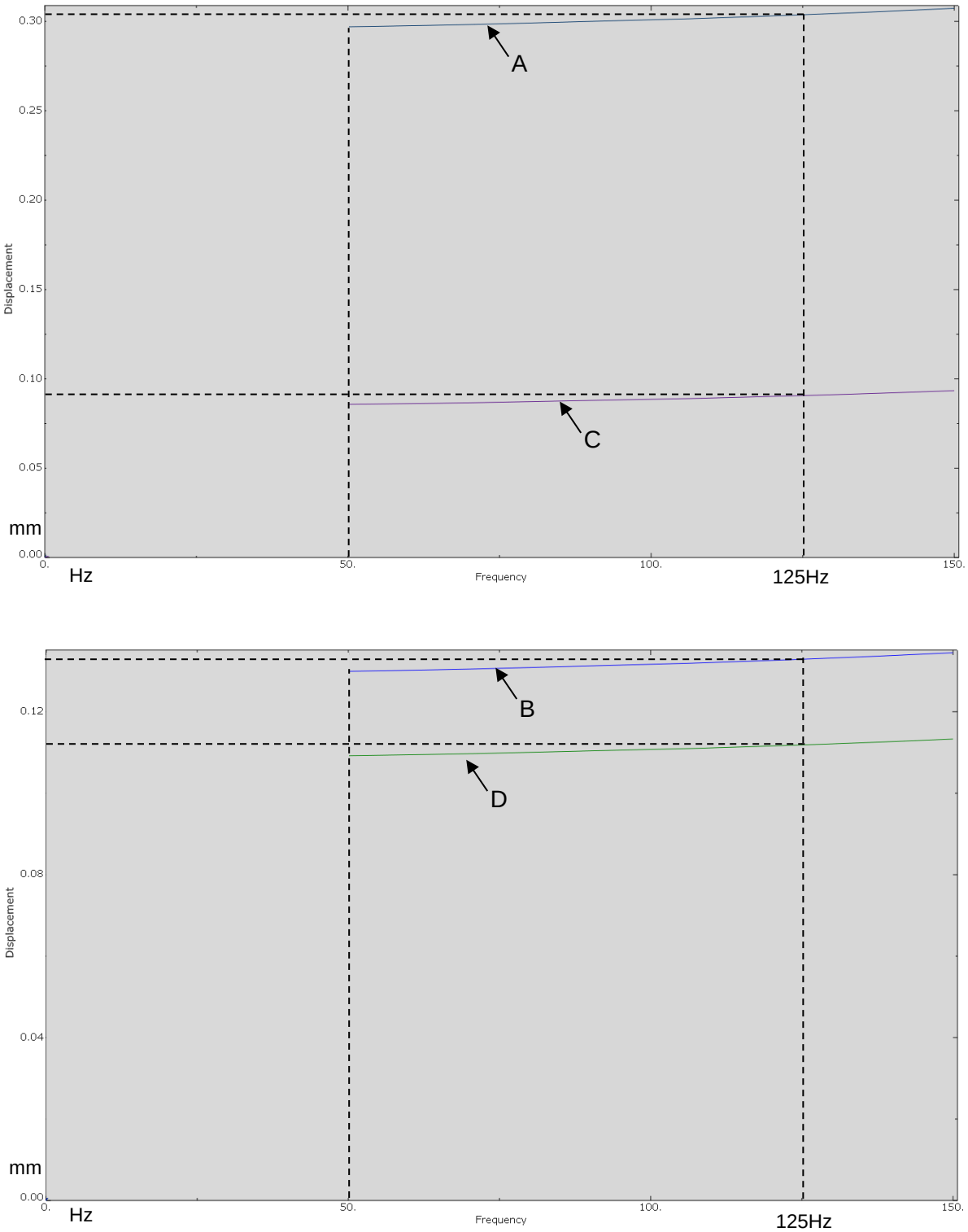


**Figure A-1:** Displacement response to 20G side frequency-based application

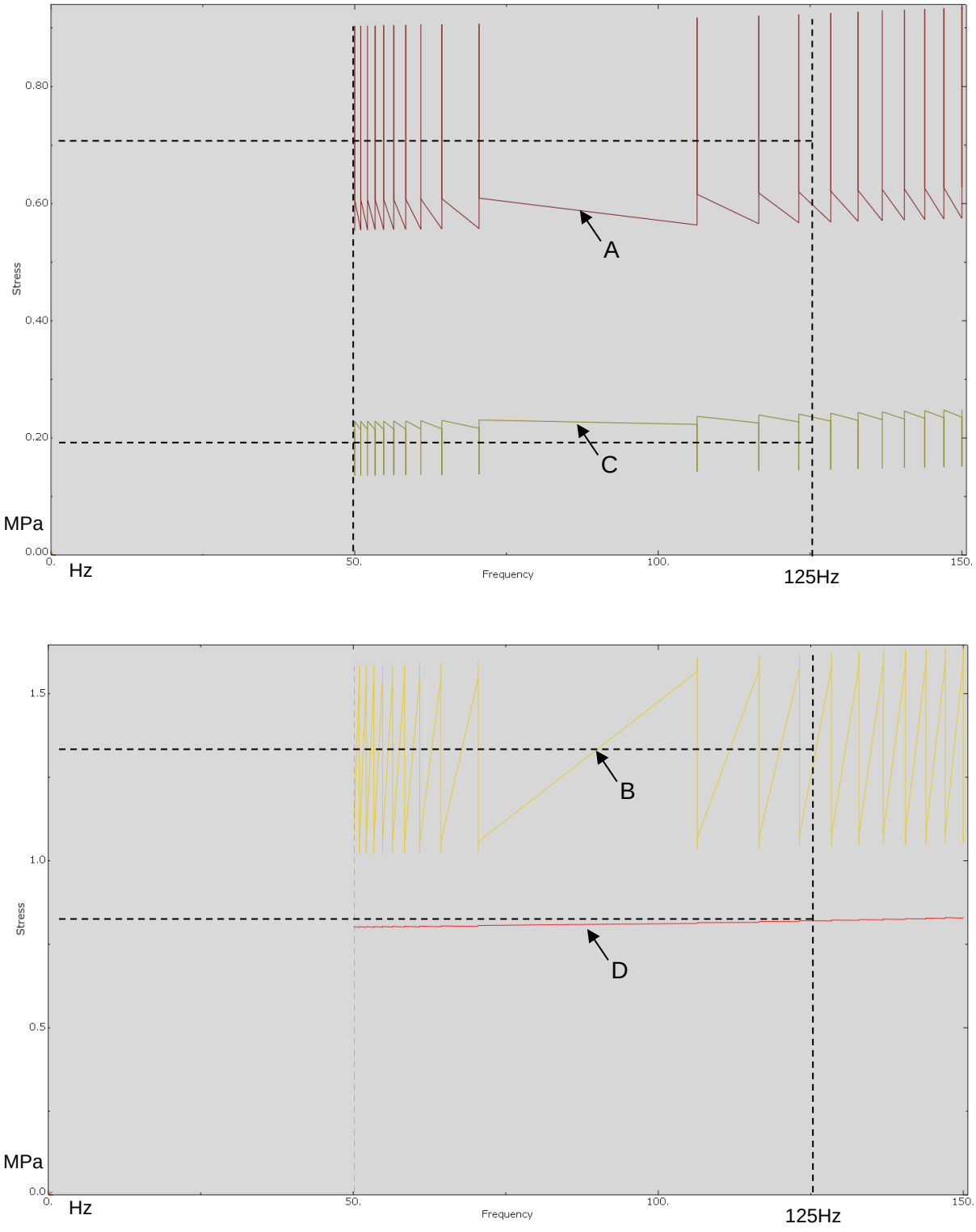


**Figure A-2:** Displacement response to 20G side frequency-based application

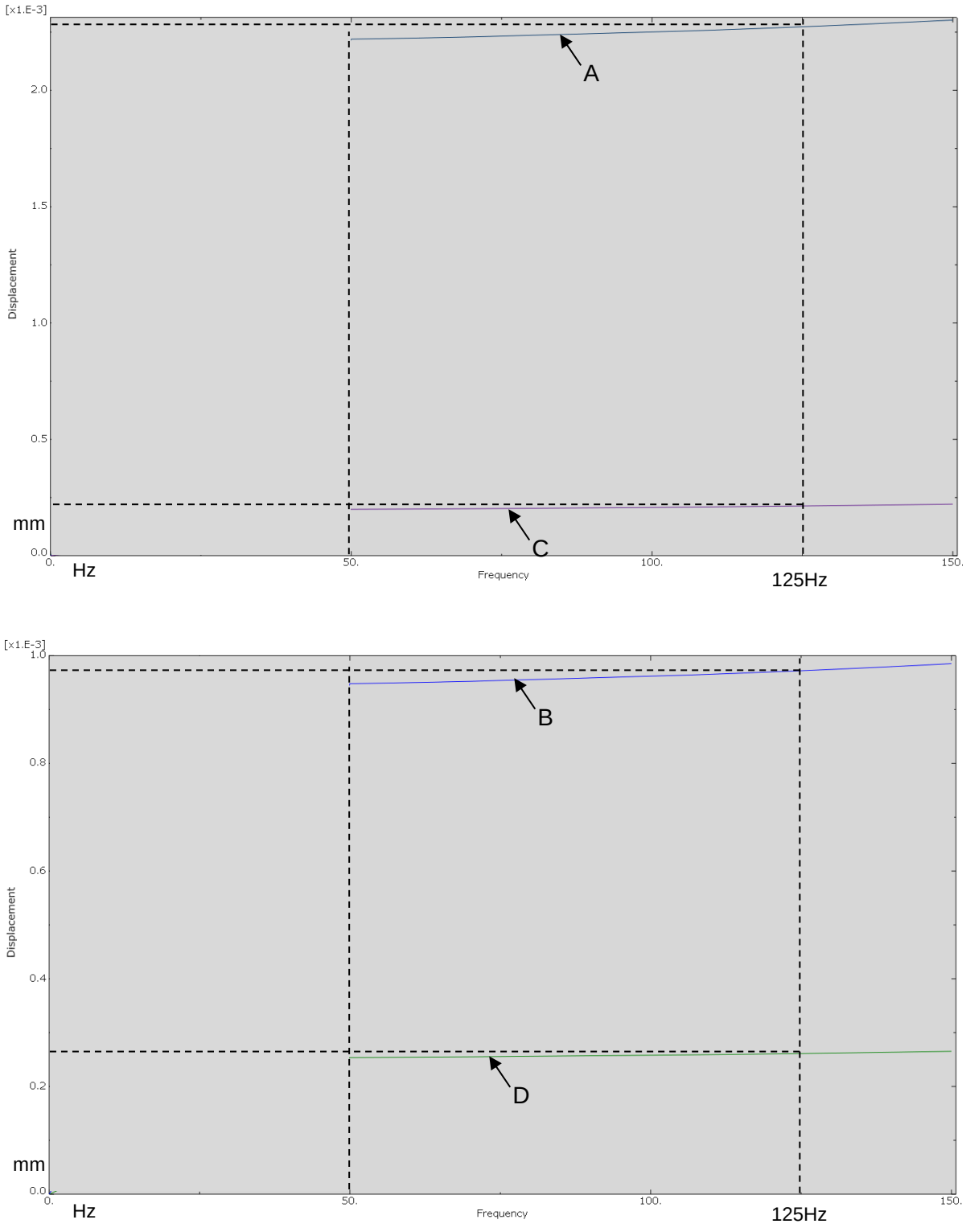


**Figure A-3:** Displacement response to 30G vertical frequency-based application

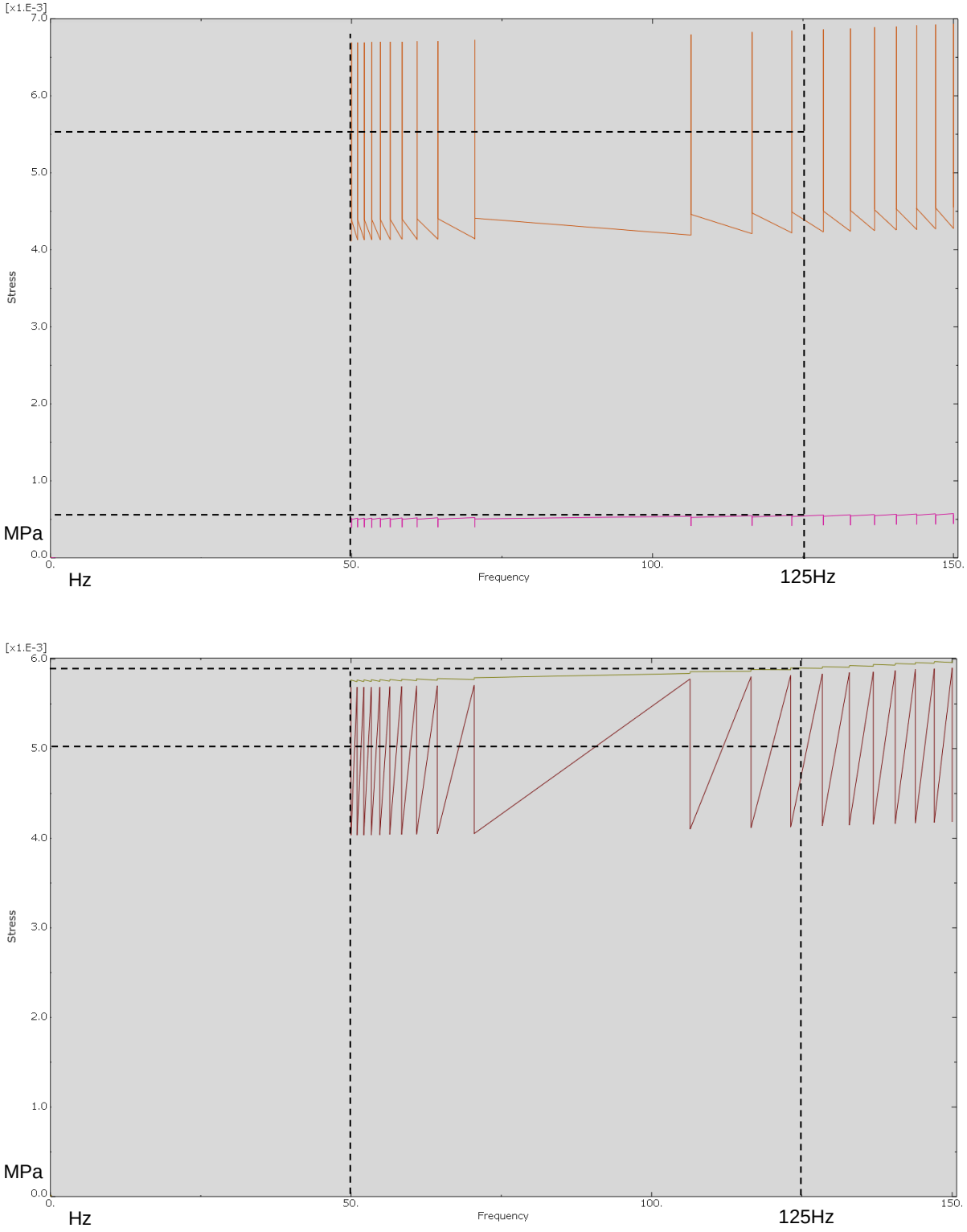


**Figure A-4:** Stress response to 30G vertical frequency-based application

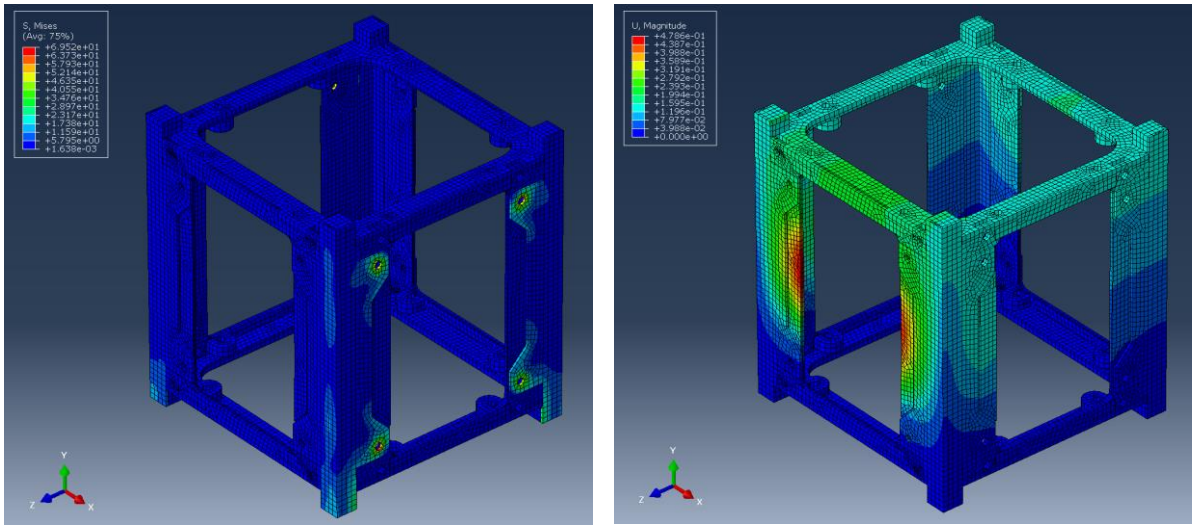


**Figure A-5:** Contours for steady state modal frequency analysis for 20G side vibrations, bottom fixed, Stress contours (left) and Displacement contours (right)

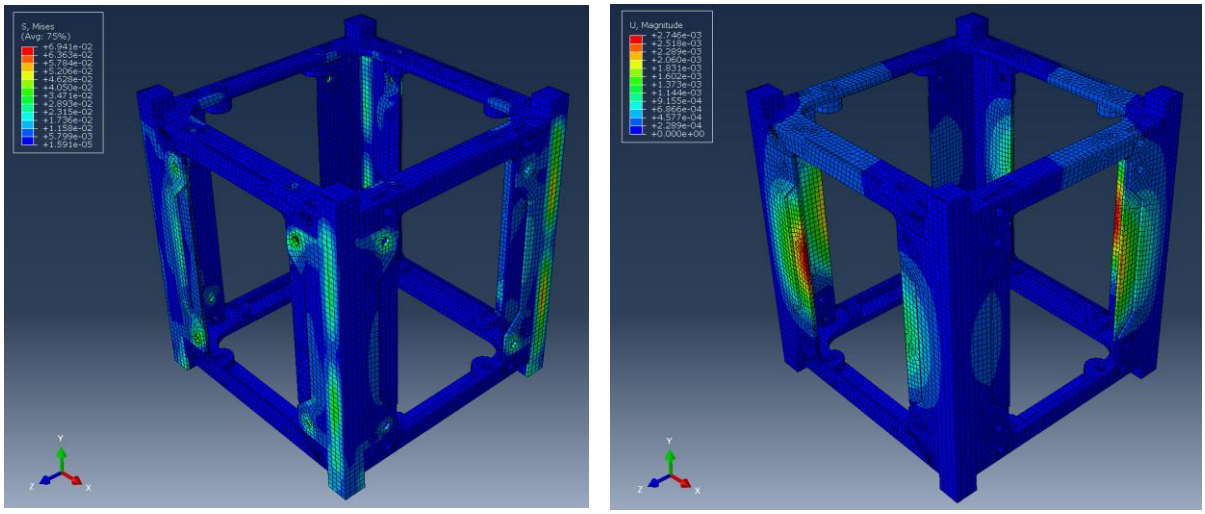


**Figure A-6:** Contours for steady state modal frequency analysis for 30G vertical vibrations, bottom fixed, Stress contours (left) and Displacement contours (right)

# Appendix B: MATLAB Code for Tumbling

```
% Average incoming power for a tumbling CubeSat

clear all
close all
clc
alt = 400;
t1 = 1711.1;
t2 = 3842.4;
solar_constant = 1367; %incoming solar heat
k = 2;
mu = 398600;
a = 6378+ alt;
n = sqrt(mu/a^3);
P = 2* pi()/n;
t0 =0;
dt = 1;
t=t0 : 1 : k*P;
cell_eff=0.30;
Id = 0.9;
cells_1U_side = 2;

current_cell=0.5044;
number_of_cell_strings=1;
number_of_cell_strings_two=1;
cell_area = 0.003018; % m^2
area_1U = cells_1U_side * cell_area;
total_surface_area = 5 * area_1U;
average_cell_area = (1/4) * total_surface_area;

battery(1) = 38.5; %Watt-hour

for j=1:length(t)

    if t(j) <= 1711.1
        Power_usage(j) = 0.672; %W
```

```
    else if t(j) <= 4773.4 && t(j) >= 1711.1
        Power_usage (j) = 0.672; %W

      else if t(j) >= 4773.4 && t(j) <= P
          Power_usage (j) = 4.12; %W

        else if t(j) >= P && t(j) <= 2*P
            Power_usage (j) = 0.672; %W
          end
        end
      end
    end
end

for j=2: length(t)

    if t(j) <= t1 || t(j) >= t2 && t(j) <= P+t1 || t(j) >= P+t2 && t(j) <= 2*P
      I(j) = abs(average_cell_area * cell_eff * 0.9 * 0.97 * 0.957 * solar_constant * cos(mod(n* t(j), 2*pi())));

    else
      I(j) = 0;
    end

    battery(j) =battery(j-1)+(- Power_usage (j)* dt/3600+ I(j)* dt/3600); %[Wh]
    if battery(j) > battery(1)
      battery(j)=battery(1) ;
    end
end

figure(1)
plot(t, I, 'Color', [0 0.75 1])
xlabel('t[s]')
ylabel('Average incoming power [W]')
title('Average incoming power over time , Case IV')

figure(2)
plot(t, battery, 'Color', [0.98, 0.47, 0])
title('Battery capacity remaining vs time for Case IV (alt = 400 km, i = 51.65°)');
xlabel('Time [s]');
```

```
ylabel('Battery capacity remaining [Wh]');

figure(3)
plot(t, P_usage)
xlabel('Time [s]')
ylabel('Power [W]')
title('Power usage and incoming power for Case IV (alt = 400 km, i = 51.65°)')
legend('Power usage [W]')
```

## Appendix C: Functional Diagrams

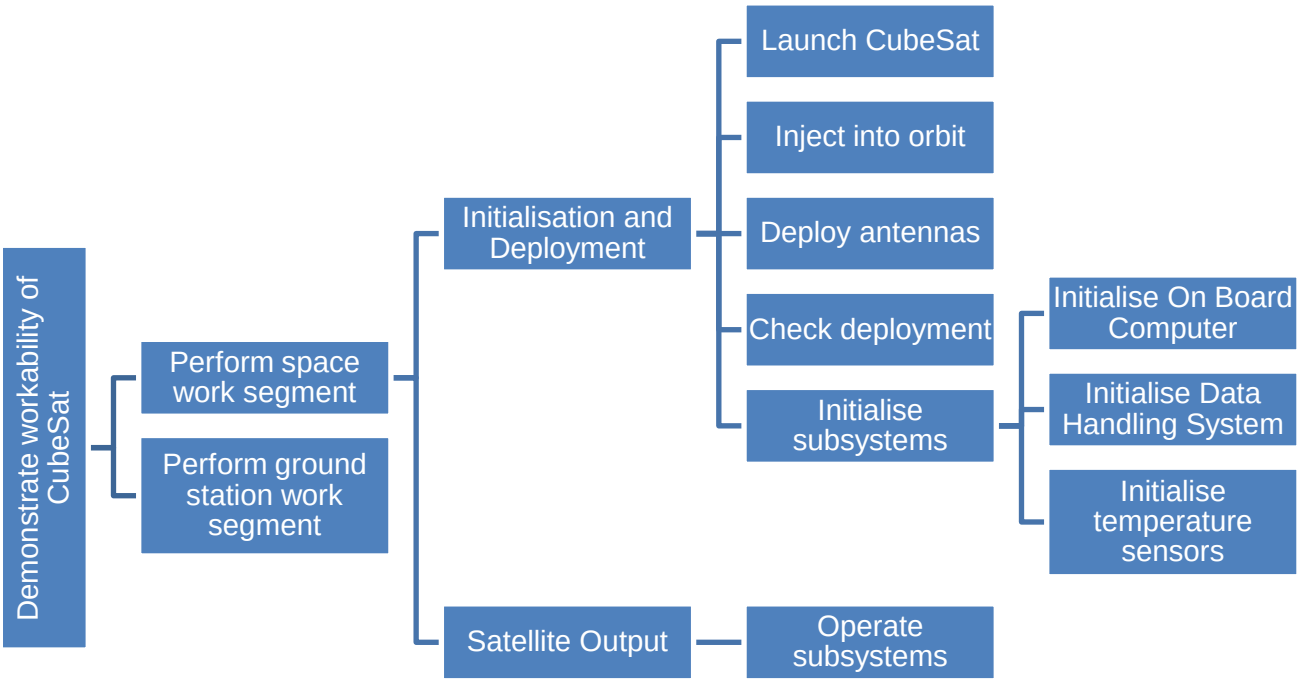


**Figure C-1:** Main functional block diagram

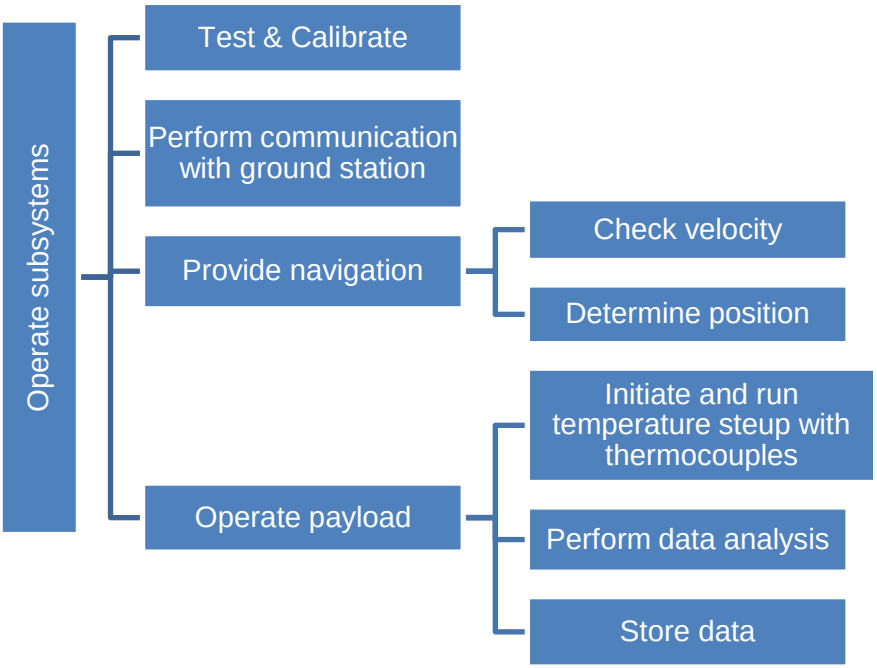


**Figure C-2:** Subsystems operation block diagram

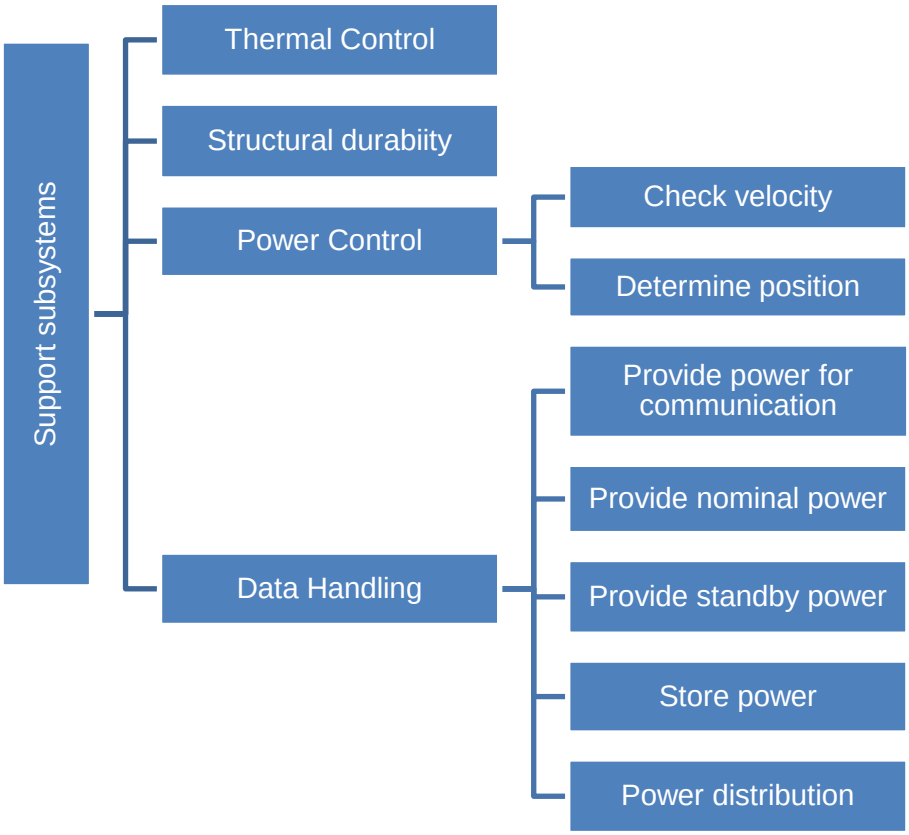


**Figure C-3:** Support subsystems operation block diagram

# Appendix D: STK Analysis of Orbit

**Facility-Groundstation-To-Satellite-Satellite2: Inview Azimuth, Elevation, & Range**

**Groundstation-To-Satellite2 - AER reported in the object's default AER frame**

| Time (UTCG) | Azimuth (deg) | Elevation (deg) | Range (km) |
|---|---|---|---|
| 21 Sep 2018 03:21:14.388 | 32.122 | 0.000 | 2294.748166 |
| 21 Sep 2018 03:22:14.000 | 43.052 | 0.855 | 2201.458728 |
| 21 Sep 2018 03:23:14.000 | 54.621 | 1.024 | 2183.354830 |
| 21 Sep 2018 03:24:14.000 | 65.971 | 0.463 | 2243.389417 |
| 21 Sep 2018 03:24:40.852 | 70.783 | 0.000 | 2294.236639 |
| 21 Sep 2018 04:53:58.850 | 324.121 | 0.000 | 2294.695483 |
| 21 Sep 2018 04:54:58.000 | 324.080 | 4.086 | 1884.685793 |
| 21 Sep 2018 04:55:58.000 | 323.977 | 9.505 | 1471.381635 |
| 21 Sep 2018 04:56:58.000 | 323.743 | 17.655 | 1066.524498 |
| 21 Sep 2018 04:57:58.000 | 323.096 | 33.044 | 688.476882 |
| 21 Sep 2018 04:58:58.000 | 318.108 | 71.153 | 421.193117 |
| 21 Sep 2018 04:59:58.000 | 147.528 | 51.953 | 498.971661 |
| 21 Sep 2018 05:00:58.000 | 145.818 | 25.595 | 829.709309 |
| 21 Sep 2018 05:01:58.000 | 145.361 | 13.979 | 1222.230922 |
| 21 Sep 2018 05:02:58.000 | 145.133 | 7.170 | 1631.500122 |
| 21 Sep 2018 05:03:58.000 | 144.981 | 2.352 | 2046.268623 |
| 21 Sep 2018 05:04:33.584 | 144.907 | 0.000 | 2293.061737 |
| 21 Sep 2018 06:34:11.381 | 247.595 | 0.000 | 2293.520003 |
| 21 Sep 2018 06:35:11.000 | 236.575 | 0.581 | 2229.618438 |
| 21 Sep 2018 06:36:11.000 | 225.224 | 0.470 | 2241.488289 |
| 21 Sep 2018 06:36:51.988 | 217.709 | 0.000 | 2293.114381 |
| 21 Sep 2018 16:27:46.935 | 203.065 | 0.000 | 2292.960166 |
| 21 Sep 2018 16:28:46.000 | 200.010 | 3.932 | 1897.057130 |
| 21 Sep 2018 16:29:46.000 | 195.255 | 8.980 | 1504.478955 |
| 21 Sep 2018 16:30:46.000 | 187.020 | 15.939 | 1134.239071 |
| 21 Sep 2018 16:31:46.000 | 170.271 | 26.017 | 819.984089 |
| 21 Sep 2018 16:32:46.000 | 133.872 | 35.620 | 651.112426 |
| 21 Sep 2018 16:33:46.000 | 90.514 | 30.152 | 736.556803 |
| 21 Sep 2018 16:34:46.000 | 68.223 | 19.115 | 1013.803483 |

| Time (UTCG) | Azimuth (deg) | Elevation (deg) | Range (km) |
|---|---|---|---|
| 21 Sep 2018 16:35:46.000 | 57.882 | 11.167 | 1370.372326 |
| 21 Sep 2018 16:36:46.000 | 52.257 | 5.566 | 1757.678316 |
| 21 Sep 2018 16:37:46.000 | 48.774 | 1.265 | 2158.084080 |
| 21 Sep 2018 16:38:06.223 | 47.884 | 0.000 | 2294.551851 |
| 21 Sep 2018 18:05:32.545 | 263.638 | 0.000 | 2293.794757 |
| 21 Sep 2018 18:06:32.000 | 272.848 | 2.400 | 2042.369490 |
| 21 Sep 2018 18:07:32.000 | 284.439 | 4.480 | 1849.364697 |
| 21 Sep 2018 18:08:32.000 | 298.146 | 5.801 | 1738.452274 |
| 21 Sep 2018 18:09:32.000 | 312.888 | 5.960 | 1725.824595 |
| 21 Sep 2018 18:10:32.000 | 326.989 | 4.902 | 1813.392851 |
| 21 Sep 2018 18:11:32.000 | 339.161 | 2.975 | 1987.449212 |
| 21 Sep 2018 18:12:32.000 | 349.026 | 0.619 | 2227.020503 |
| 21 Sep 2018 18:12:47.028 | 351.158 | 0.000 | 2294.87 |

# Appendix E: Vibration Exciter Charts

## Sinusoidal Vibration Parameters in Z-direction

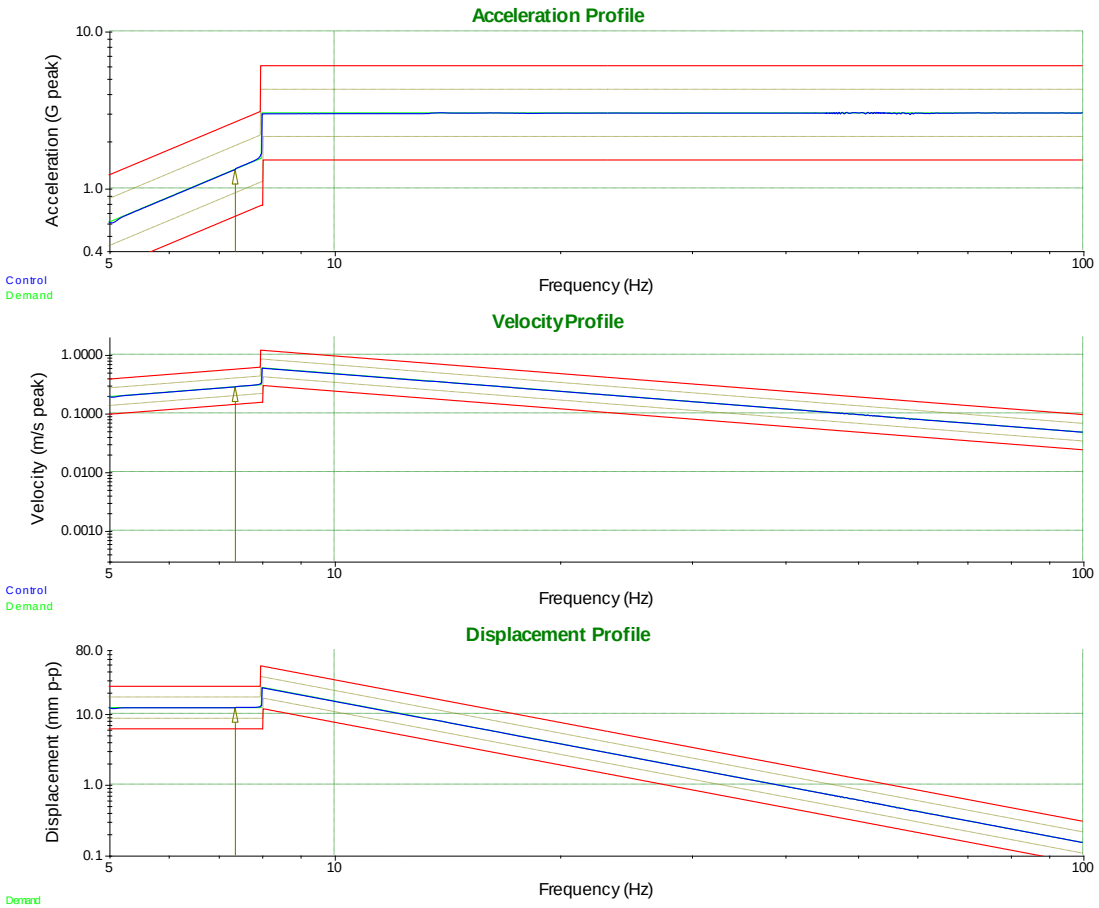


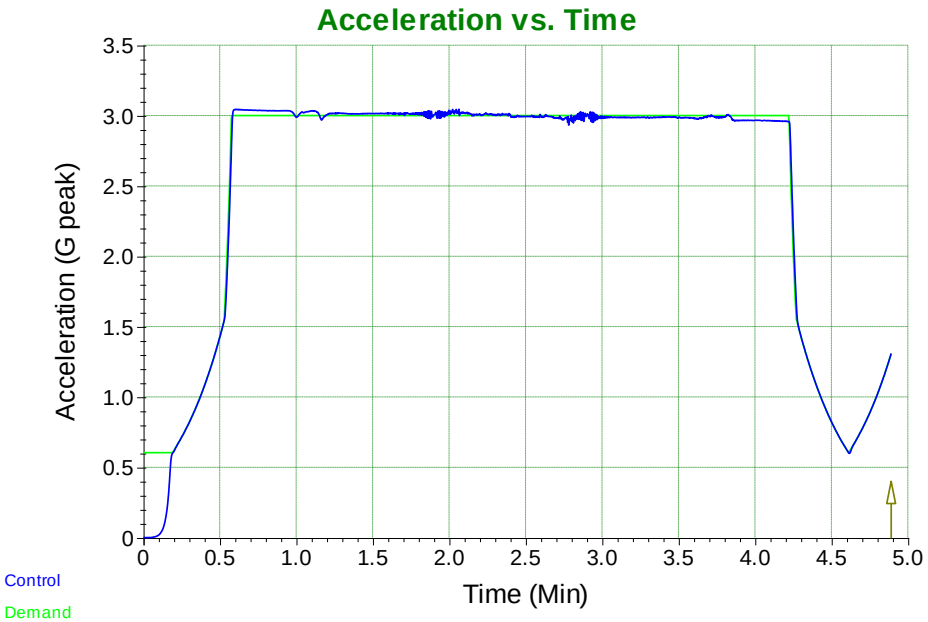

## Sinusoidal Vibration Parameters in Y-direction

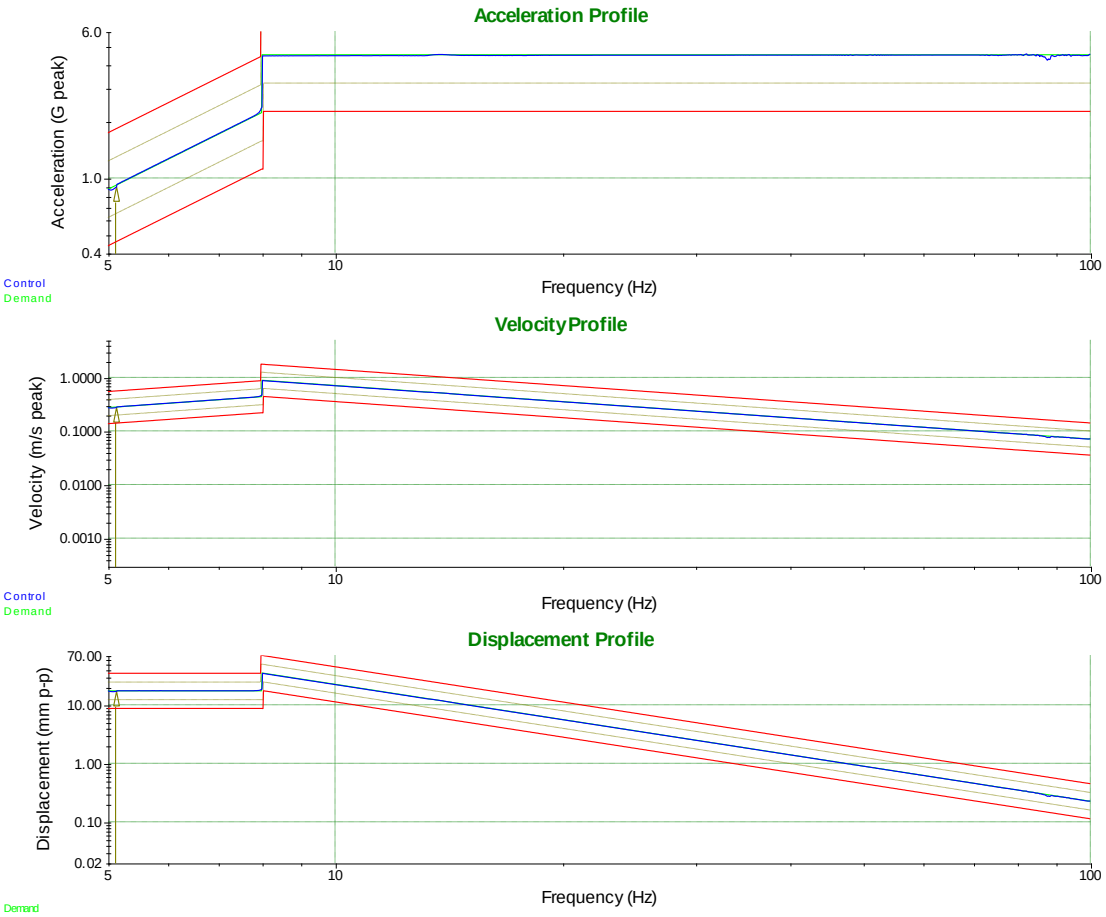


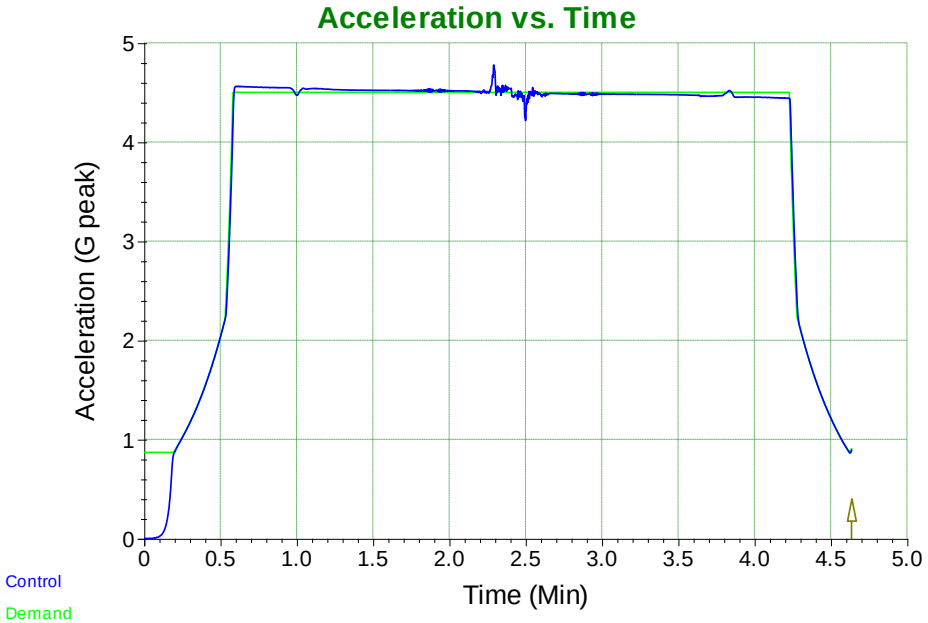

# Appendix F: Random Vibration Results

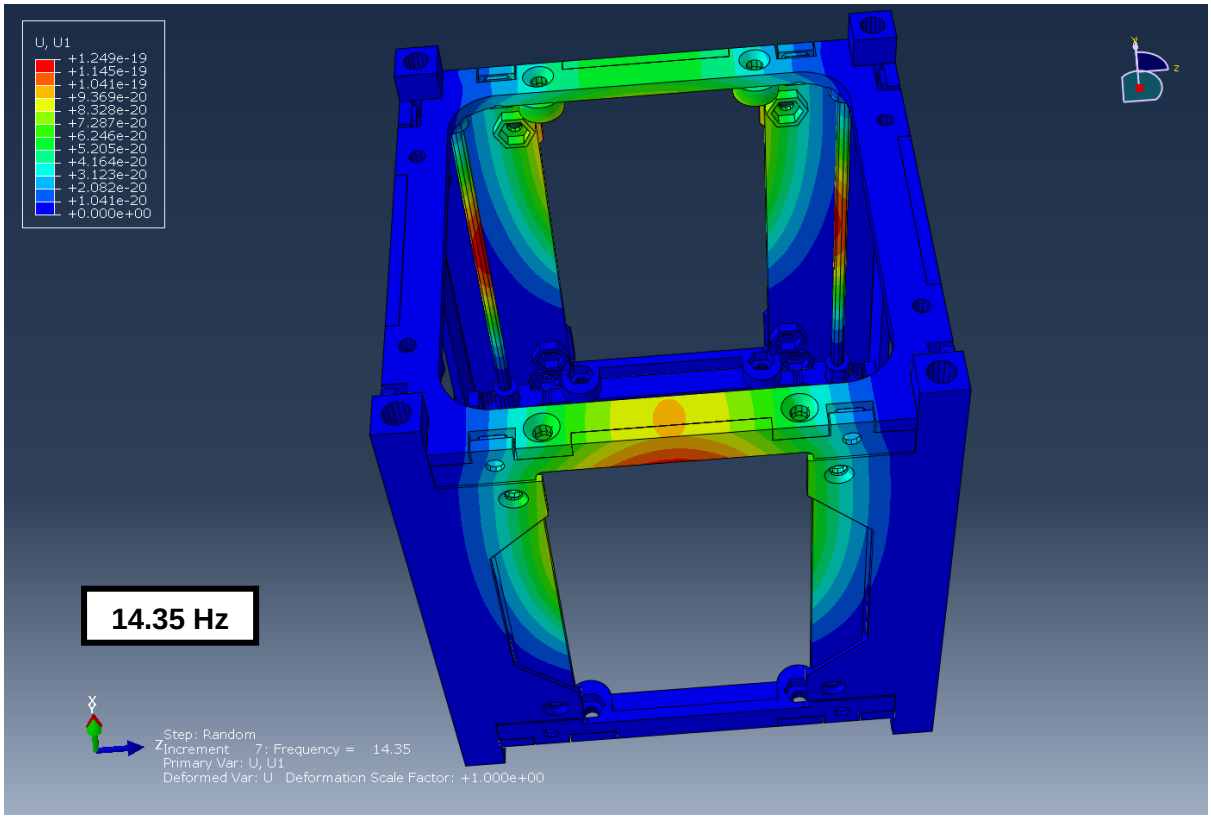


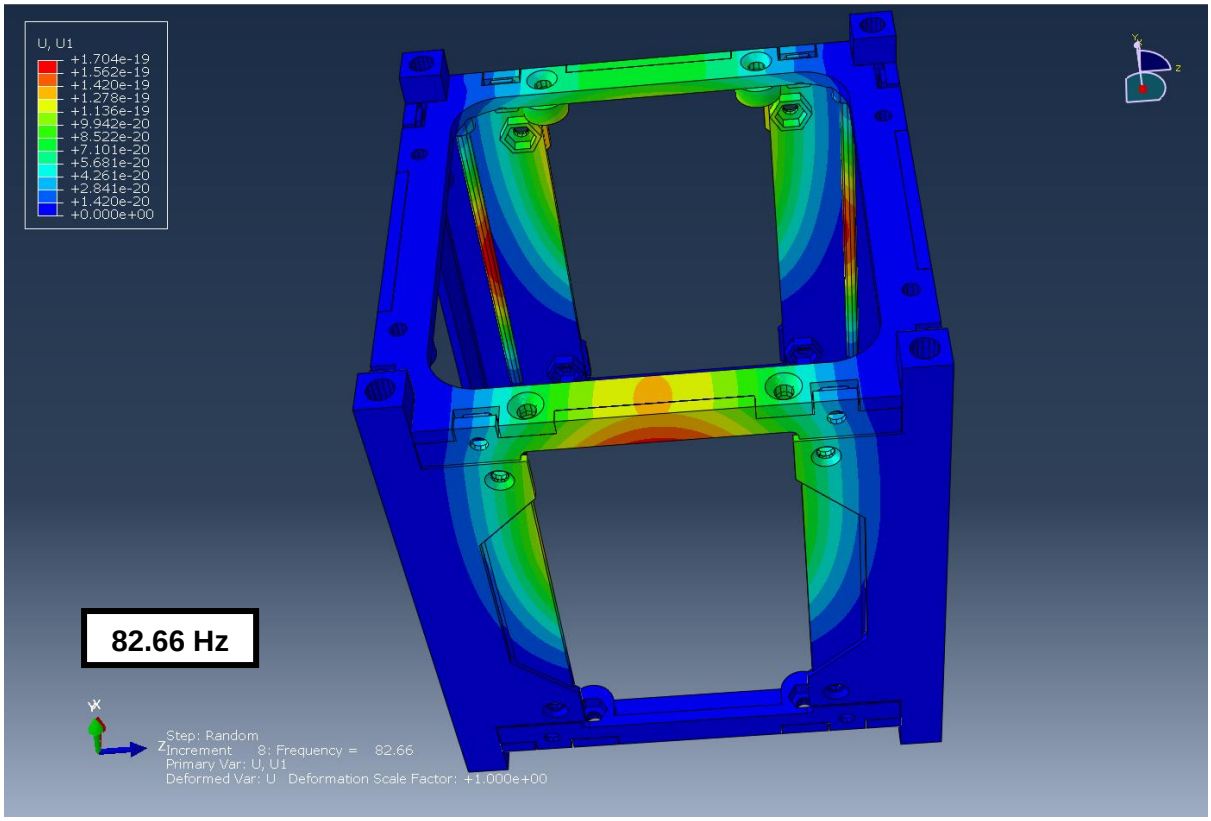

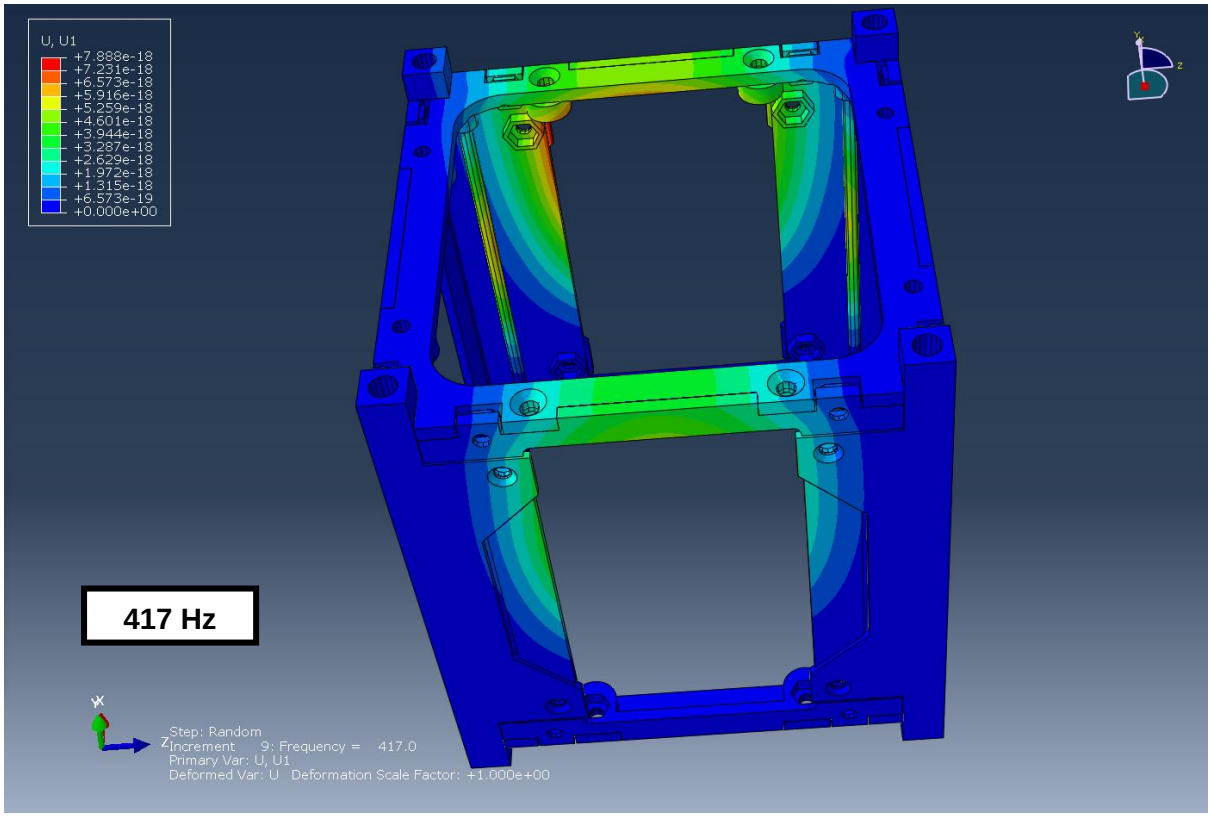
U, U1
+7.888e-18
+7.231e-18
+6.573e-18
+5.916e-18
+5.259e-18
+4.601e-18
+3.944e-18
+3.287e-18
+2.629e-18
+1.972e-18
+1.315e-18
+6.573e-19
+0.000e+00
417 Hz
Step: Random
Increment 9: Frequency = 417.0
Primary Var: U, U1
Deformed Var: U Deformation Scale Factor: +1.000e+00

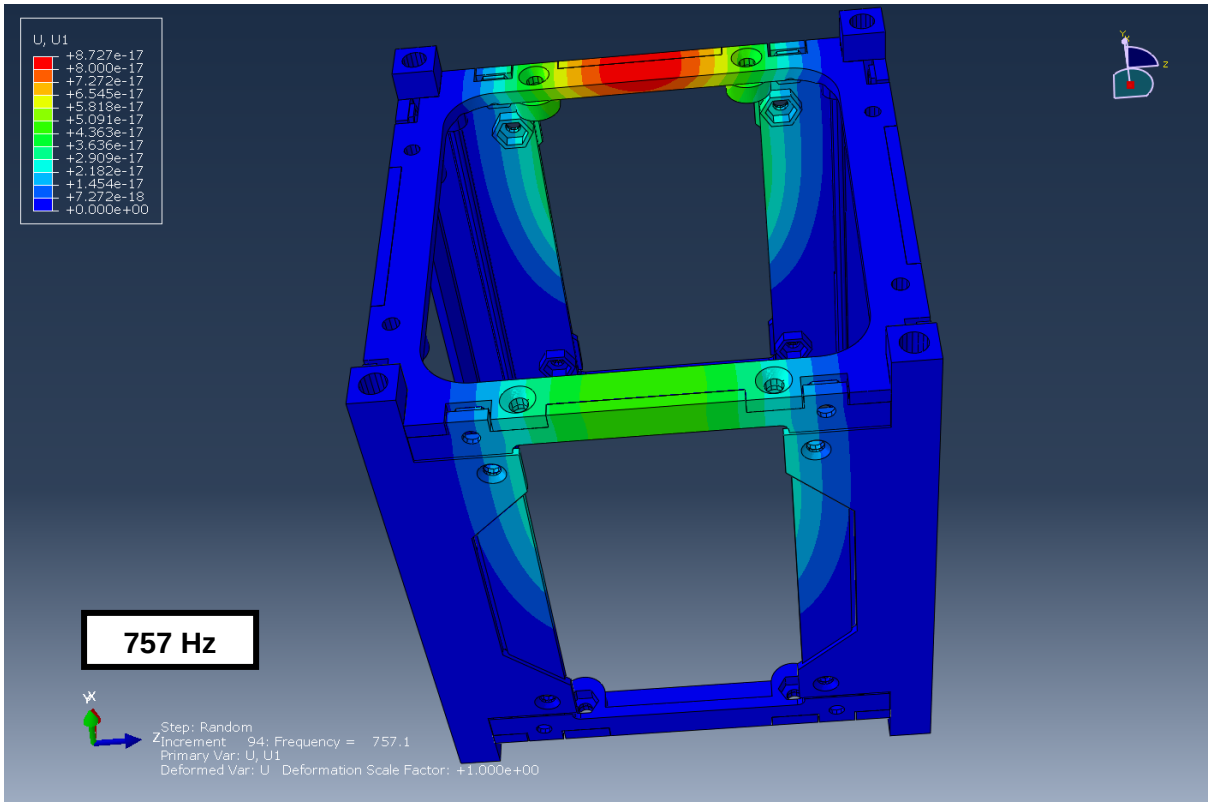
U, U1
+8.727e-17
+8.000e-17
+7.272e-17
+6.545e-17
+5.818e-17
+5.091e-17
+4.363e-17
+3.636e-17
+2.909e-17
+2.182e-17
+1.454e-17
+7.272e-18
+0.000e+00
757 Hz
Step: Random
Increment 94: Frequency = 757.1
Primary Var: U, U1
Deformed Var: U Deformation Scale Factor: +1.000e+00

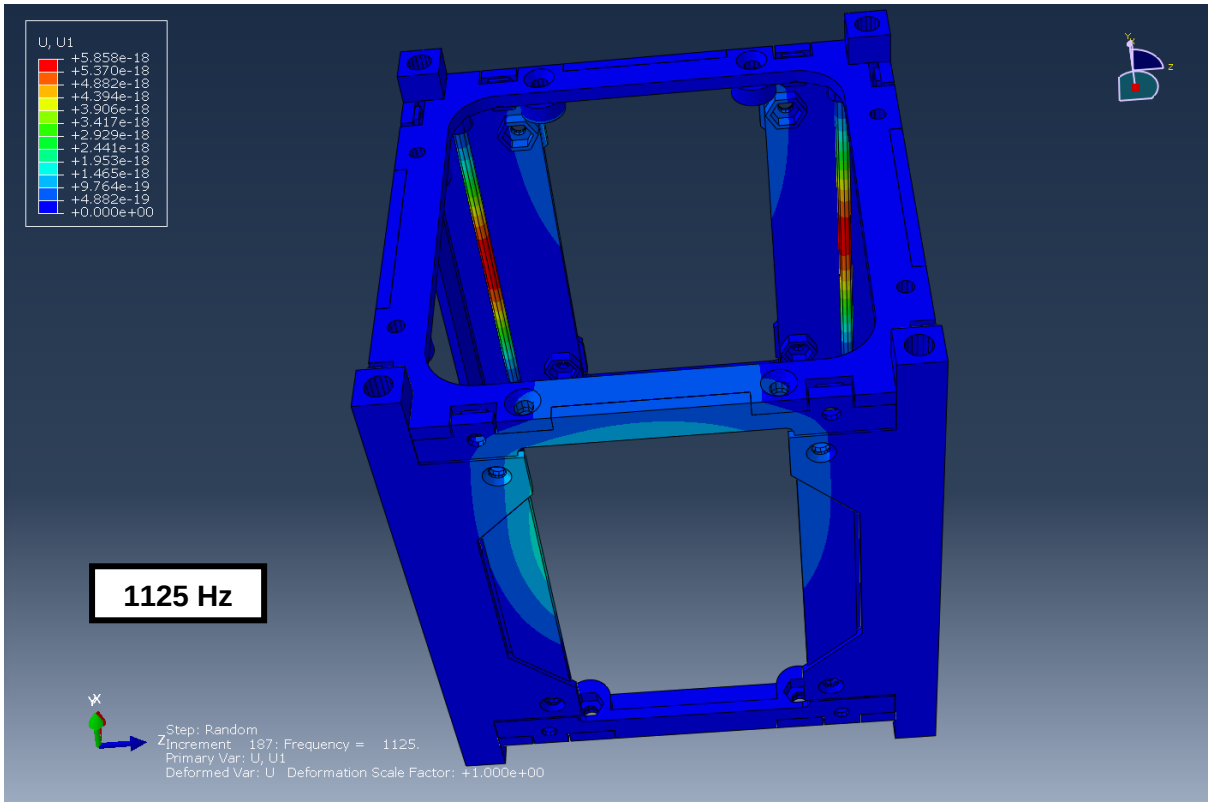
U, U1
+5.858e-18
+5.370e-18
+4.882e-18
+4.394e-18
+3.906e-18
+3.417e-18
+2.929e-18
+2.441e-18
+1.953e-18
+1.465e-18
+9.764e-19
+4.882e-19
+0.000e+00
1125 Hz
Step: Random
Increment 187: Frequency = 1125.
Primary Var: U, U1
Deformed Var: U Deformation Scale Factor: +1.000e+00

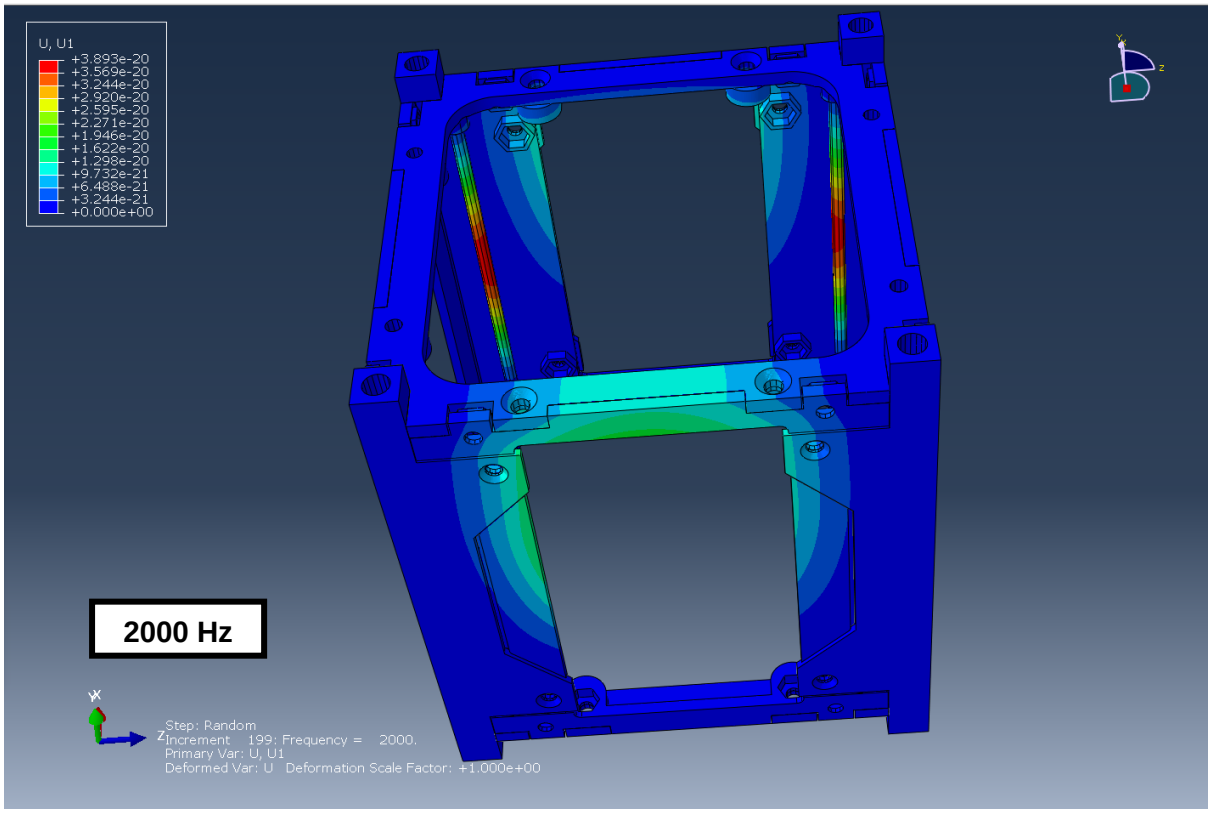
U, U1
+3.893e-20
+3.569e-20
+3.244e-20
+2.920e-20
+2.595e-20
+2.271e-20
+1.946e-20
+1.622e-20
+1.298e-20
+9.732e-21
+6.488e-21
+3.244e-21
+0.000e+00
2000 Hz
Step: Random
Increment 199: Frequency = 2000.
Primary Var: U, U1
Deformed Var: U Deformation Scale Factor: +1.000e+00